Penn Libraries
UNIVERSITY of PENNSYLVANIA

University of Pennsylvania
ScholarlyCommons

Publicly Accessible Penn Dissertations

2018

Understanding Metabolic Adaptation Of T Cells During Activation And Nutrient Limitation

Christopher Ecker
University of Pennsylvania, eckerc24@gmail.com

Follow this and additional works at: https://repository.upenn.edu/edissertations

Part of the Allergy and Immunology Commons, Immunology and Infectious Disease Commons, and the Medical Immunology Commons

Understanding Metabolic Adaptation Of T Cells During Activation And Nutrient Limitation

Abstract

Immune cells employ a diverse array of metabolic programs upon stimulation that have far-reaching consequences outside of energy production. Activated T cells require glycolysis to generate the biosynthetic intermediates for proliferation and to enhance effector functions. Due to the disorganized vasculature of solid tumors and the highly glycolytic nature of tumor cells, T cells must compete for glucose with tumor cells in a nutrient-depleted environment. We hypothesized that cells that traffic to inflamed, nutrient-limiting environments in the periphery (effector memory T cells, TEM) may have enhanced abilities to adapt to nutrient limitation compared to cells that largely reside in nutrient-rich lymphoid organs (naïve and central memory T cells, TN and TCM respectively). We demonstrate that TN and TCM rely on fatty acid metabolism to survive and proliferate when glucose is limiting, whereas TEM do not. Furthermore, we find the reliance on fatty acid metabolism in limiting glucose by TN and TCM cells regulates IFN-γ production. Thus the first section of my thesis identifies a novel regulatory interaction between fatty acid synthesis and effector function. Other byproducts of metabolic pathways can also affect immune cell function. Recent work has suggested that reactive oxygen species are released following activation, which promote proliferative signals in T cells such as IL-2 production. The second section of my thesis investigates how T cells increase reactive oxygen species (ROS) production following activation. Using transmission electron microscopy we observe dramatic alterations to mitochondrial morphology following T cell activation. Mitochondria significantly increase in size and their cristae lose parallel patterning during the first 48 hours of T cell activation. Mitochondrial swelling and cristae disturbance are glucose and mTORC1 dependent, and highly reversible. Interestingly, we find that mitochondrial swelling does not correlate to oxidative phosphorylation rate, but strongly correlates to ROS production. We speculate that these mitochondrial changes are required to create the ROS necessary for subsequent IL-2 production and T cell proliferation. Together these data demonstrate novel relationships between cellular metabolism and cytokine production in CD4 T cells. By identifying how metabolites specifically affect immune function, we hope to exploit these discoveries in future cancer immunotherapies.

Degree Type
Dissertation

Degree Name
Doctor of Philosophy (PhD)

Graduate Group
Immunology

First Advisor
James L. Riley

Keywords
effector, glycolysis, IFN-y, memory, metabolism, mitochondria

Subject Categories
Allergy and Immunology | Immunology and Infectious Disease | Medical Immunology

UNDERSTANDING METABOLIC ADAPTATION OF T CELLS DURING ACTIVATION AND
NUTRIENT LIMITATION

Christopher Michael Ecker

A DISSERTATION

In

Immunology

Presented to the Faculties of the University of Pennsylvania

in

Partial Fulfillment of the Requirements for the

Degree of Doctor of Philosophy

2018

Supervisor of Dissertation

_____

James L. Riley

Associate Professor of Microbiology

Graduate Group Chairperson

_____

David M. Allman

Professor of Pathology and Laboratory Medicine

Dissertation Committee

Taku Kambayashi, M.D., Ph.D., Associate Professor of Pathology and Laboratory Medicine

E. John Wherry, Ph.D., Richard and Barbara Schiffrin President's Distinguished Professor of

Microbiology

Kathryn E. Wellen, Ph.D., Associate Professor of Cancer Biology

Daniel J. Powell, Ph.D., Associate Professor of Pathology and Laboratory Medicine

UNDERSTANDING METABOLIC ADAPTATION OF T CELLS DURING ACTIVATION AND
NUTRIENT LIMITATION

ACKNOWLEDGMENTS

First, I would like to thank my mentor and thesis advisor Jim Riley. This work would not have been possible without his support. Jim constantly challenged my ideas and made me a better thinker, scientist and writer. He gave me the freedom to be creative, and believed in me as a scientist before I did. Jim taught me how to take informal discussions on ideas and problems into testable questions and experiments. My thesis committee have been instrumental to the development of my thesis projects and have been extremely generous with their time and guidance.

I would like to also thank all of the Riley lab members (former and current). Jim fostered a laboratory environment in which we all talk and learn from each other. Rachel Leibman and Colby Maldini were/are both brilliant graduate students that provided constant scientific and life advice and helped me create better experiments (aka the "electric factory"). Gavin Ellis, Jan Pawlicki, Kevin Tosh, and Max Richardson are incredible scientists who offered guidance, insight and support over my entire thesis. Hong Kong, Chui Lau, Kevin Gayout, Delaine Winn have also generously given their time. Whether it was lunch time conversations or random complaints about our problems, everyone has always made the lab a great place work. I would like to additionally thank Hong, Chui, and Kevin for providing me the numbers of cells needed to do many of the experiments.   Andrew Medvec was the first person in the lab I got to know well who mentored me during my rotation. Our early work fostered a lot of the conversations, ideas, and collaborations that were needed to do this thesis. Irene Su,

ABSTRACT

UNDERSTANDING METABOLIC ADAPTATION OF T CELLS DURING ACTIVATION AND
NUTRIENT LIMITATION

Christopher M. Ecker

James L. Riley

Immune cells employ a diverse array of metabolic programs upon stimulation
that have far-reaching consequences outside of energy production. Activated T cells
require glycolysis to generate the biosynthetic intermediates for proliferation and to
enhance effector functions. Due to the disorganized vasculature of solid tumors and the
highly glycolytic nature of tumor cells, T cells must compete for glucose with tumor cells
in a nutrient-depleted environment. We hypothesized that cells that traffic to inflamed,
nutrient-limiting environments in the periphery (effector memory T cells, T_{EM}) may have
enhanced abilities to adapt to nutrient limitation compared to cells that largely reside in
nutrient-rich lymphoid organs (naïve and central memory T cells, T_N and T_{CM}
respectively). We demonstrate that T_N and T_{CM} rely on fatty acid metabolism to survive
and proliferate when glucose is limiting, whereas T_{EM} do not. Furthermore, we find the
reliance on fatty acid metabolism in limiting glucose by T_N and T_{CM} cells regulates IFN-γ
production. Thus the first section of my thesis identifies a novel regulatory interaction
between fatty acid synthesis and effector function. Other byproducts of metabolic
pathways can also affect immune cell function. Recent work has suggested that reactive
oxygen species are released following activation, which promote proliferative signals in

T cells such as IL-2 production. The second section of my thesis investigates how T cells increase reactive oxygen species (ROS) production following activation. Using transmission electron microscopy we observe dramatic alterations to mitochondrial morphology following T cell activation. Mitochondria significantly increase in size and their cristae lose parallel patterning during the first 48 hours of T cell activation. Mitochondrial swelling and cristae disturbance are glucose and mTORC1 dependent, and highly reversible. Interestingly, we find that mitochondrial swelling does not correlate to oxidative phosphorylation rate, but strongly correlates to ROS production. We speculate that these mitochondrial changes are required to create the ROS necessary for subsequent IL-2 production and T cell proliferation. Together these data demonstrate novel relationships between cellular metabolism and cytokine production in CD4 T cells. By identifying how metabolites specifically affect immune function, we hope to exploit these discoveries in future cancer immunotherapies.

TABLE OF CONTENTS

LIST OF TABLES

LIST OF ILLUSTRATIONS

CHAPTER 4. Mitochondrial remodeling upon T cell activation

Chapter 1- Connecting T cell metabolism to effector function

Upon antigen encounter in T cells or toll like receptor signaling in macrophages and dendritic cells, glycolysis even in the presence of oxygen is dramatically upregulated in a phenomenon known as the "Warburg effect" (Everts et al., 2014; Frauwirth et al., 2002; Galván-Peña and O'Neill, 2014). Warburg metabolism was first described in cancer cells, in which proliferating cells rely on high rates of aerobic glycolysis (Vander Heiden et al., 2009). Much of the early focus on cancer metabolism examined why highly proliferating cells rely on aerobic glycolysis, as it is far less efficient than oxidative phosphorylation for production of ATP. A number of hypotheses were proposed to explain why proliferating malignant cells largely utilize aerobic glycolysis: 1) cancer cells are forced to use glycolysis because of mitochondrial damage from transformational mutations; 2) the rate of aerobic glycolysis occurs 10-100 fold faster than oxidative phosphorylation; 3) increased glucose uptake allows tumor cells to outcompete healthy cells in nutrient limiting environments; 4) aerobic glycolysis generates biosynthetic intermediates that can be used to produce the necessary building blocks for proliferation; and 5) aerobic glycolysis confers chromatin remodeling or other metabolic signals that drive proliferation (Liberti and Locasale, 2016; Locasale and Cantley, 2011; Vander Heiden et al., 2009). All of these proposals may not be mutually exclusive, and may differ in their importance between proliferating cancer cells and stimulated immune cells.

From a bioenergetic standpoint, it is unclear whether ATP demand ever reaches limiting values during proliferation and there are some models that propose ATP requirements for division are less than those of normal cellular maintenance (Pfeiffer et al., 2001). The most well supported view is that proliferating cells rely on aerobic glycolysis to generate the cellular building blocks necessary for proliferation. For instance, glycolytic intermediates can produce nucleotides, fatty acids, and amino acids required for creating a new cell (Vander Heiden et al., 2009). In addition, altered concentrations of metabolites can promote proliferation though epigenetic modifications and reactive oxygen species (ROS) signaling (Kong and Chandel, 2018; Reid et al., 2017). Many of the original hypotheses focused on why aerobic glycolysis was necessary for rapid cellular proliferation, and were specifically applied in the context of T cell metabolism during activation (**Fig 1-1**). However, these ideas do not sufficiently explain why macrophages and dendritic cells increase aerobic glycolysis upon TLR stimulation since these cells do not proliferate (Galván-Peña and O'Neill, 2014). It was this observation combined with early work by Chang et al. that proposed a bold new hypothesis, that aerobic glycolysis is necessary for immune cells to initiate effector programs (Chang et al., 2013).

The last decade brought enormous interest to studying the metabolism of immune cells. Two key aspects of immunometabolism were essential for the field's expansion: 1) the requirement and magnitude of metabolic changes immune cells undergo upon stimulation, and 2) the ability to tie those metabolic changes to

2

functional consequences. T cells have been at the forefront of immunometabolism because they can be easily isolated, expanded, transduced, adoptively transferred, and exhibit dramatically different metabolic states upon activation. In addition, lessons learned from T cell metabolism have been applied and translated to other immune cell types.

Historically, glycolysis has been the most studied metabolic pathway in T cells because glucose is the most consumed metabolite by activated T cells. T cell activation increases glycolysis largely by driving surface expression of the glucose transporter in T cells, Glut1, through Akt signaling (Frauwirth et al., 2002; Jacobs et al., 2008). While T cells predominantly express Glut1, T cells also express transcript for other glucose transporters including Glut 3, 6, and 8 (most of which do not increase mRNA expression following stimulation). Co-stimulation receptor expression is required for maximal Akt activation and Glut1 surface expression and subsequent glycolysis (Jacobs et al., 2008; Macintyre et al., 2014; Siska et al., 2016). Glut1 is expressed in effector T cell subsets such as CD8+ T cells and CD4+ Th1, Th2, and Th17 cells, and all of these cells strongly engage glycolysis following activation to proliferate (Macintyre et al., 2014). Glycolytic intermediates contribute to the numerous biosynthetic and energy generating pathways (the pentose phosphate pathway and serine biosynthesis pathway to generate nucleotides, to generate acetyl-CoA and TCA cycle intermediates critical for epigenetic modifications and energy, and for fatty acid synthesis from glucose-derived citrate). T cell specific deletion of Glut1 inhibits effector T cell proliferation and survival upon

3

stimulation *in vivo* (Macintyre et al., 2014). Interestingly, T regulatory cells appear in

higher numbers in those mice potentially due to increased niche space, and retain

suppressive function in *in vitro* (Michalek et al., 2011). However recent work has

suggested that glycolysis is still important in T regulatory cells for migration into

inflammatory environments and for *in vivo* and *in vitro* proliferation (Kishore et al.,

2017; Procaccini et al., 2016).   Furthermore limiting glucose availability specifically

inhibits effector function by regulating IFN-γ production by at least two independent

mechanisms: 1) available glyceraldehyde 3-phosphate dehydrogenase (GAPDH), a

glycolytic enzyme, binds to the 3' untranslated region of IFN-γ and inhibits translation,

and 2) limiting glucose lowers the cellular pool of acetyl-CoA which subsequently lowers

histone acetylation of the IFN-γ promoter (which may be highly sensitive to changes in

acetylation (Chang et al., 2013; Peng et al., 2016). These mechanisms are further

discussed in chapter 3. Interestingly, inhibiting glycolytic rate of proliferating T cells

prevents terminal differentiation and promotes memory development of adoptively

transferred T cells (Sukumar et al., 2013). The authors further demonstrated that

enforcing elevated glycolysis by overexpressing the glycolytic enzyme, phosphoglycerate

mutase-1, promoted effector function at the cost of memory differentiation. Thus

glucose works to fulfill the biosynthetic, proliferative, and functional needs of activated

T cells and regulates memory development.

Glutamine is also incredibly essential to effector T cell activation and survival.

Upon activation T cells increase mRNA and protein expression of several glutamine

transporters, including SLC38A1 and SLC38A2 (Bhutia and Ganapathy, 2016; Carr et al., 2010). Glutamine can also be routed into diverse fates critical for proliferating cells. Besides from being used for protein synthesis directly, glutamine can be metabolized into glutamate and subsequently into TCA cycle intermediates, or used for fatty acid synthesis through reductive glutaminolysis, can produce several other amino acids (alanine, aspartate, etc.), and is a critical nitrogen donor for purine and pyrimidine nucleotide synthesis (Cluntun et al., 2017; DeBerardinis and Cheng, 2010). Utilization of glutamate or cell-permeable α-ketoglutarate is not sufficient to rescue effector T cell proliferation in glutamine-deficient media (Carr et al., 2010). These data suggest that glutamine's roles outside of the mitochondria are critical for activated effector T cells. Interestingly, limiting glutamine availability also promotes T regulatory cell polarization of naïve CD4 T cells, but is reversed by adding cell-permeable α-ketoglutarate, a TCA cycle intermediate and glutamine derivative (Klysz et al., 2015).   Interestingly, glutamine utilization for oxidative phosphorylation and amino acid synthesis pathways may be increased during glucose limitation in T cells to compensate for losses in energy production (Blagih et al., 2015).

Other amino acids at least by magnitude are consumed less than glutamine, but nevertheless serve critical roles in T cell metabolism for proliferation and function. While the glycolytic intermediate 3-phosphoglycerate (3-PG) can be converted to serine, extracellular serine is required for optimal T cell expansion even when glucose availability is high (Ma et al., 2017b). Serine can be made into glycine and used for *de*

novo purine synthesis through one carbon metabolism. Ma et al. further demonstrated that dietary restriction of serine impairs T cell responses in a mouse model of *Listeria monocytogenes* infection. In addition, T cells deficient in the neutral amino acid transporter Slc7a5 (most commonly transports leucine), were unable to proliferate or differentiate into effector cells in response to antigen (Sinclair et al., 2013). Interestingly, these T cells produced equal amounts of IL-2 as wild-type cells but were compromised in glucose uptake and IFN-γ production. Limiting extracellular arginine impairs T cell glycolysis upon activation and subsequent proliferation (Fletcher et al., 2015). Furthermore, the absence of extracellular arginine in activated T cells impairs expression of CD3ε and CD3ζ and production of many cytokines such as IFN-γ, IL-5, IL-10, but not others like IL-2 (Zea et al., 2004). Tryptophan metabolites in the kynurenine pathway can be produced by the enzyme indoleamine 2,3-dioxygenase (IDO), and are expressed by many antigen presenting cells and tumor cells in the tumor microenvironment (Schafer et al., 2016). High expression of IDO can cause local depletion of tryptophan to regulate T cell proliferation, and the kynurenine metabolites can independently induce T cell apoptosis (Fallarino et al., 2002; Platten et al., 2012). Furthermore, amino acid recycling in lymphocytes is required for effective immunity in humans. Patients with loss-of-function mutations in tripeptidyl peptidase II are unable to maintain intracellular amino acid levels, exhibit impaired IFN-γ and IL-1β production, and prone to recurrent infections and autoimmunity (Lu et al., 2014).

Fatty acids perform numerous functions for the cell. They are essential components of cell membranes, act as important secondary signaling molecules during T cell activation, can post-translationally modify important proteins, and act as an energy resource.   T cells often acquire fatty acids from their environment through fatty acid transporters, but can also generate their own by *de novo* fatty acid synthesis. In CD4+ T cells, inhibition of a critical enzyme for fatty acid synthesis, acetyl-CoA carboxylase 1 (ACC1) promoted the polarization of T regulatory cells at the cost of Th1, Th2, and Th17 development (Berod et al., 2014). CD8+ T cells also require ACC1 for survival and proliferative responses during homeostasis and infection (Lee et al., 2014a). Both Berod et al. and Lee et al. demonstrated that addition of extracellular fatty acids rescues many of these alterations in polarization or defects in proliferation. These data suggest that CD8+ T cells can overcome defects in fatty acid synthesis by exogenous uptake of fatty acids, however for CD4+ T cells the source of fatty acids and the oxidation or synthesis of those fatty acids may impact polarization. Proliferating T regulatory cells require both fatty acid oxidation and glycolysis for proliferation and function (Procaccini et al., 2016). Promoting fatty acid metabolism by overexpressing carnitine palmitoyl transferase 1a (CPT1a) promotes T cell survival and memory development *in vivo* (van der Windt et al., 2012). Interestingly, driving fatty acid metabolism often has similar affects to glucose limitation by promoting memory and regulatory T cell development, and limiting effector function. This relationship between glucose limitation and fatty acid metabolism is further explored in Chapter 3.

Glucose, amino acid, and fatty acid effects on T cell polarization and memory development can partially be explained by the mammalian target of rapamycin (mTOR) activity. mTOR acts in two complexes, mTORC1 and mTORC2, and integrates nutrient availability, growth factors and energy levels (as well as other factors) to regulate metabolism and proliferation (Laplante and Sabatini, 2012; Sabatini, 2017). Glucose and many amino acids are required for mTORC1 activation following effector T cell activation. In turn, mTOR activity can regulate numerous transcription factors involved in glycolysis, fatty acid oxidation, and fatty acid synthesis like hypoxia inducible factor 1α (HIF-1α), myc, peroxisome proliferator-activated receptor alpha, peroxisome proliferator-activated receptor gamma, and the sterol regulatory element-binding protein family of transcription factors (Waickman and Powell, 2012; Zeng and Chi, 2017). Inhibition of mTORC1 in T cells promotes memory development during viral infection (Araki et al., 2009; Bengsch et al., 2016). Inversely, loss of tuberous sclerosis 1, a negative regulator of mTOR signaling, promotes effector function at the cost of memory development in a mouse model of *Listeria monocytogenes* infection (Shrestha et al., 2014). This patterning of mTOR activity is nearly identical to the observations that promoting glycolysis drives effector differentiation, while inhibiting glycolysis promotes memory development (Sukumar et al., 2013). T regulatory cell polarization and lineage stability require phosphatase and tensin homolog (PTEN), a negative regulator of Akt and mTORC1 activity, to maintain metabolic balance between glycolysis and mitochondrial metabolism (Shrestha et al., 2015) . HIF-1α is stabilized downstream of

mTORC1, promotes glycolysis and effector T cell function and polarization (Dang et al., 2011; Doedens et al., 2013). Furthermore mice with deficiency in HIF-1α are strikingly defective in Th17 polarization, while simultaneously promoting T regulatory cell polarization (Dang et al., 2011; Hsiao et al., 2015). Thus the proliferation, polarization, and function of effector, memory, and T regulatory cells are strikingly dependent on a careful balance of nutrient availability and mTOR activity.

However many of the observations listed above cannot be fully explained by simple mTOR activity. For example, metabolites and metabolic enzymes affect specific cytokine production by immune cells often in surprising and novel ways. None of our current understanding of immunometabolism could have predicted the glycolytic enzyme, GAPDH's ability to bind specifically to IFN-γ mRNA and prevent translation (Chang et al., 2013). Multiple metabolic intermediates and cofactors (i.e. α-ketoglutarate, acetyl-CoA, S-adensoylmethionine, and nicotinamide adenine dinucleotide) regulate, or are essential for, the activity of many epigenetic modifying enzymes (Etchegaray and Mostoslavsky, 2016; Wellen et al., 2009). The laboratory of Luke O'Neill has publically presented unpublished work that certain TCA intermediates like succinate may directly regulate the production of effector cytokines. Mitochondria-generated ROS are not just metabolic byproducts that cause damage to cellular structures, but can relay important proliferative signals in tumor cells and in T cells. ROS regulate the ERK MAPK, HIF-1α, and JNK signaling pathways in tumor cells, and are instrumental for IL-2 signaling and subsequent T cell proliferation (Gauron et al., 2013;

Kong and Chandel, 2018; Sena et al., 2013; Weinberg et al., 2010). In addition to their

role in energy production, mitochondria appear to serve to produce many important

metabolites that can regulate cellular signaling in numerous ways. These roles of the

mitochondria in T cell activation are further explored in Chapter 4.

Metabolism is a highly regulated network of pathways simultaneously regulating

cell processes well beyond energy production. Recent work has discovered surprising

regulatory interactions between metabolites and molecules important for immune

function.   Future work will need to expand these concepts into *in vivo* tissue biology

and mechanistic understanding of how these regulatory interactions operate with

controlled specificity.

Figures

Why do tumor cells engage in Warburg metabolism?

Competitive Advantage?

Biosynthesis

Signals that facilitate proliferation?

Tumor Cells

Proliferation

Why do stimulated immune cells engage in Warburg metabolism?

T Cells (Proliferating)   Dendritic Cells (Non-Proliferating)   Macrophages (Non-Proliferating)
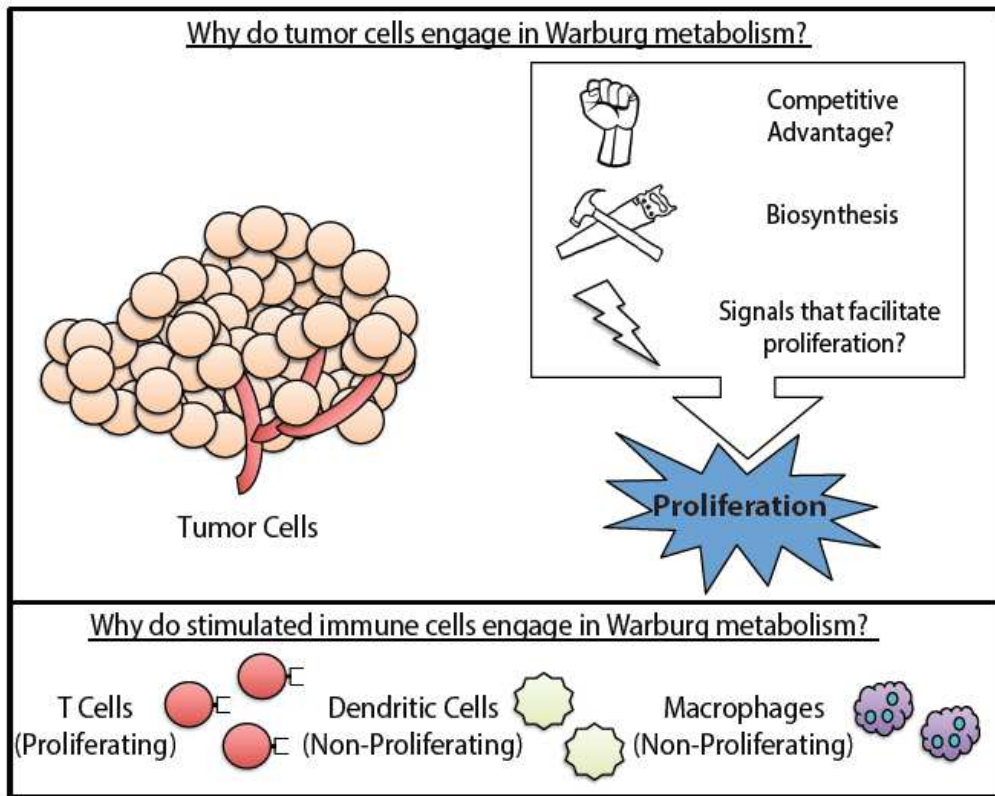
Figure 1-1

Figure 1-1: Why do cells engage Warburg metabolism?

For many years researchers questioned why tumor cells relied so heavily on ATP-inefficient Warburg metabolism instead of oxidative phosphorylation. Most of the evidence has supported three main concepts. 1) Tumor cells may gain a proliferative advantage by drastically increasing glucose uptake and consumption, and thus starving nearby cells of the nutrients needed to support proliferation. 2) Glycolytic intermediates also help to generate important cellular building blocks needed for proliferation. 3) Glycolysis promotes cellular signaling pathways that facilitate proliferation through alterations of redox potential, mitochondrial ROS production, and chromatin remodeling. Taken together, tumor cells rely on Warburg metabolism because it facilitates the signals and demands a rapidly dividing cell needs. In recent years, researchers have learned that many stimulated immune cell types also rely on Warburg metabolism. T cells stimulated through their TCR and co-stimulatory domains, or some subsets of macrophages and dendritic cells stimulated through TLRs, rapidly upregulate Warburg metabolism. However many of these immune cell populations utilize Warburg metabolism without subsequent proliferation. These ideas sparked the hypothesis that stimulated immune cells use Warburg metabolism to enhance immune function.
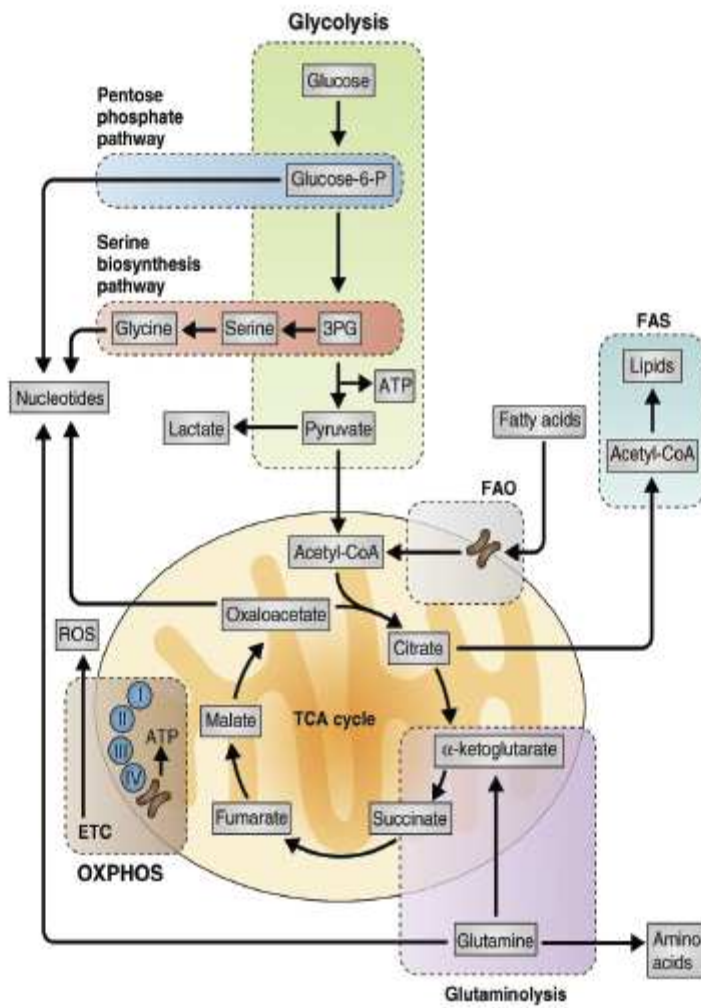
Adapted from Buck et al. T cell metabolism drives immunity. *JEM*. 2015.

Figure 1-2

Figure 1-2: Metabolic pathways generate intermediates important for biosynthesis in T cells.

During activation T cells rapidly upregulate glycolysis for energy and to generate the building blocks of a new cells. Glycolysis produces ATP and facilitates *de novo* nucleotide production through the pentose phosphate and serine biosynthesis pathway. While most pyruvate is shuttled out of the cell as lactate in activated T cells, some pyruvate can be shuttled into the mitochondria for the TCA cycle. During activation T cells also upregulate oxidative phosphorylation by increasing fatty acid oxidation, glutamine uptake. T cells can further utilize fatty acid synthesis to generate *de novo* fatty acids. Together glycolysis, oxidative phosphorylation, glutaminolysis, fatty acid oxidation and synthesis represent the most well studied metabolic pathways in T cells.

Chapter 2- The perils of using adoptive T cell approaches to study tumor/T cell metabolic competition

Exciting new technologies and conceptual advancements have re-energized the study of the metabolic competition between tumors and the adaptive immune system (Chang et al., 2015b; Ho et al., 2015a; Sugiura and Rathmell, 2018). Despite these advancements, there remains little discussion in the literature on how investigators should model nutrient depletion in the tumor microenvironment when studying immune cell/tumor cell metabolic interactions and competition. How can we more accurately distinguish and dissociate nutrient deprivation's effects on immune cells from other immunosuppressive components of the tumor microenvironment *in vivo*? Are T cells engineered with altered metabolic programming specifically overcoming a nutrient limitation or are they simply better tumor-specific T cells that function better in all nutrient environments? This essay will lay out some of the critical issues facing the field and hopefully spur the development of improved approaches for testing new immune therapies. We believe that greater mechanistic understanding of immunometabolism will fully harness the clinical potential of immune therapies.

Challenges T cells face in the solid tumor microenvironment

In vivo, tumors alter the abundance of dozens of metabolites in the interstitial fluid relative to healthy tissue (Kamphorst et al., 2015; Pavlova and Thompson, 2016). Most commonly solid tumor environments have been reported to be deprived of oxygen, glucose, glutamine, and arginine and highly acidic (**Fig 2-1 A**). Different tumors and even separate regions of the same tumor can host diverse nutrient environments and can experience intermittent blood flow and nutrient supply (DeBerardinis and Chandel, 2016; Vaupel et al., 1987). An abundance of pro-angiogenic factors (like vascular endothelial growth factor-A) promote disturbed vasculature characterized by large and leaky vessels, erratic branching, and irregular and slow blood flow which inhibits efficient nutrient delivery (Carmeliet, 2005; Lanitis et al., 2015). T cells require glucose, glutamine, and mitochondrial pathways for activation, maximal proliferation and/or effector function (Cham and Gajewski, 2005; Macintyre et al., 2014; Procaccini et al., 2016; Ron-Harel et al., 2016; Sena et al., 2013). Aerobic glycolysis serves the increased biosynthetic demands of highly proliferating cells. Glycolytic intermediates can produce nucleotides, lipids, and amino acids necessary for cellular proliferation in both T cells and cancer cells (Vander Heiden et al., 2009). Similar reliance on aerobic glycolysis between proliferating cancer cells and activated T cells intensifies a competition for limited nutrients within the tumor microenvironment. Competition for glucose also plays a clear role in limiting effective anti-tumor responses *in vivo* (Chang et al., 2015b; Ho et al., 2015a). Aerobic glycolysis is required for maximal IFN-γ production by effector T cells though two independent mechanisms. The glycolytic enzyme

glyceraldehyde-3-phosphate dehydrogenase (GAPDH) can inhibit translation of IFN-γ

mRNA, while another study has demonstrated that the glycolytic enzyme, lactate

dehydrogenase A (LDHA), promotes histone acetylation along the IFN-γ locus (Chang et

al., 2013; Peng et al., 2016). Although some attempts to increase nutrient availability

have been successful, we have little understanding how to make T cells more fit in a

nutrient limiting environment (Chang et al., 2015b; Lanitis et al., 2015).

Due to dysfunctional vasculture and the high glycolytic rate of many tumor cells,

the tumor microenvrionment is often acidic because of high lactate concentrations (**Fig

2-1 B**). Both tumor and T cells rely on monocarboxylate transporters to secrete and

uptake lactate generated from glycolysis and pyruvate. High lactate concentrations in

the environment prevent T cells from efficiently transporting lactate out of the cell and

increase intracellular acidity and inhibit functionality and NFAT activity (Brand et al.,

2016; Fischer et al., 2007).   Brand et al. demonstrated that melanoma tumor cells

engineered to have low lactate dehydrogenase A (LDHA) activity, have greater immune

infiltration and activity than tumor cells with normal LDHA expresion. LDHA is the

glycolytic enzyme required for conversion of pyruvate to lactate.   Furthermore the

administration of the proton pump inhibitor, esomeprazole, can normalize tumor pH *in

vivo* and when combined with immunotherapy can promote tumor clearance

(Calcinotto et al., 2012). While glucose deprivation and high lactate concentrations

inhibit anti-tumor responses, they also promote immunosuppressive T regulatory cell

and macrophage polarization and function (Angelin et al., 2017; Colegio et al., 2014).

As T cells become exposed to chronic antigen in the tumor microenvironment they begin to terminally differentiate and become exhausted. As exhaustion becomes more severe, T cells increase expression of multiple inhibitory receptors, while simultaneously inhibiting costimulatory receptor expression (**Fig 2-1 C**). Inhibitory receptors can inhibit co-stimulation and phosphorylation events downstream of T cell receptor (TCR) activation, and prevent activation signals (Akt and mTORC1) necessary for increasing surface expression of the major glucose transporter, Glut-1, in T cells (Jacobs et al., 2008; Siska et al., 2016). Without sufficient surface expression of Glut-1, the activated T cells are unable to properly upregulate glycolysis and have inhibited proliferation and effector function.

Chronic antigen exposure affects metabolic pathways beyond glycolysis, by inhibiting mitochondrial functions (**Fig 2-1 D**). Exhausted T cells in models of cancer or chronic virus infection often have defects in mitochondria number, size, and voltage potential and function (Bengsch et al., 2016; Scharping et al., 2016; Siska et al., 2017b). Upregulation of mitochondrial pathways (oxidative phosphorylation and one-carbon metabolism) are essential for proper T cell proliferation. (Chang et al., 2013; Procaccini et al., 2016; Ron-Harel et al., 2016; Ron-Harel et al., 2015). In addition mitochondria play roles beyond producing energy and biosynthesis, though epigenetic and signaling roles during T cell activation (Minocherhomji et al., 2012; Sena et al., 2013). The tumor microenvironment downregulates mitochondrial biosynthesis by inhibiting expression of PPAR-gamma coactivator 1α (PGC1α) by chronic Akt signaling (Scharping et al., 2016).

Furthermore, Scharping et al. demonstrated that overexpression of PGC1α in tumor-specific T cells is able to prevent downregulation of mitochondrial mass and enhance T cell functionality in the tumor microenvironment. Thus

Tumor infiltrating lymphocytes are exposed to large amounts of reactive oxygen species (ROS, **Fig 2-1 E**). ROS are highly chemically reactive and can damage cellular structures, and inhibit T cell activation. Production of ROS drastically increases in T cells exposed to hypoxia and is one of the major mechanisms of immune suppression by myeloid derived suppressor cells (Kusmartsev et al., 2004; Tafani et al., 2016). Myeloid derived suppressor cells are a heterogeneous immunosuppressive subset of cells overexpressed in patients and mice with cancer. While ROS are necessary for IL-2 production and proliferation by T cells, it remains unclear the quantities in which ROS will become harmful to T cells (Sena et al., 2013). Exposure to oxidative stress by low doses of exogenous hydrogen peroxide are sufficient to inhibit T cell functionality and survival (Ligtenberg et al., 2016).

Challenges of applying immunometabolism findings to tumor models in vivo.

Given the metabolic challenges tumor-specific T cells face, there have been numerous attempts to mitigate these effects via pharmacological or genetic modifications to improve tumor-specific T cell therapy *in vivo*. However our interpretation of *in vivo* studies has been hindered by numerous technical and biological challenges.

Distinguishing mechanism(s) of therapy

It is incredibly difficult to distinguish whether newly designed immune interventions targeting the metabolic challenges of solid tumors have generated T cells that operate better in nutrient depleted environments or simply have made a better T cell (that operates better in all environments). The key to distinguishing these possibilities are 1) identifying how a modification improves the anti-tumor response and 2) understanding how individual metabolic interactions lead to distinct functional outcomes. For example, enhancing mitochondrial fusion, increasing L-Arginine media concentrations, or inhibiting glycolytic metabolism while T cells are being expanded for adoptive cell therapy all enhance the therapeutic activity of the infused T cells (Buck et al., 2016; Geiger et al., 2016; Sukumar et al., 2013).   All of these interventions alter T cell metabolism, but do they enable T cells to function better in the tumor microenvironment? It is challenging to envision a mechanism by which temporarily expanding T cells in low glucose empowers them to function better in the tumor microenvironment. Rather, previous studies demonstrate that T cells expanded in low glucose retain a less differentiated phenotype which enables improved engraftment of the expanded T cells which correlates with improved tumor control (Gattinoni et al., 2011). Expansion in the presence of higher levels of L- arginine also results in T cells that are less differentiated and more reliant on oxidative phosphorylation instead of glycolysis (Geiger et al., 2016).   These cells have higher intracellular concentrations of L-arginine, which may make them resistant to low arginine levels in the tumor

20

microenvironment. Likewise, T cells with enhanced mitochondrial fusion are less differentiated in culture and exhibit greater reliance on oxidative phosphorylation (Buck et al., 2016). Enhanced fusion may enhance mitochondrial function and combat mitophagy frequently observed during nutrient deprivation (Rambold et al., 2011). How do we determine to what extent differentiation or improved fitness in the tumor microenvironment results in improved tumor clearance? Future studies must work to better distinguish mechanisms of metabolic immune interventions to provide mechanistic understanding of immunometabolism (**Fig 2-2 A**).

Speed of metabolic adaption and metabolite decay

Unlike standard epigenetic or transcriptional changes that often occur over several hours or days, many metabolic changes occur incredibly quickly in response to different environments. This may even be more pronounced in immune cells, because these cells readily circulate and traffic to diverse areas of the body, and thus must be able to adapt rapidly in diverse metabolic environments. While researchers can observe cell intrinsic differences of different T cell subsets *in vitro*, how much information is lost because of isolation and prolonged *in vitro* expansion (Dimeloe et al., 2016a; Pan et al., 2017; Procaccini et al., 2016; van der Windt et al., 2012)? Quantification is further complicated during conventional *in vitro* extraction techniques because of metabolite loss, leakage, or decay (Chen et al., 2016; Van Gulik et al., 2012; Vuckovic et al., 2011; Yang et al., 2017).   Thus, during commonly used isolation procedures and before any assay can be performed *in vitro,* metabolic changes are occurring (**Fig 2-2 B**). Alternative

approaches such as utilizing isotopic tracers are highly compatible with *in vivo* models, can be easily administered, and may better recapitulate *in vivo* biology (Hensley et al., 2016; Sun et al., 2017).

Utilizing relevant cell populations in nutrient depletion studies

Immune cells isolated for nutrient depletion studies should represent the cells that would traffic to sites of inflammation and nutrient depletion in the tumor microenvironment (**Fig 2-2 C**).   Many *in vitro* T cell studies have examined nutrient depletion on total T cells isolated from the blood or spleens of mice or humans. However, naïve cells that often represent the majority of T cells in circulation or in the spleen do not travel to sites of inflammation where vasculature is often disturbed or injured (Klebanoff et al., 2006; Thome et al., 2014). Differentiated effector memory T cells or tissue resident memory T cells are the cells that reside in the environments that actually encounter nutrient depletion and have distinct responses to metabolic stress (Dimeloe et al., 2016a; Ecker et al., 2018). Thus, many previous studies have lacked sufficient resolution to determine whether T cells in the blood mimic the same metabolic and adaptive features of T cells that reside in the tissue.

Missing spatial organization of nutrient availability and immune function

There remain large gaps in understanding of immune cell localization within hypoxic or glucose depleted regions of tumors. Do we truly observe anti-tumor function and immune cell proliferation only in sites of nutrient availability? Do immune cells

have higher rates of death in sites of nutrient depletion or do they simply traffic away from those sites? Which nutrients are the most essential for function *in vivo*? Regions of nutrient depletion can often be examined through florescent analogues like 2-NBDG for glucose distribution, staining with pimonidazole for regions experiencing hypoxia, or through distinct protein expression of hypoxic or nutrient depleted cells (Airley et al., 2001). These are well validated, and compatible with commonly used methods to identify immune cell localization and activity (Bennewith and Durand, 2004; He et al., 2008; Sukumar et al., 2013). Improvements in the resolution of mass spectrometry imaging techniques have also identified tissue-resident immune populations and metabolite gradients in tumors (Dilillo et al., 2017; Holzlechner et al., 2017). Additionally, sensitive reporter constructs could be useful to map the duration and regional location of nutrient limiting milieus.   Elucidating the spatial organization of nutrient availability and immune populations will be crucial for greater insight of immune surveillance in the tumor microenvironment (**Fig 2-2 D**).

The last decade of research has led to incredible findings and a growing interest in immunometabolism. Researchers have only just begun to understand how to translate the basic findings into in vivo tumor models and face many challenges. Future studies designed to overcome these challenges will be essential for providing mechanistic understanding of *in vivo* immunometabolism and for translating these approaches into the clinical arena.

Figures

METABOLIC CHALLENGES T CELLS ENCOUNTER IN THE SOLID TUMOR MICROENVIRONMENT

C. TERMINAL DIFFERENTIATION AND EXHAUSTION

B. HIGH EXTRACELLULAR LACTATE CONCENTRATIONS

D. DECREASED MITOCHONDRIAL MASS AND FUNCTION

A. NUTRIENT LIMITATION AND COMPETITION

E. HYPOXIA AND MDSC-INDUCED ROS

TUMOR SPECIFIC T CELLS

SOLID TUMOR MASS

Figure 2-1

24
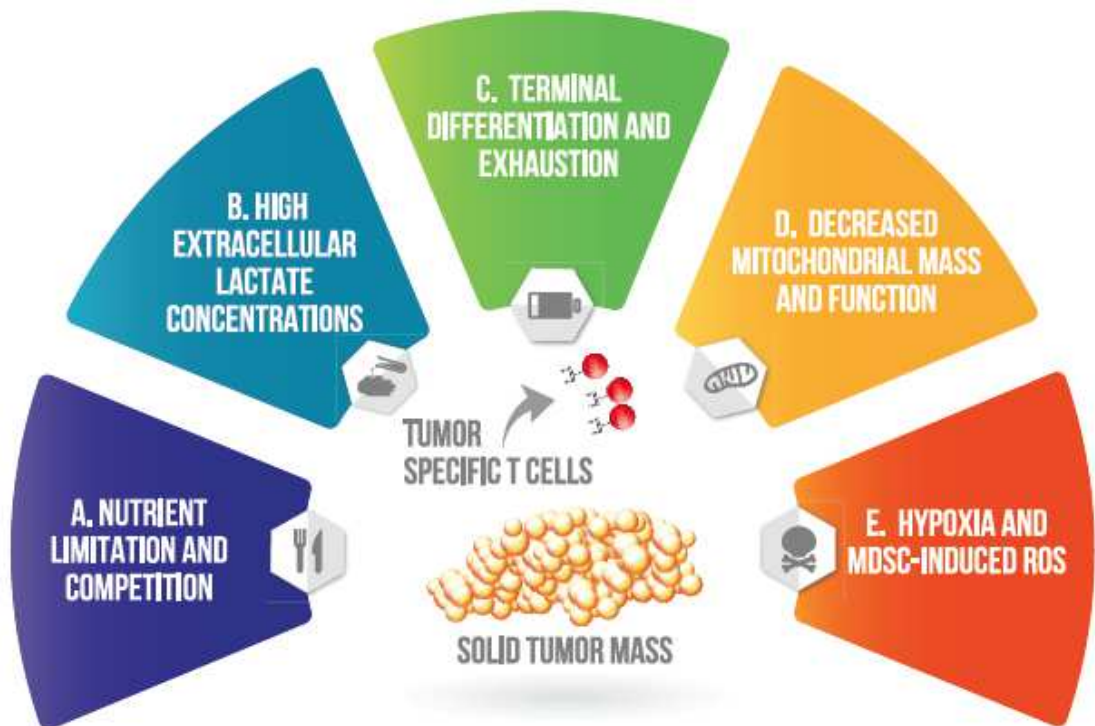
Figure 2-1: Metabolic challenges T cells encounter in the solid tumor microenvironment.

A. Nutrient limitation and competition**.** Disturbed vasculature of solid tumors are often unable to provide nutrients critical for T cell activation.   Activated T cells and proliferating tumor cells rely on aerobic glycolysis and compete for extracellular glucose. **B.** High extracellular lactate concentrations**.** Reliance on aerobic glycolysis by tumor cells promotes a large buildup of the waste product lactate in the extracellular milieu of solid tumors. High extracellular concentrations of lactate hinder T cell activation by inhibiting efficient secretion of lactic acid from the cytoplasm and acidifying intracellular pH. **C.** Hypoxia and MDSC-induced ROS**.** T cells in the solid tumor microenvironment are constantly exposed to reactive oxygen species, which are highly reactive and damage cellular structures. Hypoxia rapidly induces ROS production by T cells and myeloid derived suppressor cells frequently suppress effector T cells by secreting ROS. **D.** Decreased mitochondrial mass and function. Tumor specific T cells have defects in mitochondria biogenesis, size, cristae structure, voltage potential and function. **E.** Terminal differentiation and exhaustion. Chronic antigen exposure causes loss of co-stimulatory receptors while promoting inhibitory co-receptors that inhibit glycolytic metabolism and activation signaling.

CHALLENGES OF STUDYING IMMUNOMETABOLISM USING IN VIVO TUMOR MODELS
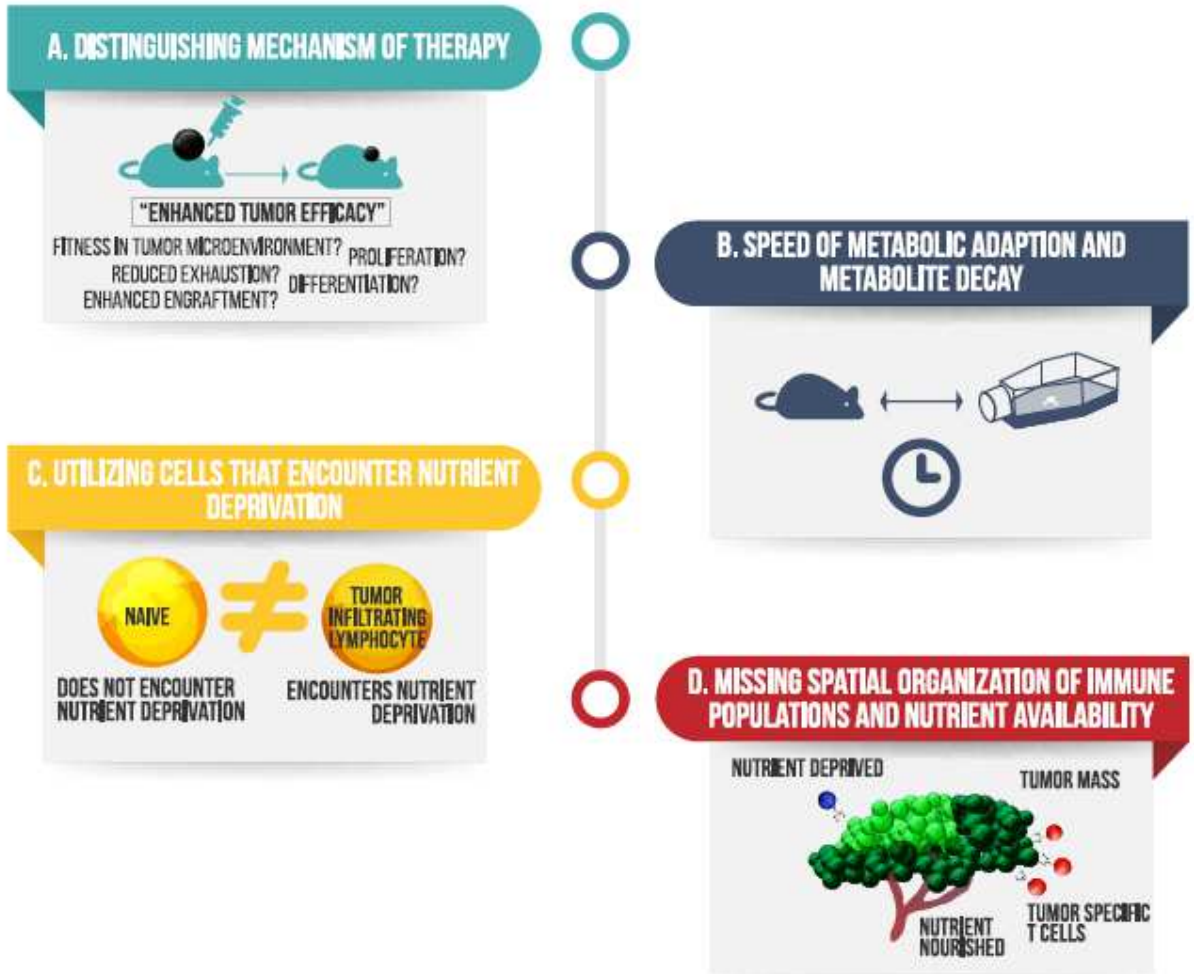
Figure 2-2

Figure 2-2: Challenges of applying immunometabolism findings to tumor models *in vivo*.

A. Many researchers have found ways to improve anti-tumor efficacy of adoptively transferred T cells through metabolic manipulation or genetic engineering. Too often though we lack the resolution to distinguish the mechanism by which enhanced tumor efficacy is reached. **B.** The speed by which cells metabolically adapt to changes in the extracellular environment during extraction procedures, and how quickly some metabolites can decay or be lost in commonly used isolation techniques hinder our understanding of *in vivo* biology. **C.** The most accessible cells in the blood or spleen (that are commonly used in metabolic studies of nutrient limitation) do not reflect the metabolic traits or adaptive properties of terminally differentiated cells found in most tumors. **D.** The field has not explored the spatial organization of nutrient depletion and immune cell infiltration in solid tumors.

Chapter 3-Differential reliance on lipid metabolism as a salvage pathway underlies functional differences of T cell subsets in nutrient poor environments.

Parts of this chapter were previously published in:

Christopher Ecker, Lili Guo, Stefana Voicu, Luis Gil-de-Gómez, Andrew Medvec, Luis Cortina, Jackie Pajda, Melanie Andolina, Maria Torres-Castillo, Jennifer Donato, Sarya Mansour, Evan R. Zynda, Angel Varela-Rohena, Ian Blair, James Riley. Differential reliance on lipid metabolism as a salvage pathway underlies functional differences of T cell subsets in poor nutrient environments. Cell Reports. 2018.

Andrew Medvec, **Christopher Ecker**, Hong Kong, Emily Winters, Joshua Glover, Angel Varela-Rohena, James Riley. Improved Expansion and In Vivo Function of Patient T Cells by a Serum-Free Medium. Mol Ther Methods Clin Dev. 2017.

Introduction

T cell responses against tumor are often blunted by the recruitment of suppressive immune cells, immune checkpoint blockade, exhaustion, and competition for vital nutrients (Chang et al., 2015a; Dunn et al., 2002; Jacobs et al., 2008; Moon et al., 2014; Sukumar et al., 2015). Both tumor cells and activated effector T cells rely heavily on glycolysis, and recent work has demonstrated that tumor cells are able to outcompete T cells for scarce glucose (Chang et al., 2015b; Ho et al., 2015a). The most

well-characterized defect in effector response due to poor glucose availability is the pronounced reduction in IFNγ production following activation of T cells (Cham and Gajewski, 2005; Chang et al., 2013; Siska et al., 2016).   Two mechanisms behind glucose-mediated IFNγ down-regulation have been proposed including: 1) GAPDH, when not involved in glycolysis, binds to the 3' UTR of IFNγ and prevents IFNγ RNA from being translated (Chang et al., 2013); and 2) the steady state levels of cytosolic acetyl-CoA is reduced in limiting glucose, reducing histone acetylation at sensitive sites like the IFNγ locus and thus lowering production of IFNγ (Peng et al., 2016). However, it is unclear whether either of these two mechanisms is operative, and equally active, in all T cell subsets.

Most data studying T cell responses in the presence of limiting glucose have used cells which are largely naïve (T_N) cells rather than human effector memory (T_{EM}) cells which are the population enriched in the tumor microenvironment (Beura et al., 2016). T cell subsets have remarkably different proliferative capacities, trafficking patterns, and effector capabilities (Sallusto et al., 1999). T_{EM} cells are defined by the lack of lymphatic homing markers such as CCR7 and CD62-L and loss of the co-stimulatory molecule CD27. T_{EM} cells do not proliferate well relative to naïve or central memory T cells (T_{CM}) but have enhanced effector functions such as cytotoxic potential and effector cytokine production.

Few studies have examined the metabolism of human T_{EM} cells because they are difficult to culture and scarce in the peripheral blood of healthy donors. The studies

that have been performed have demonstrated that T_{EM} cells in hypoxia have a survival advantage and are uniquely adapted to produce IFNγ rapidly (Dimeloe et al., 2016b; Gubser et al., 2013; Xu et al., 2016).   Human T_{EM} cells are the most common T cell to reside in the tumor microenvironment and other inflamed environments (Farber et al., 2014; Pagès et al., 2005; Thome et al., 2014). Inflammation often disrupts the vasculature and can induce hypoxia and deprive cells of valuable nutrients in the inflamed tissue (Eltzschig and Carmeliet, 2011). Thus, T_{EM} cells are often forced to function in environments that are nutrient deprived. We hypothesized that because T_{EM} cells must function in nutrient deprived environments, they may have unique metabolic mechanisms to adapt compared to T_N or T_{CM} cells. Recent work has shown that fatty acid oxidation and synthesis is essential for survival, growth, and metastatic expansion of pancreatic cancer and other cancer cells *in vivo* (Ricciardi et al., 2015; Samudio et al., 2010; Svensson et al., 2016). We speculated that if pancreatic cancer cells became reliant on fatty acids, T cells found in the same limited nutrient environment might rely on a similar metabolism.

Here we demonstrate like many cancer cells, when T_N and T_{CM} cells are starved of glucose, they augment fatty acid metabolism which drives oxidative phosphorylation and allows these two T cell subsets to survive in limited glucose. This increased reliance on fatty acid oxidation and synthesis correlated with reduced IFNγ expression upon T cell activation. In contrast, T_{EM} cells did not upregulate fatty acid synthesis and could maintain high levels of IFNγ production in low glucose upon T cell activation. Together,

these data suggest that T_{EM} cells are programmed to have limited ability to synthesize and metabolize fatty acids and as a result T_{EM} cells maintain functionality in limiting glucose conditions.

Results

Generation of a chemically-defined, customizable medium that can expand human T cell subsets in the absence of serum

To date, studies that have examined the effects of nutrient availability on T cell function *in vitro* have relied on media supplemented with dialyzed serum (Blagih et al., 2015; Chang et al., 2013; Keppel et al., 2015).   Serum is ill-defined, making characterization of key nutrients challenging. Moreover, dialysis of serum is nonspecific. To overcome these limitations, we sought to create a chemically-defined medium that could expand all human T cell subsets without supplementation of human serum. Three different basal media that contained selected groups of components, including fatty acids, metal elements, polyamines, and antioxidants were generated for the study. These media were used alone or mixed at different ratios to generate ten media for the Design of Experiments (DOE) screen (**Fig 3-1 A, Table 3-1 A)**. T cells from seven healthy donors were activated with anti-CD3/CD28 coated beads and their expansion rates were monitored in each of the ten media (**Fig 3-1 B**). Statistical analysis, harmonization to eliminate components of xenogeneic origin, and rational approaches based on spent media samples were used to further optimize the media (**Fig 3-1 C, D, Table 3-1 B, C**). Lastly, using a range of concentrations of glucose, galactose, and lipids, the carbon

source supplied to the T cells was optimized (**Fig. 3-1 E, Table 3-2**) and compared to that of medium actively being used in clinical trials of adoptive T cell therapy, X-VIVO 15™ media supplemented with 5% human serum.

There is no consensus on what is the best media to use for adoptive T cell therapy; however, most groups to date have used RPMI 1640, AIM V, or X-VIVO 15 media (Cruz et al., 2013; Lee et al., 2015; Maude et al., 2015). Both AIM V and X-VIVO 15 are defined as serum-free media, but in the T cell manufacturing process used to treat patients, human serum is universally added, largely because patient-derived T cells fail to grow optimally in serum-free media and exhibit reduced efficacies of gene transfer resulting from less than optimal T cell activation. We decided to examine which medias could maximally expand human T cells in the absence of human serum. As expected, RPMI 1640 required the addition of human serum to promote T cell expansion (**Fig 3-2 A**). T cells expanded in AIM V grew as well as T cells expanded with AIM V supplemented with human serum for 5 days. However, after 5 days, AIM V SFM could not support further T cell expansion (**Fig 3-2 B**). In contrast, both X-VIVO 15 and 1B2H supported T cell expansion nearly equivalently in the presence and absence of serum, although it is important to note that T cells expanded in the absence of serum rested more quickly than T cells expanded in the presence of serum. (**Fig 3-2 C, D**). Thus, both X-VIVO 15 and 1B2H fulfill the requirement of being a bona fide serum-free medium: similar expansion in the presence and absence of human serum.

An *in vivo* model of CAR T cell therapy was developed, which has proven

informative for predicting clinical results in humans (Grupp et al., 2013; Kalos et al.,

2011; Porter et al., 2011). In this model, NALM6, a pre-B cell leukemic cell line that

naturally expresses CD19, was engineered to express luciferase and engrafted into

NOD/SCID-$\gamma c^{-/-}$ (NSG) mice. If CD19-specific CAR T cells are added within a week, tumor

clearance is observed within 10–14 days. However, if the experiment is extended,

leukemia returns in most animals and durable cures are not observed. We sought to

determine whether T cells expanded in 1B2H could perform *in vivo* as well as T cells

expanded using X-VIVO 15 supplemented with 5% human serum—the current medium

formulation our group uses for good manufacturing practice (GMP) manufacturing of

T cells. Consistent with previous findings, we observed that CD19-specific CAR T cells

expanded in X-VIVO 15 supplemented with 5% human serum dramatically cleared

tumors from NSG mice 13 days after the infusion of T cells (**Fig 3-3 A**) (Milone et al.,

2009). However, as previously demonstrated, this control was transient, with tumor

returning to most of the mice. Surprisingly, CD19-specific CAR T cells expanded in 1B2H

SFM could provide durable control of tumors and this translated to a remarkable

difference in leukemia-free survival (**Fig 3-3 B**). Interestingly, mice treated with CAR

T cells expanded with 1B2H supplemented with 5% human serum could only transiently

control tumor burden similarly to mice treated with CAR T cells expanded in X-VIVO 15

supplemented with 5% human serum, suggesting that expanding T cells in the presence

of serum is detrimental to *in vivo* performance of engineered T cells. Both humanized

mouse studies and clinical data from patients have shown a strong correlation with the level of T cell persistence after adoptive transfer and the ability to provide durable control of tumors (Maude et al., 2014; Milone et al., 2009). Likewise, we observed superior T cell engraftment that was sustained for much longer in cells expanded in the absence of serum (**Fig 3-3 C, D**). Together, these data suggest that human serum is not only dispensable, but is also hindering the ability of CAR T cells to function, persist, and control tumor growth.

Traditionally most CAR studies have focused on ex vivo transduction and expansion and subsequent autologous transfer of a patient's own cells, which are highly differentiated and poorly proliferative compared to a healthy donor's T cells. Thus we examined the functional properties of the multiple myeloma patient T cells expanded in X-VIVO 15 or 1B2H, with and without serum. Here, the addition of serum did not significantly alter the functional profile of the expanded CD19-specific CAR T cells because there were no consistent differences between T cells grown in 1B2H or X-VIVO 15 (**Fig 3-4 A, B**), suggesting the functional abilities of fully differentiated T cells are not modulated by the presence of human serum or media in which they are expanded. We then addressed the ability of these expanded T cells to control NALM6 tumors *in vivo*. As a control, we also expanded CD19-specific T cells from a healthy individual so we could compare *in vivo* function of T cells from healthy donors and multiple myeloma patients. All T cell populations showed transient control of NALM6 tumors; however, 2 of the 6 mice that were treated with T cells expanded by X-VIVO 15 SFM still had significant

tumor burden after 12 days of treatment (**Fig 3-4 C**) and none of these mice durably

controlled tumor growth (**Fig 3-4 D**). As before, the leukemia relapsed in most mice

treated with CD19-specific T cells expanded in either 1B2H or X-VIVO 15 supplemented

with human serum. Impressively, T cells isolated from multiple myeloma patients

engineered to be CD19 specific and expanded in 1B2H SFM provided durable control of

tumor in all mice treated and had equivalent therapeutic potency as similarly

engineered and expanded T cells isolated from a healthy donor.

While physiological glucose concentration in human blood is around 5mM, we

found that the static optimal glucose concentration that allowed maximal T cell

expansion and maintained high glucose concentrations throughout culture conditions is

35mM (**Table 3-2**). To ensure that our medium, called 1B2H, could be customized to

study T cell metabolism, we generated 1B2H variants that were glucose or glutamine

free. We found that T cells could not divide in media free of glucose or glutamine,

demonstrating that our media contained no nutrients that could substitute for either

glucose or glutamine (**Fig 3-5 B**). To examine how well human T cell subsets grew in our

created medium in the absence of serum, we sorted T_N, T_{CM} and T_{EM} CD4 T cells and

compared expansion in our created medium (1B2H) supplemented with or without

human serum. We found that all subsets could grow equally well in 1B2H medium with

or without serum supplementation (**Fig. 3-5 C-E**), and this level of T cell expansion is

consistent with serum supplemented commercial media that is currently being used for

adoptive T cell therapy (Medvec et al., 2018). Thus, 1B2H is a bona fide serum-free,

medium that can facilitate the study of metabolic differences between human T cell subsets. We were able to utilize our collaboration with Thermofisher Scientific to further customize this defined media to add and withdraw specific nutrient components specifically, without the need for dialysis.

Effector Memory T cells are resistant to glucose-mediated IFNγ suppression

We next examined how low glucose altered human T cell subsets' ability to expand, adapt functionally, and differentiate.   We sorted T_N, T_{CM}, and T_{EM} (**Fig 3-6 A-I**) and stimulated them with anti-CD3/CD28 coated beads in the presence of optimal glucose (35mM) or low glucose (0.35mM).   As expected, all T cell subsets have substantially reduced growth in low glucose (**Fig 3-7 A**).   We next examined the ability of freshly sorted human T cell subsets to produce IFNγ in the presence of optimal or low glucose after PMA/ionomycin stimulation. T_N and T_{CM} cells made less IFNγ in low glucose, consistent with previous reports (Cham and Gajewski, 2005; Chang et al., 2013; Chang et al., 2015b; Ho et al., 2015a).   However, T_{EM} cells made equivalent levels of IFNγ (**Fig 3-7 B, E**), suggesting that the effector functions of T_{EM} cells are not compromised in poor nutrient environments. Interestingly IL-2 and TNFα (**Fig 3-7 B,C, Fig. 3-8 A-F**) are not affected by glucose availability. Therefore, we expanded T cells from **Fig 3-7B** for 10-12 days and determined their ability to make IFNγ and IL-2 upon re-stimulation. We observed expanded T_N cells still have a profound defect in their ability to produce IFNγ in low glucose, whereas both expanded T_{CM} and T_{EM} cells produced equivalent IFNγ after being expanded in both optimal and low glucose (**Fig 3-7 C, F**). The

36

ability of expanded but not freshly isolated T_{CM} cells to make high levels of IFNγ in the presence of optimal or low glucose is likely tied to their more differentiated phenotype after expansion **(Fig 3-7 D, G, H)**. Furthermore, we found that while all cells up-regulate CD25, the IL-2 receptor, following anti-CD3/CD28 bead activation in both optimal and low glucose, T_N and T_{CM} cells lost CD25 expression quickly following activation in low glucose whereas T_{EM} cells were able to maintain heightened CD25 expression in limiting glucose (**Fig 3-9 A-D**), suggesting that they can maintain an activated phenotype in poor nutrient conditions. Cumulatively these data show that T_{EM} cells maintain function in low glucose whereas T_N and T_{CM} make less IFNγ and lose CD25 expression.

Effector memory T cells do not augment oxidative phosphorylation in low glucose

Past studies have linked T cell metabolism to IFNγ production (Cham and Gajewski, 2005; Chang et al., 2013; Ho et al., 2015a). To better understand the relationship between T cell metabolism and function, we performed metabolic assays on activated human T cells cultured in media with 35mM, 3.5mM, 0.35mM or no glucose. In agreement with previous studies, we found that T cells cultured in lower amounts of glucose had reduced glycolysis as measured by extracellular acidification rate (ECAR) and compensated for this loss in glycolysis by up regulating oxidative phosphorylation measured by oxygen consumption rate (OCR, **Fig 3-10 A, B**). Previous reports have demonstrated the importance of fatty acid oxidation in T cells to their ability to utilize and upregulate their OCR (O'Sullivan et al., 2014; van der Windt et al., 2012). We also found that OCR increases were dependent upon fatty acid oxidation as

the increase in OCR in limiting glucose was blocked by etomoxir, a drug that blocks fatty

acid intake into the mitochondria by inhibiting carnitine palmitoyltransferase (**Fig 3-10**

D). However, etomoxir treatment did not significantly alter ECAR, intracellular lactate or

extracellular lactate production (**Fig 3-10 C, G, H**). T_N and T_{CM} cells behave in a similar

fashion to total T cells by exhibiting reduced glycolysis and augmented OCR when

cultured in low glucose (**Fig 3-10 E, F)**. Furthermore, etomoxir inhibited the OCR of all T

cell subsets only in low glucose, without altering their glycolytic rate (**Fig 3-10 I-N)**.

These data show that effector memory T cells metabolically respond to low glucose

distinctly from other T cell subsets by not augmenting oxidative metabolism.

Effector memory T cells contain fewer lipid droplets than other T cell subsets in optimal

glucose

Because T_N and T_{CM}, but not T_{EM} could compensate for low glucose by

augmenting oxidative phosphorylation in a fatty acid dependent manner, we wanted to

examine the supply of lipids stored within the cell. Lipid droplets are dynamic

organelles that play a key role in the regulation of lipid metabolism and serve as a ready

to use source of lipids (Barneda and Christian, 2017). We first isolated total CD4 T cells

and examined the number of lipid droplets in resting and activated cells in both optimal

and low glucose. T cell activation was required for the formation of lipid droplets as we

did not observe lipid droplets in resting T cells. Moreover, we found that activated CD4 T

cells grown in optimal glucose had dramatically more lipid droplets per cell than cells

activated in low glucose (**Fig 3-11 A, F**). We hypothesized that T cells expanded in low

38

glucose could not store lipid droplets, because they were using lipids as fuel for oxidative phosphorylation. To determine whether lipids were being consumed in T cells when cultured in low glucose, we first activated T cells in optimal glucose for 48 hours, and then placed them in low glucose for an additional 0, 4, 8, 24, or 48 hours. We further quantified lipid droplets by staining cells with the lipophilic dye bodipy 493/503 which is commonly used to mark neutral lipids (Singh et al., 2009).   Significant decreases in bodipy florescence of stained lipid droplets were observed after placing cells in low glucose for greater than 24 hours, indicating that T cells consume lipid droplets when placed in nutrient poor conditions (**Fig 3-11 B, Fig 3-12 A)**. After 6 days of culture, we observed significant number of autophagosomes (**Fig 3-12 B)**. Under normal conditions autophagic protein microtubule-associated protein 1 light chain-3B (LC3B) consists largely of its cytoplasmic form LC3B-1. However during autophagy, LC3B becomes conjugated to phosphatidylethanolamine forming LC3B-II and is recruited to the membrane of autophagosomes (He et al., 2003). We found that T cells cultured in optimal glucose maintained higher levels of LC3B-I compared to LC3B-II whereas T cells cultured in low glucose had much more LC3B-II than LC3B-I (**Fig 3-11 C-E, Fig 3-12 D-E)**, confirming that T cells were performing autophagy in response to low glucose.

Previous studies have implicated autophagy in fatty acid consumption (Liu and Czaja, 2013; Singh et al., 2009). We found that T cells were unable to consume their lipid droplets in low glucose when treated with an autophagy inhibitor, Lys05 (**Fig 3-12 C)**. To further investigate whether autophagy was responsible for the breakdown of

lipid droplets, we transduced T cells with a lentiviral vector expressing LC3B fused to mCherry, a pH insensitive fluorescent reporter. We found that lipid droplets marked by bodipy 493/503 often co-localized with the autophagosomes (**Fig 3-11 D**), suggesting that autophagy was responsible for lipid droplet breakdown and consumption. Furthermore, we found that inhibiting mTORC1 via rapamycin, a well-known method of inducing autophagy, increased T cell growth in low glucose but not in optimal glucose. We found that the enhanced growth by rapamycin was blocked when co-administering Lys05, while expansion was not significantly inhibited by Lys05 alone in low glucose (**Fig 3-12 F-H**). These data support the idea that promoting autophagy can increase T cell expansion in low glucose possibly by increasing lipid consumption. Next, we isolated T cell subsets to examine if T_{EM} cells may fail to up-regulate oxidative phosphorylation because they cannot uptake lipids and store them as well as T_N or T_{CM} cells. We observed T_N and T_{CM} cells cultured in optimal glucose had significantly higher amounts of lipid droplets per cell per micrograph than T_{EM} cells (**Fig 3-11 E, G**). These data demonstrate that T_{EM} cells acquire fewer lipid droplets in optimal glucose, suggesting that lipids may not be the preferred alternative fuel for T_{EM}.

Effector memory T cells are unable to perform reductive glutaminolysis for fatty acid synthesis when cultured in low glucose

Next, we wished to examine whether other salvage pathways were differentially regulated in T cell subsets in response to low glucose. An increased consumption of glutamine has been shown to be a salvage pathway to drive T cell metabolism in low

glucose (Blagih et al., 2015). We quantified the rates of consumption/production of glucose, amino acids and a few organic acids in the supernatant of activated T cells (**Table 3-3 A, B**). As expected, T cells primarily consumed glucose and glutamine. Additionally, we observed high consumption of serine, supporting recent findings that serine is essential for *de novo* nucleotide biosynthesis (Ma et al., 2017a). T cells in low glucose regardless of subset, consumed fewer amino acids, likely due to overall reduced level of T cell activation. Interestingly glutamine was equally consumed by T cells at optimal or low glucose; thus, relative to other amino acids, glutamine was preferentially consumed by T cells cultured in low glucose. Surprisingly, TCA cycle intermediates demonstrated different patterns of abundance, suggesting complex regulation of the TCA under nutrient stress (**Fig 3-13 A-G)**. To examine how glutamine was utilized, we cultured T cells in the presence of labeled glutamine and examined how it was metabolized within the cell. The differential labeling of citrate can be used to interpret glutamine metabolic pathways (**Fig 3-14 A**) (Fendt et al., 2013; Metallo et al., 2011). A citrate with 4 heavy carbons (marked mass +4 or M+4) suggested typical oxidative glutaminolysis, where glutamine is incorporated into the TCA cycle and then spread across other TCA cycle intermediates. We found that T cells cultured in low glucose had less labeled M+4 citrate and this was observed in all T cell subsets examined (**Fig 3-14 B**). To extend this finding, we examined other TCA intermediates and found equivalent levels of M+4 labeling, suggesting that oxidative glutaminolysis functions similarly in all T cell subsets in both optimal and low glucose (**Fig 3-14 E-G**).

A citrate with 5 heavy carbons suggests reductive glutaminolysis where glutamine is being routed into fatty acid synthesis (**Fig 3-14 B**). We found that T_N and T_{CM} cells had higher relative amounts of citrate M+5 when cultured in low glucose, suggesting that some of the glutamine imported into T cells was being converted to fatty acids (**Fig 3-14 A**). T_{EM} cells, on the other hand, did not to appear to upregulate fatty acid synthesis in the presence of low glucose since the relative percentage M+5 was the same regardless of the T cells being cultured in optimal or low glucose. To confirm this, we examined both M+2 and M+4 palmitate which would directly show glutamine being converted to fatty acids. Interestingly, we observed that T_N and T_{CM} cells expanded in optimal glucose had higher levels of M+2 palmitate than their respective groups grown in low glucose, but higher M+4 palmitate (**Fig 3-14 H-J**). In contrast, T_{EM} cells have low levels of M+2 palmitate when cultured in both optimal and low glucose, suggesting that very little glutamine gets converted to fatty acids in T_{EM} regardless of the glucose levels present. These data indicate that reductive glutaminolysis is occurring at a higher rate in T_N and T_{CM} cells cultured in low glucose. Only small amounts of M+4 palmitate was detected in T_{EM} cells further confirming very little glutamine is converted to fatty acids in T_{EM} regardless of the glucose levels present.

A citrate with 6 heavy carbons suggests that some fraction of glutamine is being converted into pyruvate and this pyruvate is then being used to generate citrate (**Fig 3-14 A**). We found that all T cell subsets expanded in low glucose had higher levels of citrate M+6, indicating that the differential use of glutamine by T_{EM} cells is confined to

reductive glutaminolysis (**Fig 3-14 D**).   Interestingly, all T cells subsets redirect glutamine

into production of pyruvate by having increased M+3 labeling of pyruvate, making an

estimated 20% of the intracellular pool in low glucose (**Fig 3-14 K**). Additionally, ~10% of

the intracellular pool of lactate is made from glutamine, suggesting that this glutamine-

derived pyruvate is converted into lactate (**Fig 3-14 L**). We found that all subsets when

cultured in optimal glucose secreted approximately 1.5 moles of lactate per mole of

glucose consumed, consistent with previous reports showing that most of the glucose

utilized is converted into lactate (Frauwirth et al., 2002). However, when T cells were

cultured in low glucose, we found that lactate/glucose ratios exceeded 2, suggesting

that a carbon source other than glucose was being used to produce lactate (**Fig 3-14 M**).

Together, T cells appear to be adept at using glutamine to fulfill a diverse array of

metabolic needs when glucose is limiting with the notable exception that T_{EM} cells are

unable to use glutamine to produce fatty acids.

Effector memory T cells are less reliant on fatty acid metabolism for survival and

expansion at low glucose

With evidence of fatty acid droplets being consumed in low glucose and data

demonstrating that glutamine was being redirected into fatty acid synthesis by T_N and

T_{CM} cells, we sought to explore the importance of fatty acid metabolism for the survival

and expansion of T cells in low glucose.   We treated activated T cells in optimal or low

glucose with 5-(Tetradecyloxy)-2-furoic acid (TOFA), an inhibitor of fatty acid synthesis,

or vehicle (DMSO). We saw little to no effect of TOFA on T cell expansion in optimal

glucose and significant inhibition of T cell expansion in low glucose (**Fig 3-15 A, B**). We

further examined how TOFA affected the expansion of T cell subsets grown in low

glucose. T_N and T_{CM} cells behaved in a similar manner to total T cells and suffered

severe proliferative defects when cultured in low glucose (**Fig 3-15 C**). In contrast,

expansion of T_{EM} cells was only marginally affected by TOFA in both optimal and low

glucose. However, T cells can also uptake fatty acids from exogenous sources

(O'Sullivan et al., 2014). We quantified surface expression of CD36, a scavenger

receptor that is thought to be important for uptake of long-chain fatty acids (Glatz and

Luiken, 2016; Schwenk et al., 2010). We observed that T_N and T_{CM} cells could up-

regulate CD36 when grown in low glucose, while T_{EM} cells did not (**Fig 3-15 D-E**).

Together these data suggest that T_{EM} cells are not as reliant as T_N or T_{CM} cells on fatty

acid synthesis or uptake of exogenous fatty acids to expand in limiting glucose.

To further characterize which T cell subsets, if any, are dependent on exogenous

fatty acids we prepared fully defined, serum free media that lacked all species of lipids

(Fat-Free). Despite an early defect in proliferation, we found that total T cells in optimal

glucose in the absence of lipids expanded nearly as well as T cells in the presence of

lipids (**Fig 3-15 F**). However, in low glucose, the lack of fatty acids severely impaired T

cell expansion. This pattern remained consistent in T_N and T_{CM} cells, their expansion was

severely inhibited in fat free media when grown in low glucose (**Fig 3-15 G**).

Surprisingly, T_{EM} cells grew equally well in the presence and absence of lipids in low

glucose. Next, we wanted to quantify how much different T cell subsets incorporated

exogenous lipids into the TCA cycle. In agreement with our data in **Figure 2**, we found

that all subsets equally increased their incorporation of exogenous fats into acetyl CoA

(**Fig 3-15 H**). We examined the viability of T cells and observed that most of the T_N and

T_{CM} cells were dead in low glucose, fat-free media whereas T_{EM} cells had near equivalent

viability in the presence and absence of lipids (**Fig 3-15 I-J**). Cumulatively, these results

show that T_{EM} cells are not as reliant as T_N or T_{CM} cells on lipid metabolism to expand or

survive in low glucose.

Impairment of fatty acid synthesis in naïve T cells augments IFNγ expression

Our data demonstrate a strong correlation between a T cell subset's ability to

utilize fatty acids and subsequent ability to produce IFNγ in limiting glucose. To

determine whether there is a relationship between IFNγ expression and fatty acid

metabolism, we first asked whether a reduction in fatty acid synthesis would augment

IFNγ production. To do this, we used a dose of TOFA (5µM) that permits T_N cells to

survive in low glucose and then examined their ability to make IFNγ. Blocking fatty acid

synthesis in T_N cells significantly increased their ability to make IFNγ (**Fig 3-16 A,B**). This

did not however impact T_{EM} cells ability to produce IFNγ, further confirming the notion

that T_{EM} cells are not actively synthesizing fatty acids and thus are insensitive to TOFA.

Interestingly, blocking fatty acid synthesis did not impact the production of other

cytokines such as IL-2 in any of the subsets (**Fig 3-16 C**), suggesting that IFNγ is

specifically targeted by fatty acid metabolism. Furthermore, TOFA did not alter IFNγ or

IL-2 production in T_N cells or any other subset in optimal glucose (**Fig 3-17 A, B**). This is

consistent with our mass spectrometry data, suggesting that T cells activated in optimal glucose do not utilize fatty acid synthesis to a significant extent.

Next, we sought to determine whether increasing the concentration of exogenous lipids in the media would cause decreased production of IFNγ by T cells. To do this, we added a defined minimal lipid concentration that permitted T cell expansion in low glucose to our lipid-free media. To investigate how individual subsets reacted to the presence of exogenous lipids, we added increasing doses of exogenous lipids to sorted subsets and examined IFNγ and IL-2 production. We found that in minimal lipids, IFNγ production by all subsets was higher than that of cells in normal amounts of lipids (1x) in low glucose (**Fig 3-16 D, E**). Furthermore, we found that as we increased lipid concentration, IFNγ production further decreased in all subsets. Moreover, the addition of exogenous lipids caused decreases in not only IFNγ but also IL-2 in T_N and T_{CM} cells but not T_{EM} cells (**Fig 3-16 C-F)**, further highlighting T_{EM} cells' relative resistance to modulate their effector functions due to fatty metabolism. Together, these data demonstrate that lipid metabolism regulates IFNγ production.

Decreased mitochondrial mass in lung T cells in non-small cell lung cancer patients

In recent months we have asked how our new data on effector memory T cell metabolism may apply to tumor infiltrating lymphocyte (TIL) metabolism. Through a collaboration with Steve Albelda's group, we have been able to receive human samples from non-small cell lung cancer (NSCLC) patients . We are able to isolate CD4 and CD8 T

cells from the blood, adjacent lung tissue , and tumor tissue within the lung. Recent

work has demonstrated that TILs (which are mostly terminally differentiated cells with

similar phenotype to effector memory T cells) have lower mitochondrial mass compared

to T cells in the blood, spleen or lymph node (Scharping et al., 2016). Furthermore the

remaining mitochondria are often dysfunctional and hyperpolarized due to chronic

antigen exposure and tumor-intrinsic singals (Bengsch et al., 2016; Siska et al., 2017b).

Because our data suggests T cells may utilize mitochondrial-related pathways during

glucose deprivation in the tumor microenvironment, we examined the mitochondrial

mass of T cells from NSCLC patient blood, adjacent lung tissue, and tumor tissue. In

agreement with earlier findings, we find that CD8+ T cells (and to some extent CD4+ T

cells) have a severe defect in mitochondrial mass in the tumor compared to T cells from

the peripheral blood (**Fig 3-18 A-D)**.   Surprisingly though we found this mitochondrial

mass defect affected the adjacent lung, and not only the T cells present within the

tumor. Furthermore, differentiation was not significantly responsible for these

mitochondrial mass differences **(Fig 3-18 E)**. This data may suggest that there are tissue-

specific signals and not tumor-specific signals that alter mitochondrial mass.

Furthermore, we are currently working to examine how decreased mitochondrial mass

impact TIL reliance on mitochondrial pathways during glucose limitation.

Discussion

Over the past few years, it has become increasingly clear that T cell metabolism plays a crucial role in driving T cell differentiation and function (Pollizzi and Powell, 2014). Our studies uncovered that T cell subsets respond distinctly to the same metabolic stress. In response to low glucose, T_N and T_{CM} cells increase oxidative phosphorylation, rely on fatty acid metabolism, increase autophagy, and redirect glutamine into pathways that produce both fatty acids and pyruvate. We show that unlike T_N or T_{CM} cells, T_{EM} cells do not rely on fatty acid synthesis or increase oxidative phosphorylation in low glucose. We further demonstrate that by being less reliant on fatty acid pathways T_{EM} cells can maintain functionality during nutrient stress (**Fig 3-19 A,B**).

Our studies suggest that the relative ratio of glycolysis to fatty acid metabolism within a single effector T cell determines its functional capabilities. By limiting fatty acid metabolism in T_N, we could significantly augment their IFNγ production. Conversely, by culturing T_{EM} in high levels of lipids, we selectively decreased their ability to make IFNγ. Thus, our studies show a strong link between active fatty acid metabolism and the ability to make IFNγ, adding to a number of mechanisms a T cell employs to regulate IFNγ production (Chang et al., 2013; Peng et al., 2016; Siska and Rathmell, 2016). There are many challenges associated with translating *in vitro* findings on T cell metabolism to *in vivo* models (Ecker and Riley, Submitted). Simple adoptive transfer studies favor less differentiated T cell due to their ability to expand and differentiate into effector

memory T cells (Gattinoni et al., 2011). Models in which the metabolic milieu and the number infiltrating T lymphocytes can be carefully controlled and monitored will be necessary to confirm our findings *in vivo*. To date, the best in vivo data supporting our in vitro studies comes from studies that correlate the number of T_{EM} within the tumor microenvironment with patient survival (Farber et al., 2014; Pagès et al., 2005; Thome et al., 2014).

Immune cells are one of the few groups of cells in the body that must travel to a wide-spectrum of environments. These environments have a diverse array of metabolic requirements and immune cells must be able to function in all of them. Our work and others demonstrate that T cells can downregulate activation, proliferation, and transcription to lower energy consumption, while relying on salvage pathways to utilize diverse fuel sources (Blagih et al., 2015). Previous work has demonstrated that glucose is not only essential for generating energy quickly through glycolysis but glycolytic intermediates are necessary for effective T cell activation and proliferation (Ho et al., 2015a). Thus, these salvage pathways do not simply need to meet the energy demands for the cell when traditional nutrients are scarce, but need to supply the building blocks to generate proteins, fatty acids and nucleic acids required for T cell expansion and differentiation (Pearce and Pearce, 2013). Our data that glutamine can be shunted into all metabolic pathways examined in glucose limiting conditions, driving increased oxidative phosphorylation and increased biosynthetic production of fatty acids and pyruvate, demonstrates how different carbon sources could be utilized in nutrient poor

conditions. Increased oxidative phosphorylation in limiting glucose likely amplified the need for fatty acid oxidation and exogenous fatty. The incredible flexibility of T cells to manufacture the building blocks of many synthetic pathways underlies their ability to function throughout the body. Our studies highlight how the salvage pathways that T cells choose to alter their eventual functionality. Understanding the metabolic demands of T cell subsets and how to modulate traditional and salvage metabolic pathways may yield more effective cellular therapies for cancer and other diseases.

Materials and Methods

Study Design

The purpose of this study was to characterize human T cell subsets and identify metabolic and functional outcomes when grown in sufficient and deficient conditions. The number of replicates per experiment are indicated in the figure legends and performed in a controlled and non-blinded manner.

Immune Cell Purification and Sorting

De-identified human CD4 T cells were obtained from the Human Immunology Core at the University of Pennsylvania under an IRB approved protocol and stained using antibodies for CD4 (BD Pharmingen, 562424), CD45RA (BD Pharmingen, 337167), CD25 (BD Pharmingen, 557138), CCR7 (Biolegend, 353218) and CD27 (Biolegend, 353218). Naïve (N, CD45RA$^+$, CCR7$^+$, CD27$^+$, CD25$^-$), central memory (CM, CD45RA$^-$, CCR7$^+$, CD27$^+$, CD25$^-$) and effector memory (EM, CD45RA$^-$, CCR7$^-$, CD27$^-$, CD25$^-$) were sorted to high purity using a BD FACS AriaII.

Cell Culture and Activation

Sorted CD4 T cells were washed twice in PBS, and then placed in IB2H serum-free medium containing optimal (35mM), medium (3.5mM) or low (0.35mM) glucose concentrations.   The medium was supplemented with 1x (500uL), or 2x (1000uL) or 3x (1500uL) when indicated, of a chemically defined lipid mixture (ThermoFisher Scientific, 11905031, individual lipid concentrations available online) and 8mM L-glutamine.   Cells were then activated at 1 million cells per mL using Dynabeads® Human T-Expander CD3/CD28 (ThermoFisher Scientific, 11131D) at a concentration of 3 beads per cell. Additional volumes of medium were added on Day 3 and every day after so that each culture was at 0.5 million cells/mL after feeding. Cells were treated with TOFA (5, 10μM, Sigma Aldrich, T6575), or etomoxir (200, 400 μM Sigma Aldrich, E1905). cDNA encoding LC3B was synthesized (IDT) and transferred into pTRPE, a lentiviral transfer vector (Leibman et al, submitted). Lentiviral supernatants and T cell transduction were generated and performed as previously described (Parry et al., 2003)

Intracellular Cytokine Staining

Sorted cells were treated with 1μg of PMA (Sigma Aldrich, P1585) per mL of media, 3μg of ionomycin (Sigma Aldrich, 407950) per mL of media and GolgiStop (BD Pharmingen 554724) for 6 hours at 37°C immediately following sorting or 9-11 days post-activation after cells had rested and stopped dividing. Cells were stained with Live/dead Aqua (ThermoFisher Scientific, L34957) according to manufacturer's instructions. Cells were

washed with 1x PBS, and fixed using Fixation Medium A (ThermoFisher Scientific, GAS001S100) for 15 minutes at room temperature. Cells were then washed again with 1x PBS. Cells were then permeabilized using Permeabilization Medium B (ThermoFisher Scientific, GAS002S100) and stained with antibodies for IFNγ (eBioSciences, 45-7319-42), IL-2 (BD Pharmingen, 554567), and TNFα (BD Pharmingen 557647) for 15 minutes at room temperature. Cells were then washed 1x with PBS, and analyzed using the BD LSR II flow cytometer.

Western Blotting

Cells were lysed with 1x RIPA Buffer (Cell Signaling Technology, 9806) and 1mM PMSF (Cell Signaling Technology, 8553S) according to manufacturer's instructions. Proteins were resolved by SDS-PAGE and transferred to nitrocellulose. Blots were probed with anti-LC3B (Cell Signaling Technology, 3868) and anti-β-actin (Cell Signaling Technology, 4970). Protein was visualized using Odyssey CLx LI-COR instrument.

Confocal Microscopy

To quantify neutral lipid droplets, cells were stained with 500n/mL Bodipy 493/503 (ThermoFisher Scientific, D3922) in serum free medium at 37 degrees Celsius for 30 minutes. Cells were then washed 2x with PBS and placed in their respective media. Cells were live imaged at 37 degrees Celsius using a stage heater on the Leica TCS SP8 Confocal microscope.

Metabolite extraction, derivatization and LC-MS measurements

Cells were activated with anti CD3/CD28 beads in media supplemented with 8mM [U-^{13}C]-glutamine (Cambridge Isotope Laboratories, CNLM-1275-H-PK) for 48 hours when indicated. The isolation and LC-MS measurements of organic acids were performed as described previously with slight modification (Angelin et al., 2017; Guo et al., 2016). Briefly, cells were washed twice with PBS before extracting using 750 µL of ice-cold methanol/water (4/1 v/v). For metabolites quantification, samples were spiked with internal standards (250 ng [^{13}C$_4$]-succinate, 250 ng [^{13}C$_6$]- citrate, 250 ng [^{13}C$_3$]-pyruvate, 1 µg [^{13}C$_3$]-lactate, 25 ng [^{13}C$_4$, ^{15}N]-aspartate, 1 µg [^{13}C$_5$, ^{15}N]-glutamate and 250 ng [^{13}C$_6$]-glucose 6-phosphate). Samples were pulse-sonicated for 30 s with a probe tip sonicator and centrifuged at 16,000 g for 10 min. The supernatant was transferred to a new tube before evaporation to dryness under nitrogen. For quanitfying pyruvate, α-ketoglutarate and oxaloacetate, 1 mg phenylhydrazine was included in the 750 µL methanol/water (4/1 v/v) for metabolite extraction. Samples were suspended in 50 µL before LC-MS analysis using an Agilent 1200 series high performance liquid chromatography system coupled to an Agilent 6460 triple quadrupole mass spectrometer equipped with an electrospray ionization source. Analytes were separated by reversed-phase ion-pairing chromatography utilizing a Xselect HSS C18 column (150 × 2.1 mm, 3.5 µm, 100 Å; Waters). For samples that needed to be analyzed for the isotopic distribution of acetyl-CoA, cells were extracted using methanol/water as described above except that the samples were re-suspended in 50 µL of water with 5%

5-sulfosalicylic acid before LC-MS analysis. The quantification of acetyl-CoA was performed as described previously with slight modification (Snyder et al., 2015)). Briefly, cells were quenched with 750 µL of ice-cold 10% trichloroacetic acid (TCA) in water spiked with yeast extract labeled with $[^{13}C_3\ ^{15}N_1]$-pantothenate. Samples were pulse-sonicated for 30 s with a probe tip sonicator and centrifuged at 16,000 g for 10 min. The supernatants were loaded to Oasis HLB 1cc (30 mg) SPE columns (Waters) conditioned with 1 mL methanol. After 1 mL wash with water, the samples were eluted with 1 mL of 25 mM ammonium acetate in methanol and dried under nitrogen. The samples were re-suspended in 50 µL of water with 5% 5-sulfosalicylic acid. The acetyl-CoA was analyzed by an Ultimate 3000 autosampler coupled to a Thermo Q Exactive HF Hydro Quadrapole-Orbitrap Mass spectrometer as previously described (Frey et al., 2016). The same LC conditions and column were used as described for the organic acid analysis.

Transmission Electron Microscopy

Tissues for electron microscopic examination were fixed with 2.5% glutaraldehyde, 2.0% paraformaldehyde in 0.1M sodium cacodylate buffer, pH7.4, overnight at 4°C. After subsequent buffer washes, the samples were post-fixed in 2.0% osmium tetroxide for 1 hour at room temperature, and then washed again in buffer followed by water. After dehydration through a graded ethanol series, the tissue was infiltrated and embedded in EMbed-812 (Electron Microscopy Sciences, Fort Washington, PA). Thin sections were stained with uranyl acetate and lead citrate and examined with a JEOL 1010 electron microscope fitted with a Hamamatsu digital camera and AMT Advantage image capture

software. To quantify lipid droplets, 30-40 cells per sample group were examined in two

separate experiments and lipid droplets were counted by eye.

Seahorse XF Assay

OCR and ECAR were measured using a 96-well XF extracellular flux analyzer (Seahorse

Bioscience). 250k cells per well at 48 hours post-activation in optimal or low glucose

IB2H medium , washed with PBS, and transferred to warm, optimal or low glucose

supplemented, XF Seahorse medium.

NSCLC T cell Isolation

PBMC and TIL were isolated from NSCLC patients and extracted as described (Huang et al.,

2017).

Statistics

Statistical analysis was performed using a 2-tailed Student's t-test or Mann-Whitney test

after the analysis of distribution of variables. In the case of multiple comparisons, one-

way ANOVA followed by Tukey LSD was performed. Significance determined at $p < 0.05$,

and error bars indicating mean plus or minus SEM. All calculations were made using

GraphPad Prism 5 software (GraphPad Software Inc.) or Microsoft Excel.
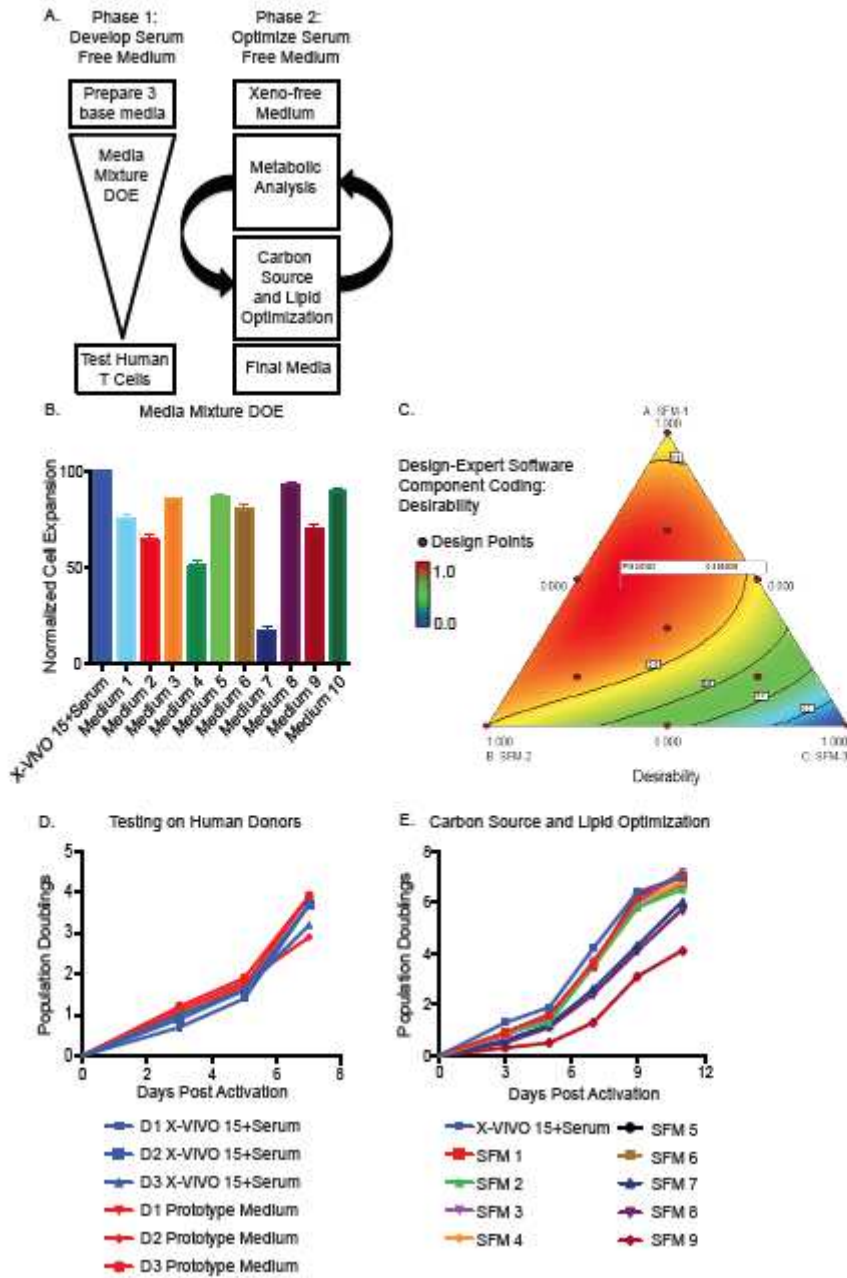
Figures

Figure 3-1

Figure 3-1: Development and testing of IB2H media.

A. The first phase of generating a serum free medium that can expand all human T cell subsets, consisted of creating 10 prototype media by mixing different ratios of 3 base media that contain different concentrations of amino acids, vitamins, trace elements, antioxidants, metal ions, polyamines, and lipids. These prototype media were tested for their ability to expand activated primary human T cells using anti-CD3/CD28 coated beads and reiterated with a Design of Experiments (DOE) statistical quadratic model through Design-Expert® 9.0.1 software with a desired response to maximally expand human T cells without serum supplementation. Phase 2 consisted of eliminating xenogeneic components, examining metabolites consumed in serum-supplemented X-VIVO^TM-15 medium and prototype media from phase 1, and modifying media so that concentrations of metabolites are maintained upon feeding of activated T cells. The final phase focused on optimizing carbon sources, lipid concentrations, lentiviral transduction efficiency, and cytokine production post-activation on activated human T cells. **B**. Primary human T cells were stimulated with anti-CD3/CD28 coated beads and cultured in one of ten custom media. Population doublings for each medium were normalized to the expansion obtained with X-VIVO^TM 15 supplemented with 5% human AB serum. Data are representative from at least seven experiments. Error bars reflect SEM. These data were used for the statistical analysis to optimize cell expansion. **C**. Contour and response surface plots for designing the optimal media for T cell expansion. Statistical analysis performed on StatEase Design-Expert® 9.0.1 based on a Quadratic

model with a desired response of maximum T cell serum-free expansion generated from results of prototype medias in A. Based on this analysis, a predicted optimal medium mixture formulation was generated. **D.** Total T cells were stimulated with anti-CD3/CD28 coated beads in X-VIVO^{TM} 15 supplemented with 5% human AB serum or in the Design of Experiments (DOE) predicted medium (A). Data are representative of 3 donors. **E.** Total T cells were stimulated with anti-CD3/CD28 coated beads in X-VIVO^{TM} 15 supplemented with 5% human AB serum or in the variants of the predicted medium containing a range of concentrations of glucose, galactose and lipids. Data are representative of 5 donors.
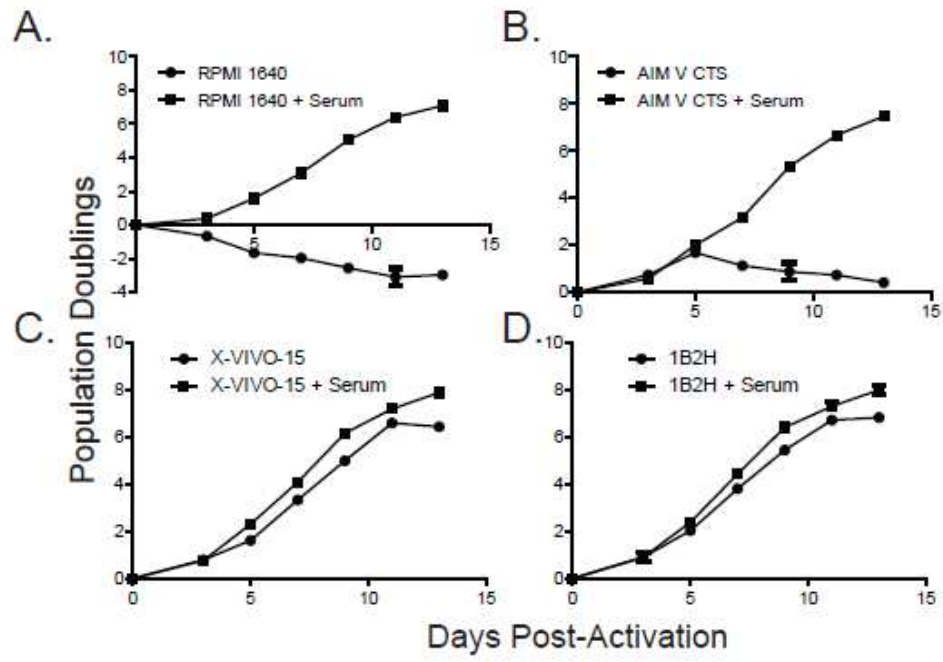
Figure 3-2

Figure 3-2: 1B2H Supports and Robustly Expands Human T Cells in the Absence of Serum

A-D. Primary human CD4 and CD8 T cells were mixed at a 1:1 ratio, activated with CD3/28-coated beads, and cultured in (A) RPMI, (B) AIM V CTS, (C) X-VIVO 15, or (D) 1B2H media with no serum (circles) and with serum (squares). The population doubling rate was measured by cell counting on the days indicated by a symbol. Error bars represent SEM.

A.

X-VIVO-15 Untransduced | X-VIVO-15 Serum CD19 CAR | 1B2H CD19 CAR | 1B2H Serum CD19 CAR

Day -1
Day 13
Day 49

B.

Percent survival / Days

- - - X-VIVO-15 Serum Untransduced
—— X-VIVO-15 Serum CD19 CAR
- - - 1B2H CD19 CAR
—— 1B2H CD19 Serum CAR

C. Day 14

CD3+ Cells/ul of blood

Media:	X-VIVO -15	X-VIVO -15	1B2H	1B2H
Serum:	Yes	Yes	Yes	No
T cells:	Untrans-duced	CART19	CART19	CART19

D. Day 40

X-VIVO-15	1B2H	1B2H
Yes	Yes	No
CART19	CART19	CART19

Figure 3-3

61

Figure 3-3: Durable Tumor Control by CAR T Cells Expanded in the Absence of Human Serum

A. NALM6 tumor cells expressing luciferase were engrafted in NSG mice, and 7 days later (day −1), luciferase expression was determined. Mice were then randomized into treatment groups and 10 million of the indicated T cells (described in Figure 3) were infused on day 0. Luciferase expression within each mouse was measured on days 13 and 43 after T cell infusion. **B.** Kaplan-Meier curve showing tumor-free survival of each of the indicated groups. **C-D.** 14 (C) and 40 (D) days after T cell infusion, peripheral T cell levels were measured using TruCount beads. Each symbol represents data collected from a single mouse.
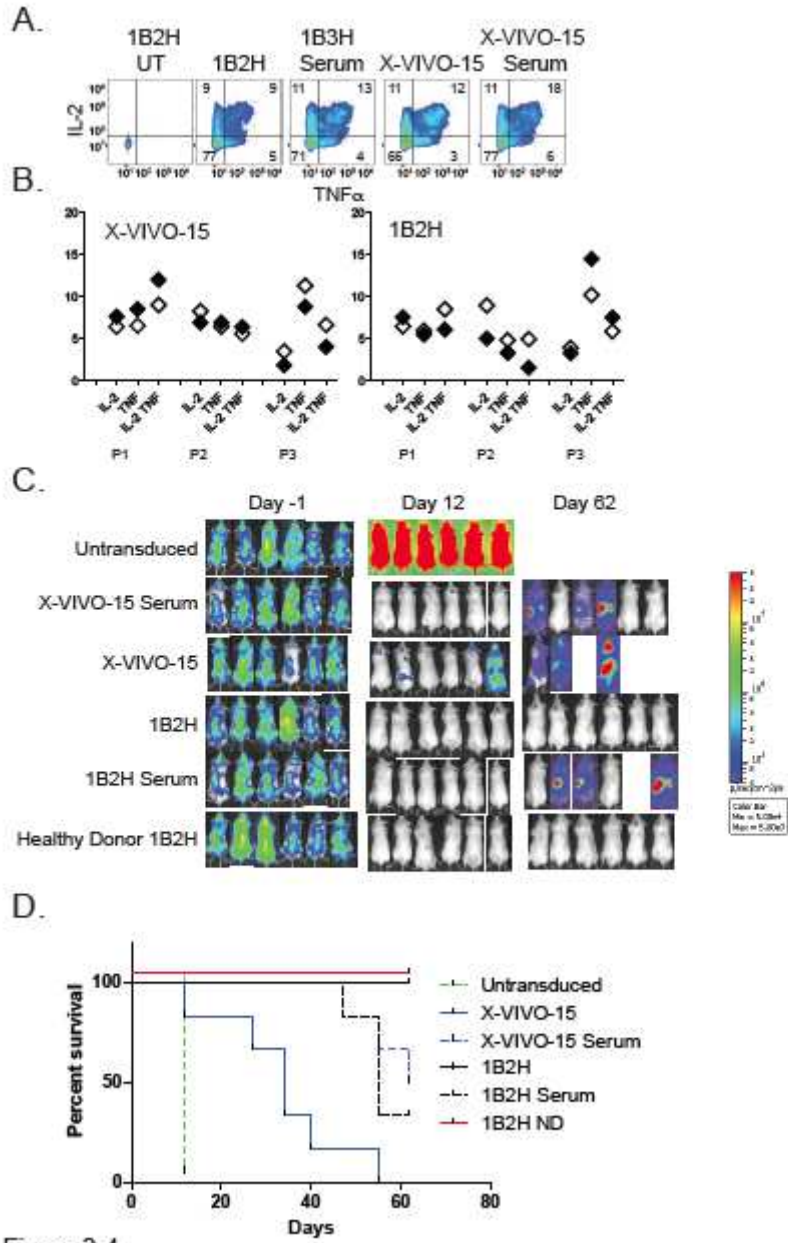
Figure 3-4

Figure 3-4: Durable Control of Tumor Growth of Patient T Cells Expanded with 1B2H SFM

A. CD19 CAR transduced T cells from Figure 5 were diluted with untransduced (UT) T cells so that each population contained 40% transduced T cells. These cells were then incubated with CD19-expressing K562 for 5 hr, and intracellular IL-2 and TNF-α were measured by flow cytometry. **B.** Summary data for 3 multiple myeloma patients from the data described in (A). Filled symbols represent T cells expanded in serum, and open symbols represent T cells expanded in the indicated media in the absence of serum. **C.** NALM6 tumor cells expressing luciferase were engrafted in NSG mice, and 7 days later (day −1), luciferase expression was determined. Mice were then randomized into treatment groups and 10 million of the indicated T cells (described in Figure 5) were infused on day 0. Luciferase expression within each mouse was measured on days 12 and 62 after T cell infusion. **D.** Kaplan-Meier curve showing tumor-free survival (animals that maintained less than the 1×10^7 light units) of each of the indicated groups.
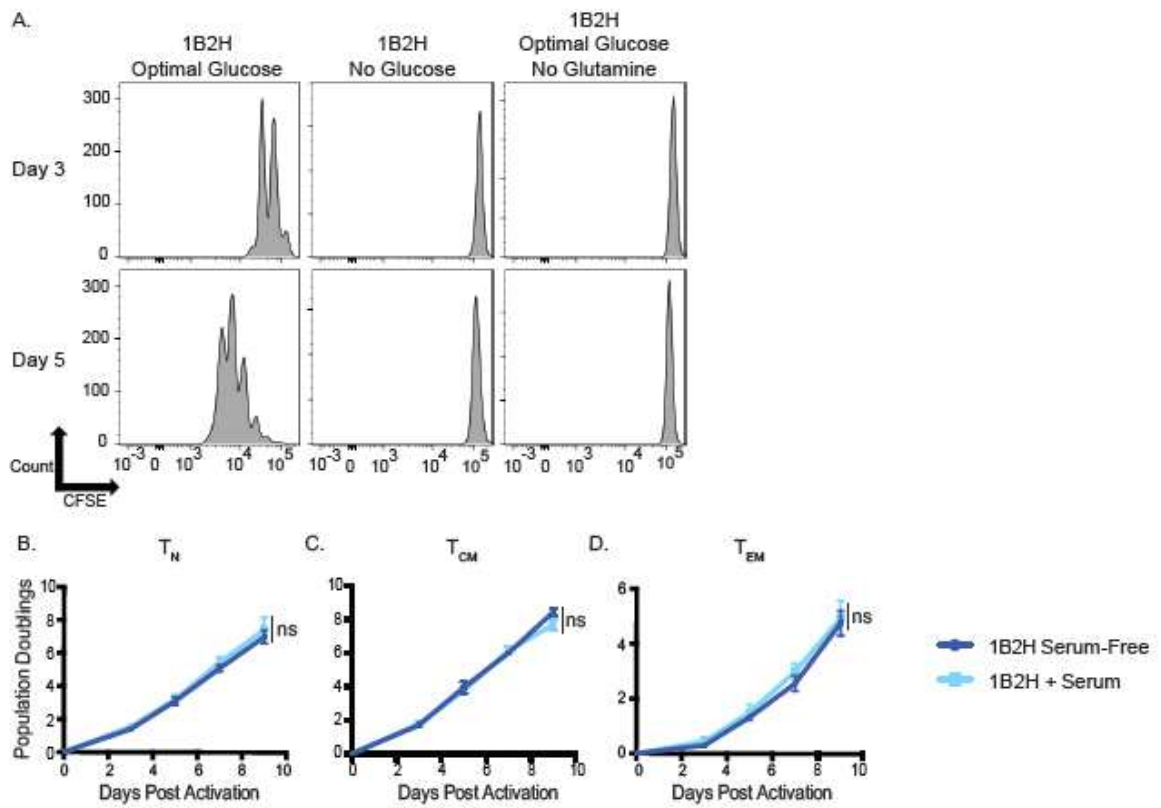
Figure 3-5

Figure 3-5: Generation of a chemically defined, customizable media that can expand human T cell subsets in the absence of serum.

A. Total CD4 T cells were labeled with CFSE and activated by anti-CD3/CD28 coated beads in 1B2H medium containing optimal glucose, no glucose, or optimal glucose without glutamine. T cell proliferation was measured by CFSE dilution by flow cytometry. Data is representative of 3 independent experiments. **C-E.** Primary human CD4 T cells were sort-purified into T_N (CD25-, CD45RA+, CCR7+, CD27+), T_{CM} ((CD25-, CD45RO+, CCR7+, CD27+) and T_{EM} (CD25-, CD45RO+, CCR7-, CD27-) and stimulated with anti-CD3/CD28 coated beads in 1B2H medium with or without 5% human serum. (See **S2** for gating strategy). Cell expansion was monitored by Coulter counter on the indicated days. Data is representative of 2-3 donors and independent experiments. *p <0.05, **p<0.01, paired two-tailed Student's T test on day 9 population doublings. ns = not significant.
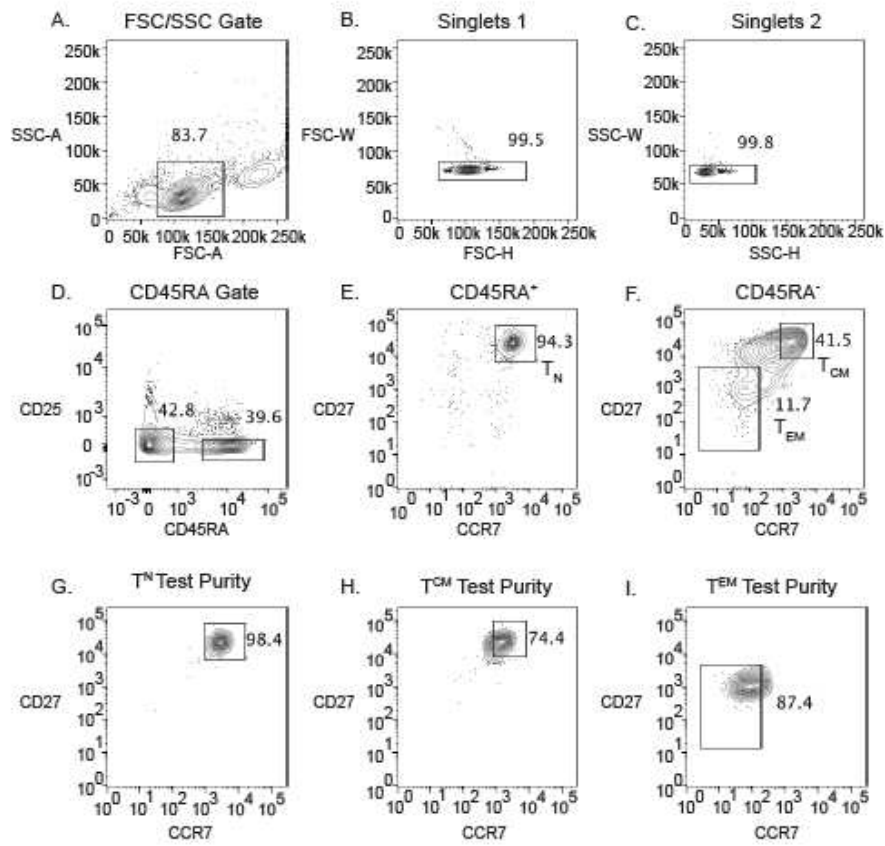
Figure 3-6

Figure 3-6: Gating strategy and purities for sorting human naïve, central memory, and effector memory CD4 T cell subsets.

A-F. T cells for subset experiments were sorted using this gating strategy. Human CD4 T cells were isolated from peripheral blood mononuclear cells (PBMC) and obtained from the Human Immunology Core at the University of Pennsylvania. Cells were sorted in the following order by FSC-A/ SSC-A gating, singlet 1 gating, singlet 2 gating, CD45RA and CD25 gating, and then by CCR7 and CD27. **E.** Naïve (T_N) T cells were designated as cells that are CD45RA$^+$, CD25$^-$, CCR7$^+$, CD27$^+$. **F.** Central memory (T_{CM}) T cells were designated as cells that are CD45RA$^-$, CD25$^-$, CCR7$^+$, CD27$^+$. Effector memory (T_{EM}) T cells were designated as cells that are CD45RA$^-$, CD25$^-$, CCR7$^-$, CD27$^-$. **G-I.** Sorted populations were immediately re-run through the sorter to measure CCR7 and CD27 expression to determine sorting purity. Data is representative of dozens of sorts performed for publication.
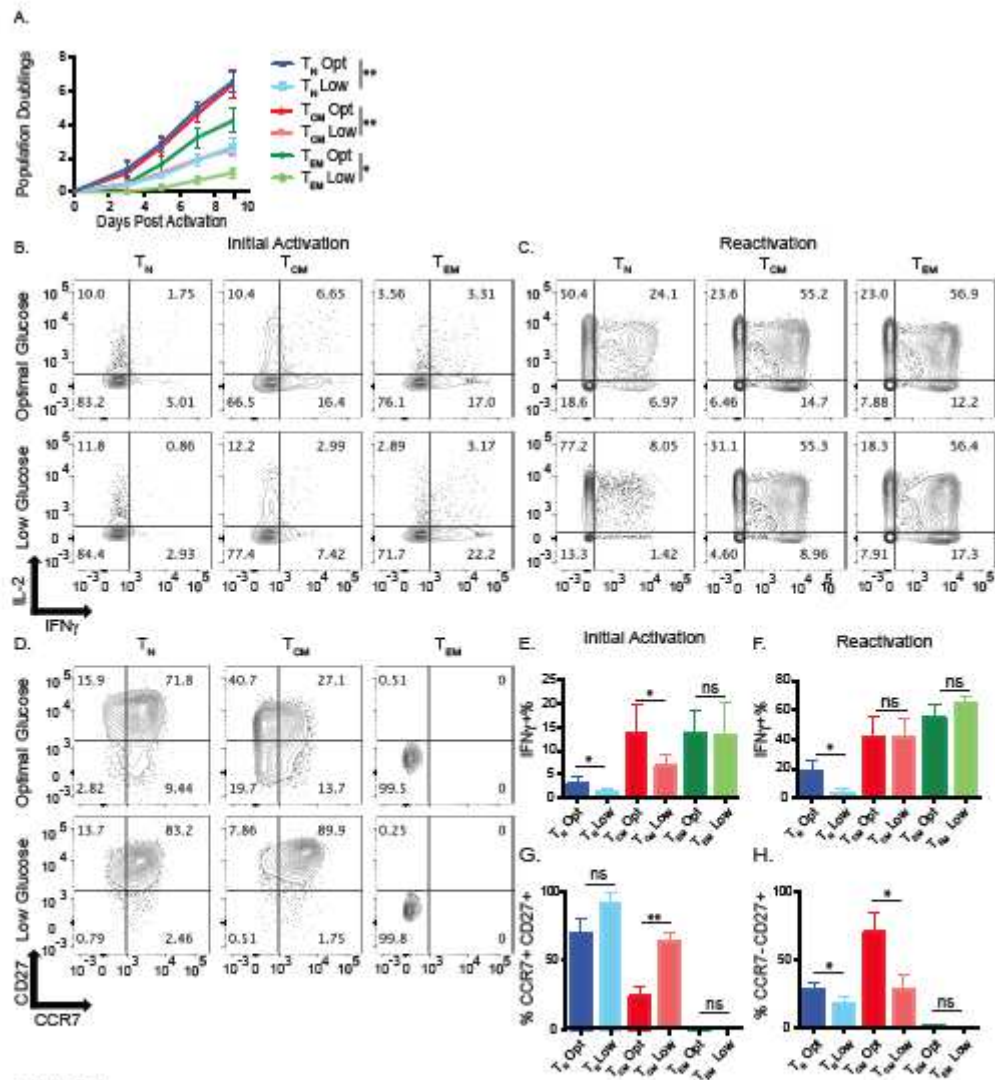
Figure 3-7

Figure 3-7: Effector Memory T cells are resistant to glucose-mediated IFNγ suppression.

A. The indicated subsets were stimulated with anti-CD3/CD28 coated beads in the presence of optimal (35mM) or low (0.35mM) glucose. Cell expansion was monitored by Coulter Counter on the indicated days. Statistics were performed on day 9 population doublings. **B-C.** T cell subsets that were expanded for 24 hours with anti-CD3/CD28 coated beads or expanded for 9-11 days with anti-CD3/CD28 coated beads before IFNγ/IL-2 production was measured after PMA/ ionomycin treatment. **D.** CCR7 and CD27 expression measured on T cell subsets described in A. seven days after T cell expansion. **E-F.** Data from B-C. are summarized from three independent experiments and donors (See **S3** for IL-2 and TNFα quantification). **G-H.** Data from D. summarized from three independent experiments. Error bars reflect SEM. *p <0.05, **p<0.01, paired two-tailed Student's T test. ns = not significant.
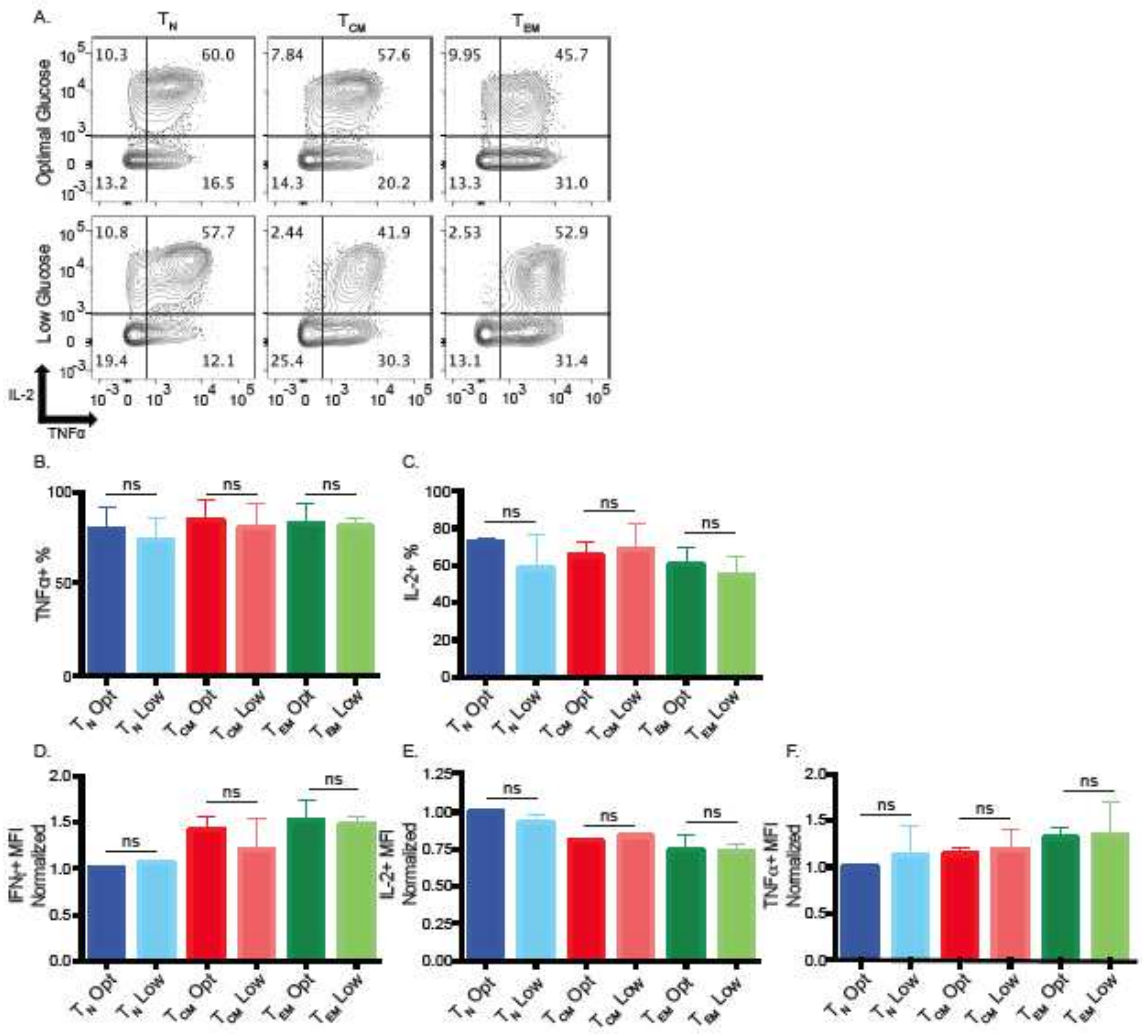
Figure 3-8

Figure 3-8: IL-2 and TNFα production is not significantly affected by glucose in human CD4 T cells.

A. T cell subsets were activated as described in 2C and TNFα production was measured 9 days post-stimulation after PMA/ionomycin treatment. **B-C.** Percentages of TNFα and IL-2+ cells were quantified from A. **D-F.** Quantification of MFI from IFNy, IL-2, TNFα positive cells in optimal or low glucose 9 days post-stimulation after PMA/ionomycin treatment. Error bars reflect SEM. All data is representative of 3 independent experiments. *p <0.05, **p<0.01, paired two-tailed Student's T test. ns = not significant.

A. Day 3 Post Activation

B. Day 7 Post Activation

C. Day 3 Post Activation

D. Day 7 Post Activation

Figure 3-9

73
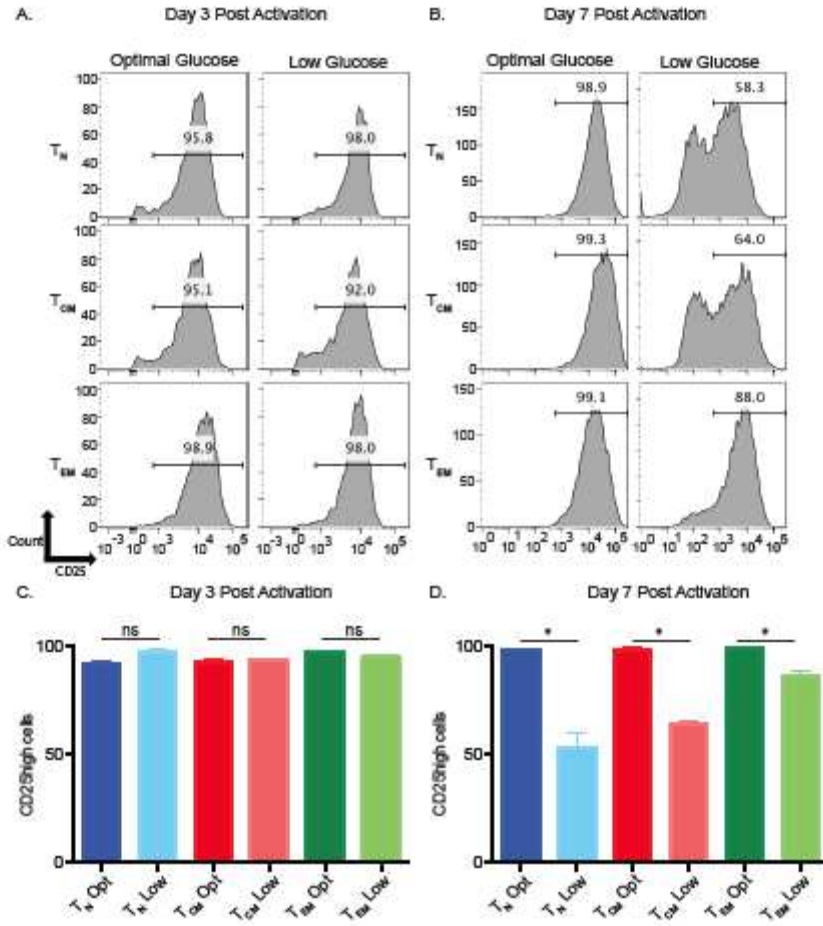
Figure 3-9: Effector memory T cells express CD25 for a longer duration post-activation in limiting glucose.

A-B. Indicated T cell subsets were activated for 3 (A) or 7 days (B) using anti-CD3/CD28 coated beads and CD25 expression was measured. **C-D.** Percentage of CD25 high expressing cells on days 3 and 7 post-activation were quantified from A. and B. respectively. Error bars reflect SEM. Data are representative of 3 independent experiments. *p <0.05, **p<0.01, paired two-tailed Student's T test.
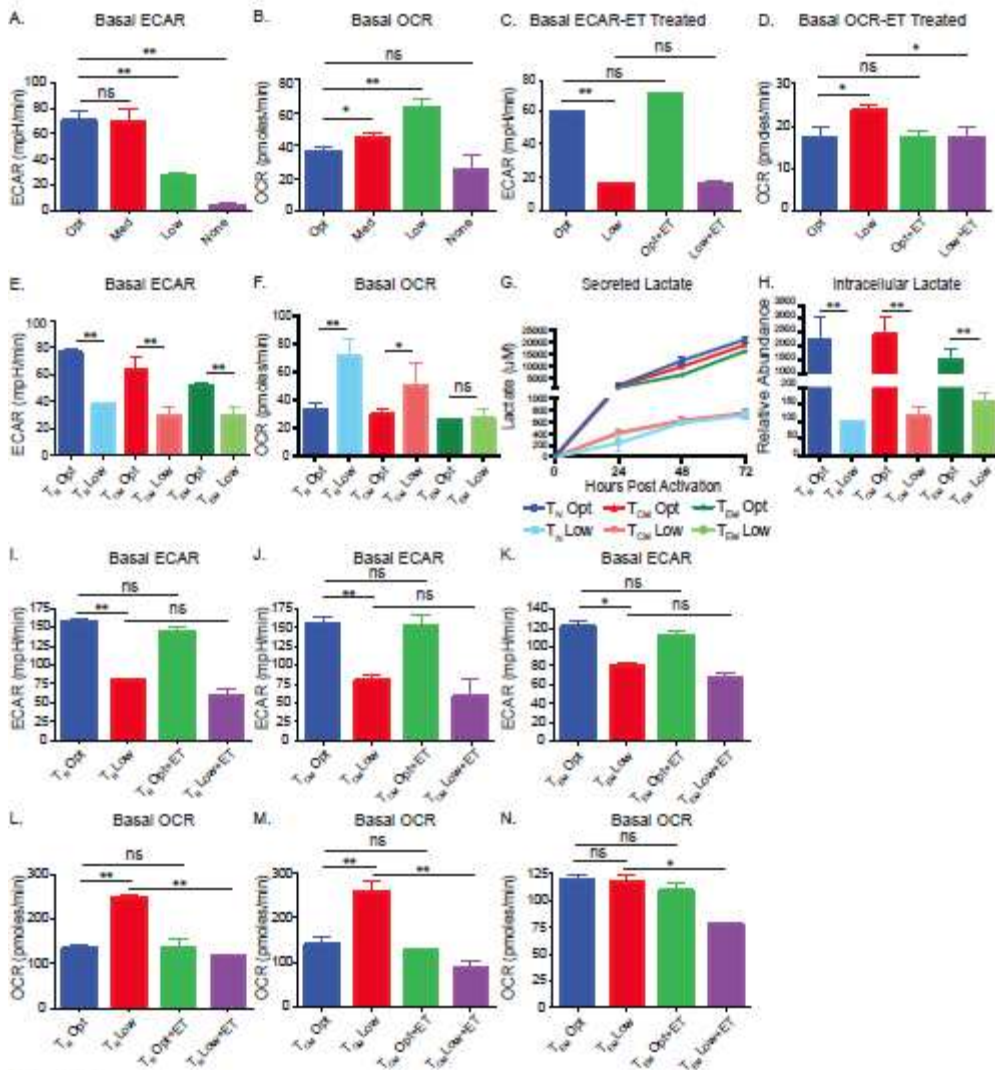
Figure 3-10

Figure 3-10: Effector memory T cells are unable to augment oxidative phosphorylation in low glucose.

A-B. Total CD4 T cells were activated with anti-CD3/CD28 coated beads in optimal (35mM), medium (3.5mM), low (0.35mM), or no glucose (0mM) for 48 hours and basal extracellular acidification rate (ECAR) and basal oxygen consumption rate (OCR) were measured by XF Seahorse Analyzer. **C-D.** Total CD4 T cells were activated with anti-CD3/CD28 coated beads in optimal and low glucose and pre-treated in the presence of etomoxir (ET) or vehicle (DMSO) for 48 hours before basal oxygen consumption rate (OCR) and extracellular acidification rate (ECAR) was measured by XF Seahorse Analyzer. **E-F.** Same as A., but the indicated T cell subsets were studied. **G**. Lactate was measured in the media of indicated T cell subsets after 24, 48, or 72 hours of culture using HPLC. **H.** Relative intracellular abundances of lactate from sorted activated T cell subsets at 48 hours by LC-MS, normalized by cell number and cell volume. **I-N.** Same as C and D., but the indicated T cell subsets were studied. Error bars reflect SEM. All data is representative of 4 independent experiments and donors. *p <0.05, **p<0.01, paired two-tailed Student's T test or in case of multiple comparisons, one-way ANOVA followed by Tukey LSD. ns = not significant.

A.   Unactivated   Optimal Glucose   Low Glucose

2 microns   2 microns   2 microns

B.   Optimal Glucose   Optimal to Low Glucose 4 hrs   Optimal to Low Glucose 24 hrs   Optimal to Low Glucose 48 hrs

2 microns

C.   Day 3   Day 5
Opt   Low   Opt   Low

B actin

LC3B-I
LC3B-II

D.   Bright Field   Bodipy 493/503   LC3B-mcherry   Merge

2 microns

E. T_N T_{CM} T_{EM}

Optimal Glucose

2 microns

Low Glucose

2 microns

F.
Lipid droplets per micrograph
Opt   Low   Unactivated

G.
Lipid droplets per micrograph
T_N Opt T_N Low T_{CM} Opt T_{CM} Low T_{EM} Opt T_{EM} Low

Figure 3-11

77

Figure 3-11: Effector memory T cells contain fewer lipid droplets than other T cell subsets at optimal glucose.

A. Total CD4 T cells were left unactivated or activated with anti-CD3/CD28 coated beads in optimal or low glucose. After 2 days of culture, T cells were examined using transmission electron microscopy. Arrow indicates presence of lipid droplets. Scale bars representing length of 2 microns is indicated below the panel. **B**. Total CD4 T cells were activated with anti-CD3/CD28 coated beads in optimal glucose for 48 hours and then transferred into medium with low glucose and cultured for up to an additional 48 hours. Bodipy 493/503 was used to stain the cells at the indicated time points after being transferred to low glucose for 0, 4, 24, or 48 hours. Fluorescence was visualized via confocal microscopy, 30-40 randomly selected cells per experiment were imaged (See **S5** for quantification). C. Total CD4 T cells were activated with anti-CD3/CD28 coated beads for 3 or 6 days in optimal or low glucose. Cell lysates were probed for LC3B isoforms and β-actin (See **S5** for quantification). Data are representative of 3 independent experiments and donors. **D.** T cells were stimulated with anti-CD3/CD28 coated beads and transduced with LC3B-mcherry. After 48 hours of activation, cells were stained with Bodipy 493/503 and co-localization was visualized via confocal microscopy. 30-40 randomly selected cells per experiment were imaged. Data is representative of 3 independent experiments and donors. **E.** Indicated subsets were stimulated with anti-CD3/CD28 coated beads in the presence of optimal or low glucose. After 2 days of culture, T cells were examined using transmission electron microscopy.

Scale bar representing length of 2 microns is indicated below the panel. **F-G.** The

number of lipid droplets per micrograph were quantified from approximately 40 images

per group per experiment in two independent experiments. Error bars reflect SEM. *p

<0.05, **p<0.01, one-way ANOVA followed by Tukey LSD. ns = not significant.
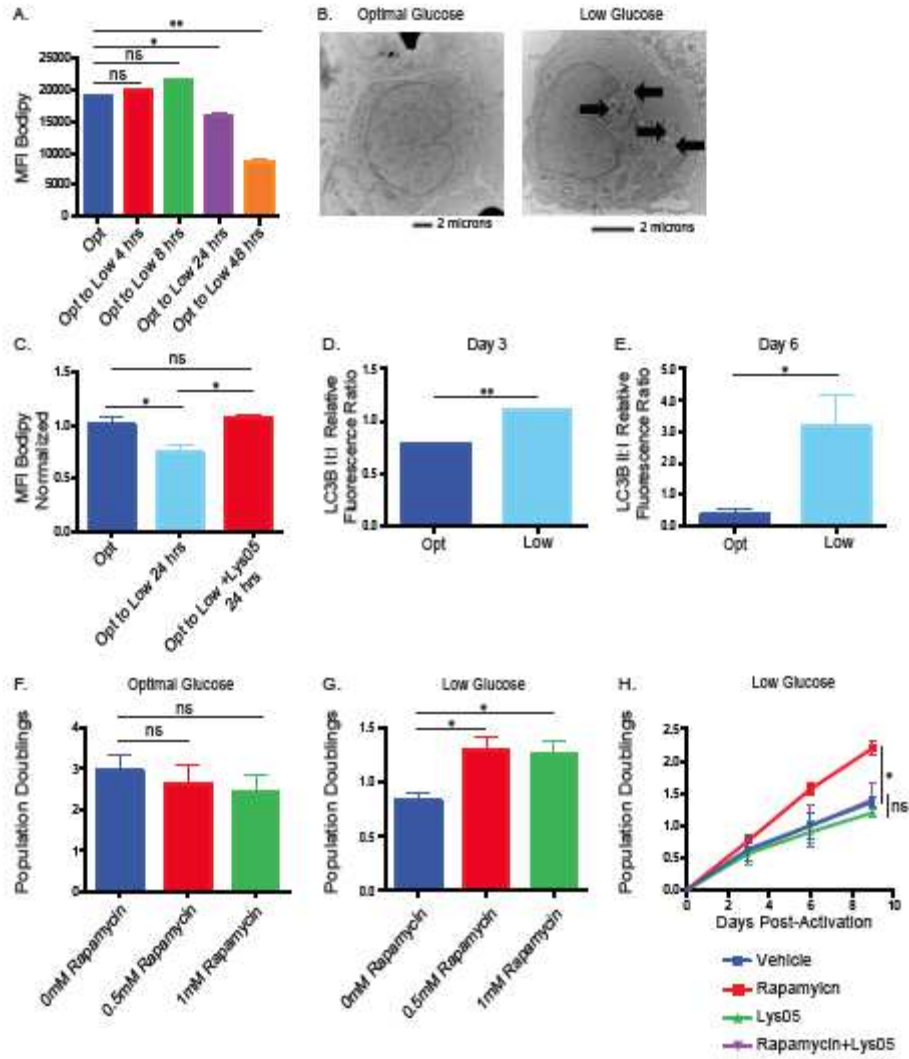
Figure 3-12

Figure 3-12: Quantification of loss of lipid droplets and autophagy by activated T cells in limiting glucose.

A. Total CD4 T cells were activated as described in Figure 4B. Mean fluorescence intensity (MFI) was measured by flow cytometry. Error bars reflect SEM. Data are representative of 3 independent experiments. **B.** Total CD4 T cells were activated with anti-CD3/CD28 coated beads and placed in optimal or low glucose. After six days, T cells were examined using transmission electron microscopy. Arrows indicate presence of autophagosomes. **C.** Total CD4 T cells were activated with anti-CD3/CD28 coated beads in optimal glucose for 48 hours and then transferred into medium with low glucose or low glucose plus Lys05 for an additional 24 hours. Bodipy 493/503 was used to stain the cells at the indicated time points after being transferred to low glucose for 0, 4, 24, or 48 hours. **D-E.** Sorted T cells were activated with anti-CD3/CD28 coated beads for 3 or 6 days in optimal or low glucose. Cell lysates were probed for LC3B isoforms and β-actin. Western data is quantified via densitometry. **F-G.** Total CD4 T cells were activated with anti-CD3/CD28 coated beads for 5 days in optimal or low glucose in the presence or absence of rapamycin. Population doublings were quantified at day 5 post-activation.   **H.** Total CD4 T cells were activated with anti-CD3/CD28 coated beads for 9 days in optimal or low glucose in the presence or absence of rapamycin, Lys05, or both rapamycin and Lys05. Data is representative of 3 independent experiments and donors. Error bars reflect SEM. *p <0.05, **p<0.01, paired two-tailed Student's T test or in case of multiple comparisons, one-way ANOVA followed by Tukey LSD**.** ns = not significant.
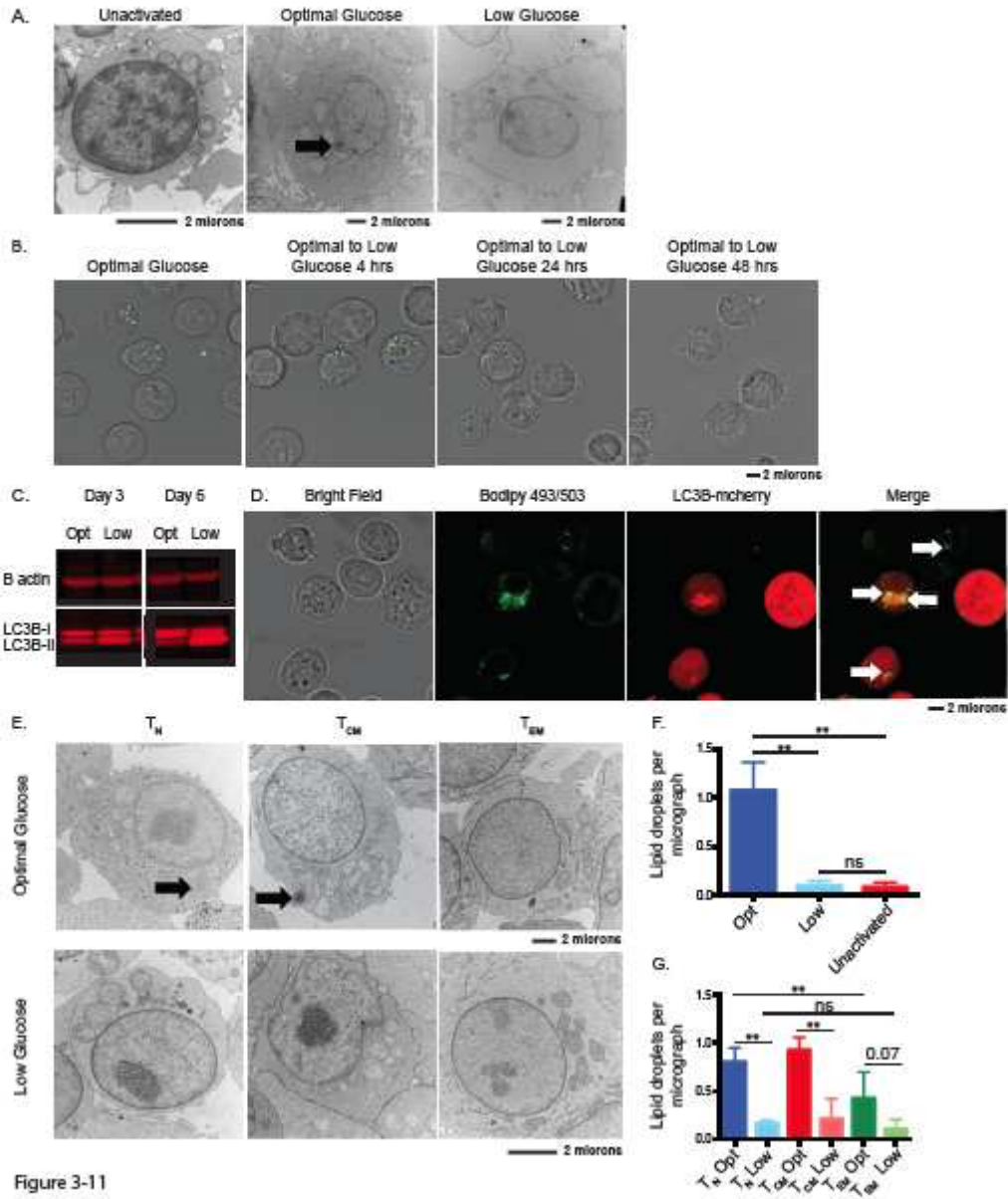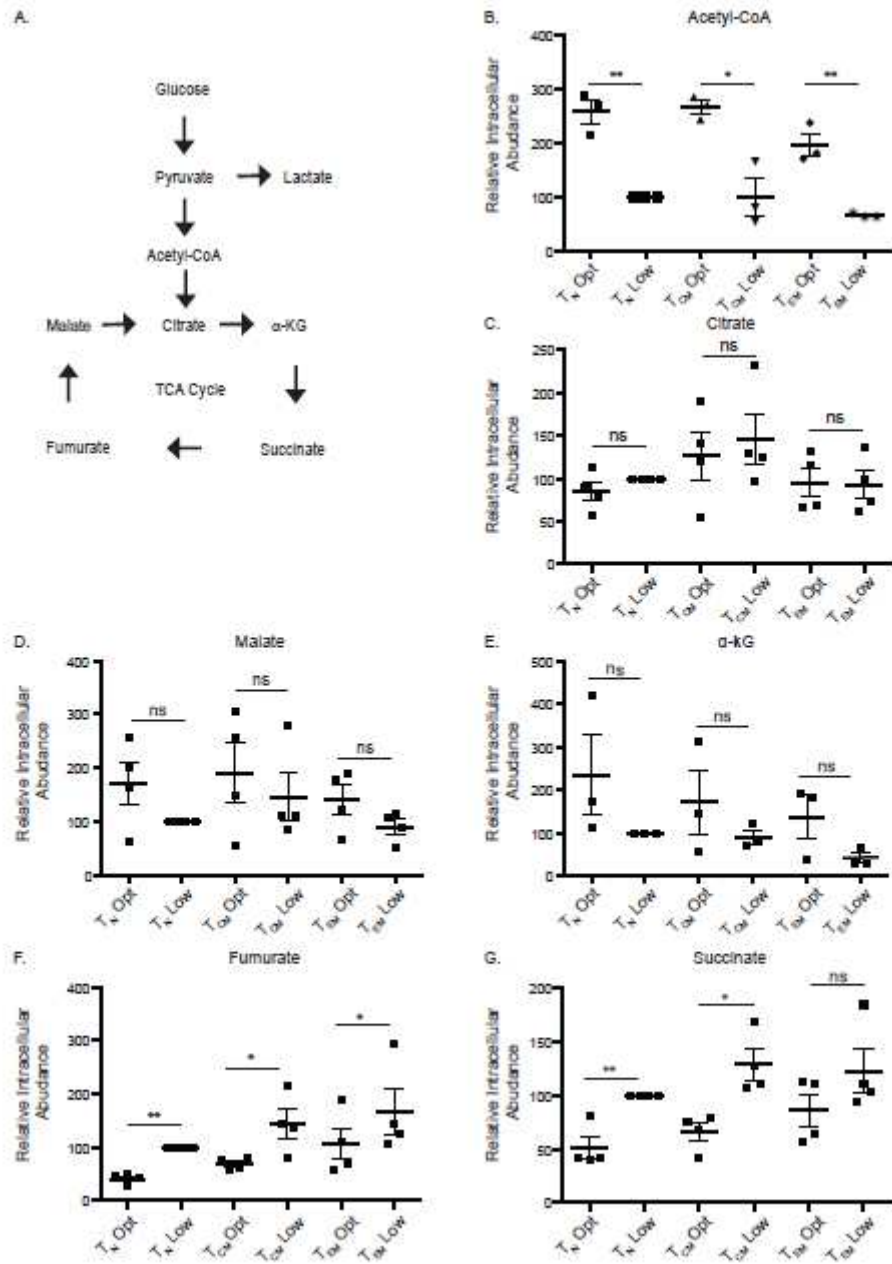
Figure 3-13

Figure 3-13: Intracellular abundances of acetyl-CoA and TCA intermediates in activated T cell subsets.

A. Diagram depicting glycolysis and TCA cycle. **B-G.** Relative intracellular abundances of acetyl-CoA, citrate, malate, α-ketoglutarate (α-KG), fumurate, and succinate respectively from indicated subsets at 48 hours by LC-MS, normalized by cell number and cell volume. Error bars reflect SEM. All data is representative of 3-4 independent experiments. *$p < 0.05$, **$p < 0.01$, paired two-tailed Student's T test. ns = not significant.
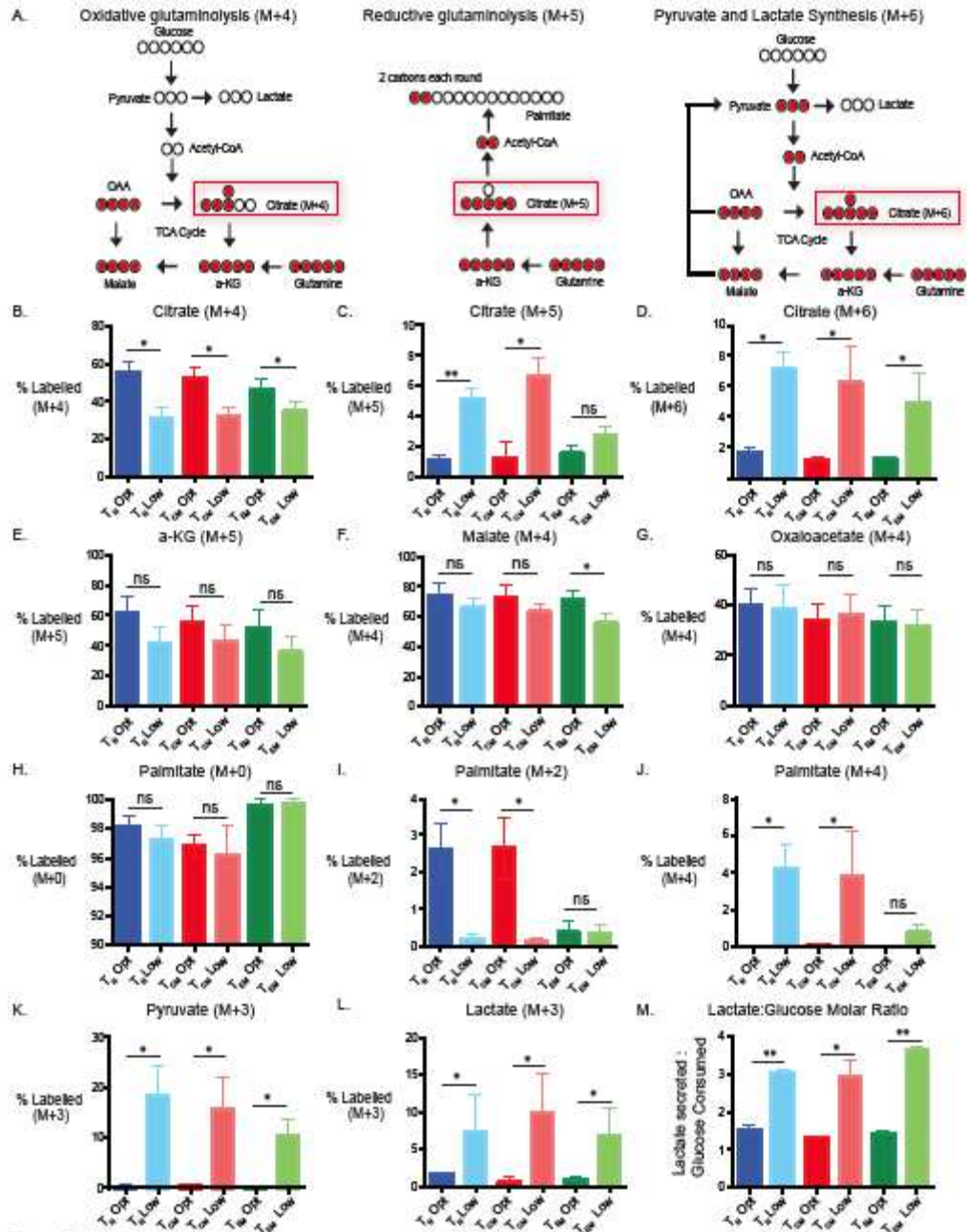
Figure 3-14

Figure 3-14: Effector Memory T cells cannot perform reductive glutaminolysis for fatty acid synthesis in low glucose.

A. Model depicting how heavy glutamine is incorporated into citrate in a M+4, M+5, or M+6 manner and how each of those inform how glutamine is routed intracellularly. **B-D.** Indicated T cell subsets were activated with anti-CD3/CD28 coated beads in optimal or low glucose supplemented with heavy glutamine for 48 hours. Percentage of M+4, M+5, M+6 citrate calculated from the total intracellular citrate pool of each subset by LC-MS is indicated. **E-G.** Indicated T cell subsets were treated identically to B. Graphs show percentage of M+5 α-ketoglutarate, M+4 malate, and M+4 oxaloacetate calculated from the total respective intracellular pools of each metabolite for each subset by LC-MS. **H-J.** Indicated T cell subsets were treated identically to B. Percentages of M+0, M+2, and M+4 palmitate were calculated from the total intracellular pool of palmitate for each subset by LC-MS. **K-L.** Indicated T cell subsets were treated identically to B. Percentage of M+3 pyruvate, M+3 lactate from the total respective intracellular pool of each subset by LC-MS. **M.** Ratios of lactate secreted and glucose consumed were calculated from moles of lactate secreted and moles of glucose consumed in supernatant of T cell subsets determined by HPLC following 48 hours post-activation. Error bars reflect SEM. All data is representative of 3-4 independent experiments. (See **S6** for overall relative metabolite abundances of each subset.) *p <0.05, **p<0.01, paired two-tailed Student's T test. ns = not significant.
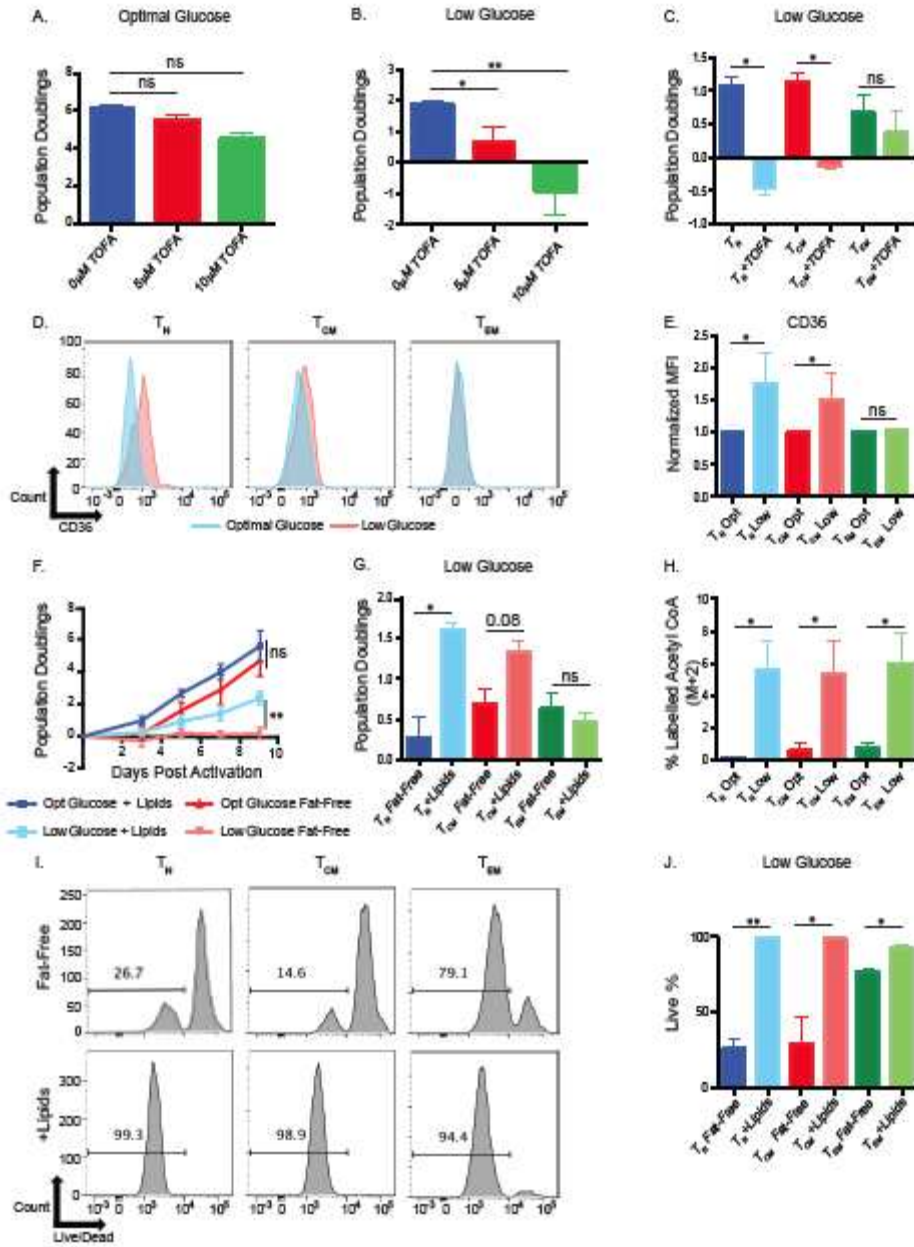
Figure 3-15

Figure 3-15: Effector memory T cells are less reliant on fatty acid metabolism for survival and expansion in low glucose.

A-B. Total CD4 T cells were activated with anti-CD3/CD28 coated beads in optimal or low glucose in the presence of TOFA or with vehicle (DMSO) for 5 days. Total cell expansion is recorded on day 5 post-activation. **C.** Indicated T cell subsets were activated with anti-CD3/CD28 coated beads in low glucose in the presence of TOFA or vehicle DMSO for 5 days. Cell expansion is recorded on day 5 post-activation. **D.** Indicated T cell subsets were activated with anti-CD3/CD28 coated beads in optimal or low glucose and CD36 expression was measured at 48 hours post-activation. **E.** Quantification of D. from three independent experiments and donors. **F.** Total CD4 T cells were activated with anti-CD3/CD28 beads in optimal or low glucose in media without any exogenous lipids (fat-free) or supplemented with exogenous lipids for 9 days. Cell expansion was monitored by Coulter counter on the days indicated. **G.** Indicated T cell subsets were activated with anti-CD3/CD28 coated beads in low glucose, fat-free medium with or without supplementation of exogenous lipids for 5 days. Cell expansion was recorded on day 5 post-activation. **H.** Indicated subsets were treated with heavy palmitate for 24 hours. Percentages of M+2 acetyl CoA were calculated from the total acetyl CoA pool by LC-MS. **I.** Indicated T cell subsets were activated with anti-CD3/CD28 coated beads in fat-free medium in low glucose with or without exogenous lipids. Live cells were identified with Live/Dead Aqua by flow cytometry on day 5 post-activation. **J.** Quantification of live cells from H. Error bars reflect SEM. All data is

representative of 3 independent experiments. *p <0.05, **p<0.01, paired two-tailed

Student's T test or in case of multiple comparisons, one-way ANOVA followed by Tukey

LSD. ns = not significant.
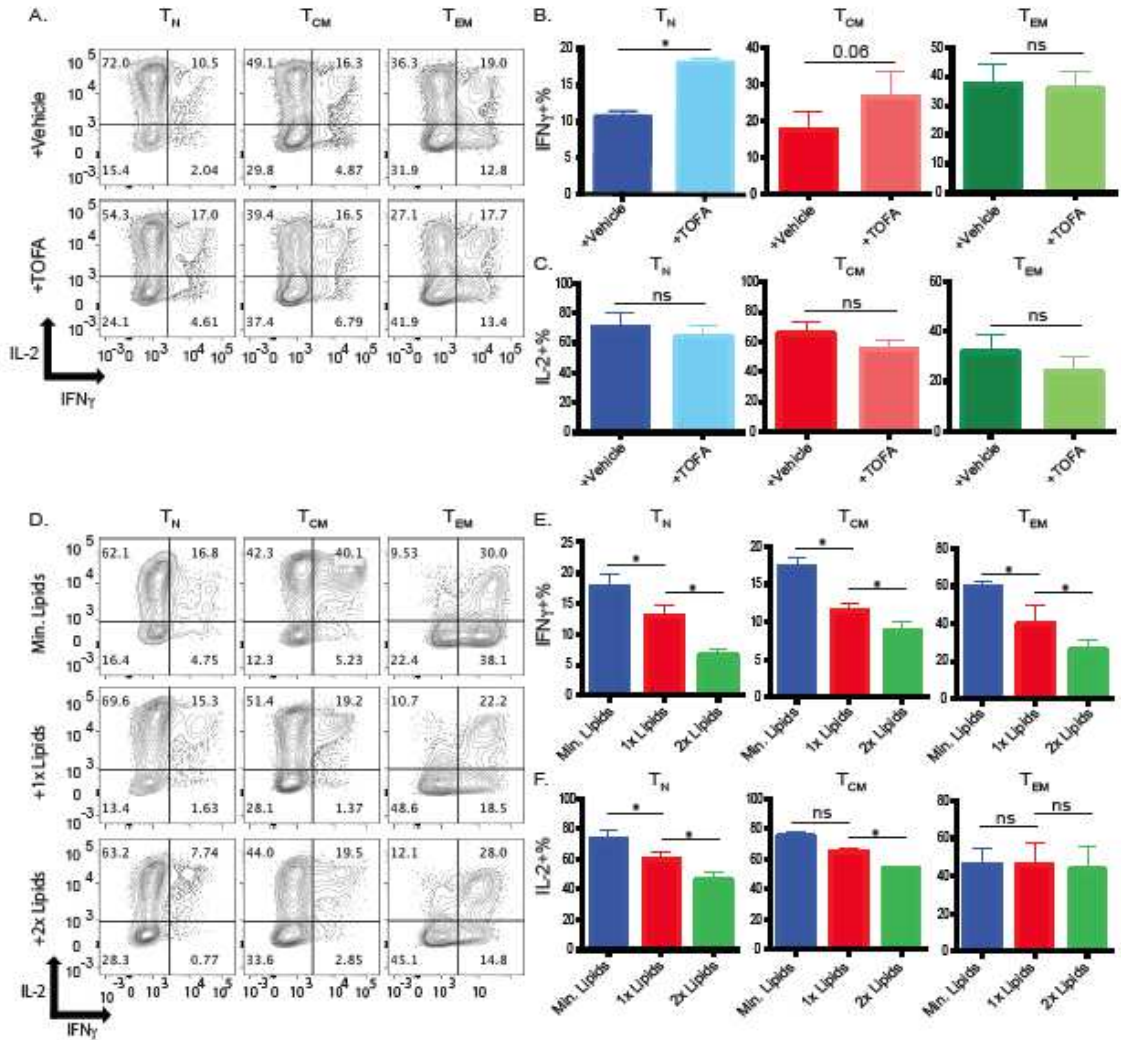
Figure 3-16

Figure 3-16: Reliance on fatty acid metabolism in low glucose inhibits IFNγ production.

A-C. Indicated T cell subsets were activated with anti-CD3/CD28 coated beads in low glucose in the presence of vehicle (DMSO) or low dose TOFA for 5 days before IFNγ and IL-2 production was measured after PMA/ionomycin treatment. For optimal glucose data, see **Figure S7**. **B-C.** Quantification of A. from 4 independent experiments. **D.** Indicated T cell subsets were activated with anti CD3/CD28 coated beads in low glucose, in the presence of minimal, 1x, or 2x exogenous lipid concentrate in fat-free medium for 5 days post-activation before IFNγ production was measured following PMA/ionomycin treatment. **E-F.** Quantification of D. from 3 independent experiments. Error bars reflect SEM. *p <0.05, **p<0.01, paired two-tailed Student's T test. ns = not significant.
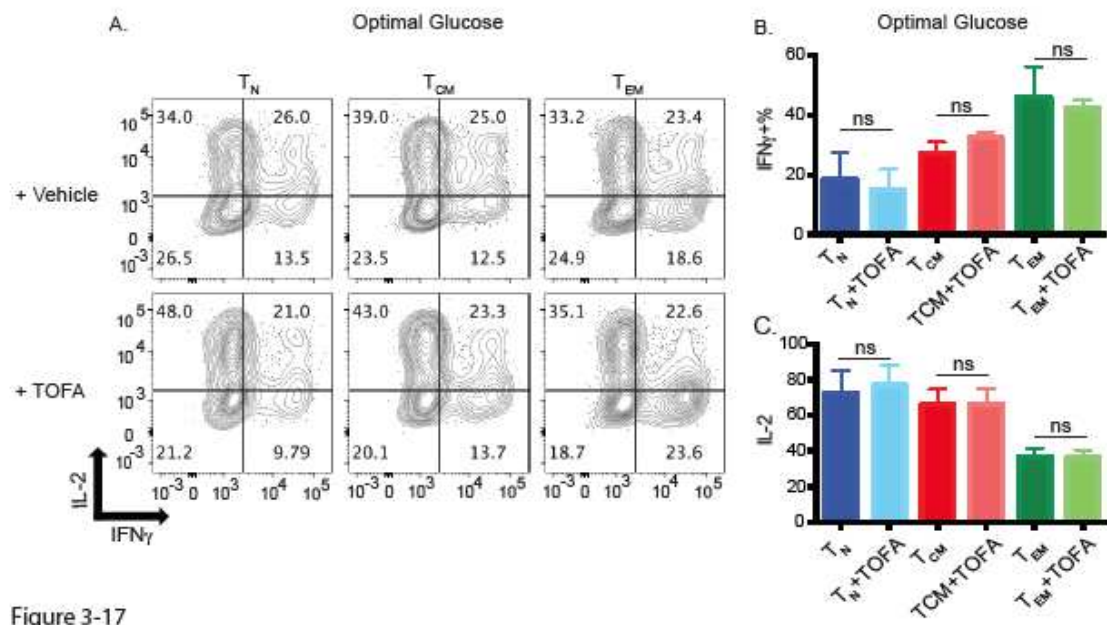
Figure 3-17

Figure 3-17: Inhibition of fatty acid synthesis does not significantly affect cytokine production in optimal glucose.

A. Indicated subsets were activated as in Fig 6A and cytokine expression was measured after PMA/ionomycin treatment in optimal glucose. **B-C.** Data from A. quantified in 4 independent experiments. Error bars reflect SEM. *p <0.05, **p<0.01, paired two-tailed Student's T test. ns = not significant.
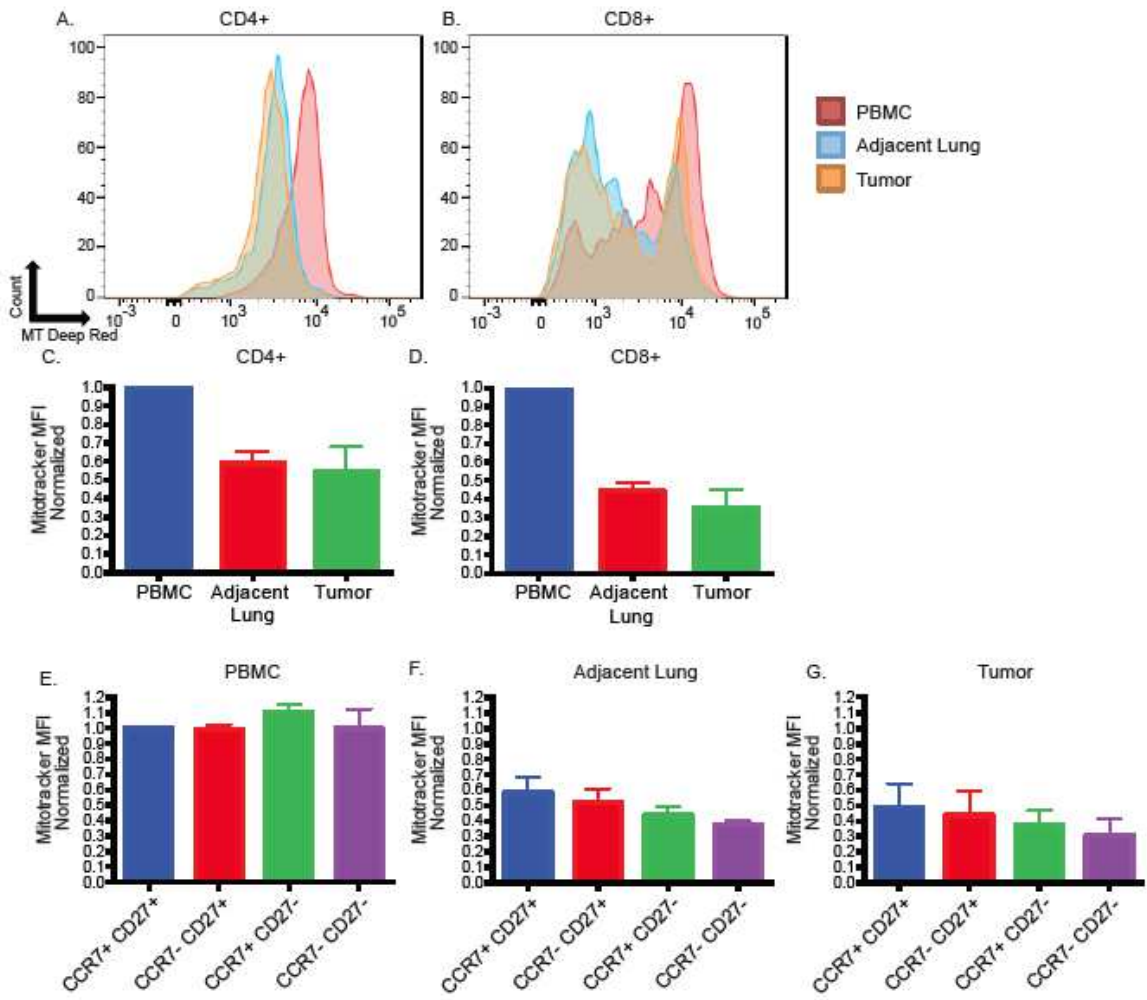
Figure 3-18

Figure 3-18: Tissue-specific signals and not tumor-specific signals may regulate mitochondrial mass in T cells from non-small cell lung cancer patients.

A-B. CD4+ (A) and CD8+ (B) T cells were isolated and stained with Mitotracker Deep Red from the peripheral blood, adjacent lung tissue, and lung tumor tissue of non-small cell lung cancer patients. **C-D.** Data from A-B quantified from 3 patients and 3 independent experiments. **E-G.** CD8$^+$,CD45RA$^-$ T cells from the peripheral blood (E), adjacent lung tissue (F), and lung tumor tissue (G) were stained with Mitotracker Deep Red.

Working Model:
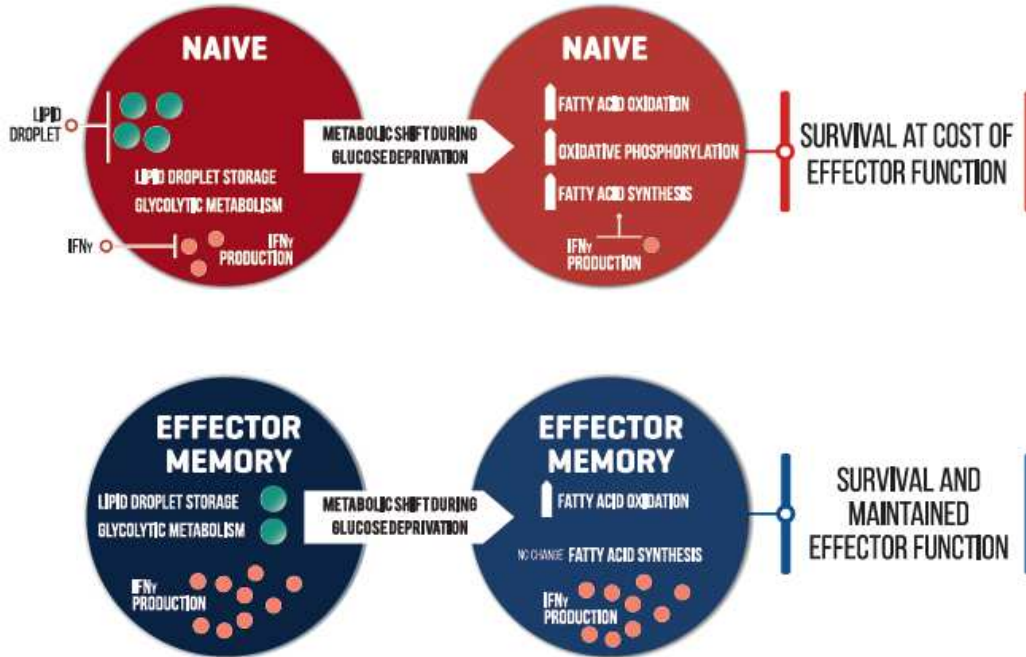
Figure 3-19

Figure 3-19: Working model for subset-specific adaption to limiting glucose.

A. When activated in sufficient glucose, naïve T cells perform glycolysis and uptake lipids from their environment and make a small amount of IFN-γ. When activated in limiting glucose, naïve T cells increase their reliance on fatty acid oxidation, oxidative phosphorylation, and fatty acid synthesis. The reliance on fatty acid synthesis inhibits IFN-γ production by naïve T cells. **B.** When activated in sufficient glucose, effector memory T cells perform glycolysis and uptake less lipids from their environment than naïve T cells, and make a large amount of IFN-γ. When activated in limiting glucose, effector memory T cells increase their reliance on fatty acid oxidation, but do not increase oxidative phosphorylation or fatty acid synthesis pathways. By not relying on fatty acid synthesis, effector memory T cells are able to maintain large amounts of IFN-γ production in limiting glucose.

Tables

Table 3-1:

A.

Prototype Media	Base 1 **Lean media with balanced AA and vitamins**	Base 2 **Non-essential AA, vitamins, trace elements and proteins**	Base 3 **Concentrated AA, vitamins, trace elements, metal ions, antioxidants, polyamines and lipids**
1	1.00	0.00	0.00
2	0.50	0.00	0.50
3	0.50	0.50	0.00
4	0.00	0.50	0.50
5	0.33	0.33	0.33
6	0.00	1.00	0.00
7	0.00	0	1.00
8	0.66	0.17	0.17
9	0.17	0.17	0.66
10	0.17	0.67	0.17

B.

X-VIVO™ 15 Media + 5% Serum	Day 0 **(% Remaining)**	Day 3 **(% Remaining)**	Day 3 Post-Feed **(% Remaining)**	Day 6 **(% Remaining)**
L-Arginine	100	62	91	52
L-Glutamine	100	58	91	28
L-Leucine	100	69	93	64
L-Methionine	100	62	91	52

L-Serine	100	7	78	nq
L-Tryptophan	100	26	91	nq
Ethanolamine HCl	100	nq	70	nq

C.

Prototype Media	Day 0 (% Remaining)	Day 3 (% Remaining)	Day 3 Post-Feed (% Remaining)	Day 6 (% Remaining)
L-Arginine	100	78	95	76
L-Glutamine	100	66	94	62
L-Leucine	100	67	91	58
L-Methionine	100	60	91	58
L-Serine	100	nq	83	14
L-Tryptophan	100	nq	92	nq
Ethanolamine HCl	100	48	96	40

Table 3-1: Creation of prototype media and spent media analysis for development of 1B2H medium.

A. Proportions of SFM1, SFM2, and SFM3 used to create ten media variants for 1B2H media creation are indicated. These ten media variants were then used in Figure S1. B. Total T cells were activated with anti CD3/CD28 coated beads in XVIVOTM-15 media supplemented with 5% human serum. Relative amounts of amino acids were analyzed at indicated time points by HPLC. Cells were counted on Day 3, and every other day afterward so that new media could be added to keep the concentration of cells at 500k cells/mL. nq = below limit of detection, not quantifiable. C. Total T cells were activated with anti-CD3/CD28 coated beads in 1B2H media. Relative amounts of amino acids were analyzed at indicated time points by HPLC. Cells were counted on Day 3, and every other day afterward so that new media could be added to keep the concentration of cells at 500k cells/mL. nq = below limit of detection, not quantifiable.

Table 3-2:

Glucose Concentration (mM)	Day 0 (% Remaining)	Day 3 (% Remaining)	Day 5 (% Remaining)	Day 7 (% Remaining)	Day 9 (% Remaining)
35.0	100	82.72727	68.78788	69.39394	72.72727
24.5	100	74.65619	55.59921	54.6169	38.25137
17.5	100	67.75956	36.61202	38.79781	29.46955
10.5	100	49.76744	1.395349	nq	nq
7.0	100	31.46853	nq	nq	nq
3.5	100	9.859155	nq	nq	nq
0	nq	nq	nq	nq	nq

Table 3-2: Determination of the optimal glucose concentration in 1B2H media.

Total T cells were activated with anti-CD3/CD28 coated beads in 1B2H media supplemented with the indicated amounts of glucose. Relative amounts of glucose remaining in the media were determined at the indicated time points by HPLC. Cells were counted on Day 3, and every other day afterward so that new media could be added to keep the concentration of cells at 500k cells/mL. nq= below limit of detection, not quantifiable

Table 3-3:

A.

Metabolites consumed	T_N Optimal (mg/L)	T_N Low (mg/L)	T_{CM} Optimal (mg/L)	T_{CM} Low (mg/L)	T_{EM} Optimal (mg/L)	T_{EM} Low (mg/L)
Glucose	10785.74+/-1326.96	237.85+/-64.74	9257.99+/-1177.92	237.89+/-64.75	6333.86+/-607.04	78.28+/-21.31
L-Glutamine	288.31+/-17.49	278.38+/-13.77	270.38+/-9.02	264.85+/-7.86	260.23+/-13.89	272.65+/-17.42
L-Serine	26.45+/-3.59	14.70+/-4.58	24.15+/-1.79	11.77+/-1.71	15.74+/-0.60	9.98+/-1.19
L-Lysine HCl	16.14+/-1.42	6.25+/-1.80	17.61+/-1.72	4.93+/-1.62	12.75+/-1.53	5.91+/-1.71
L-Arginine	13.96+/-4.03	6.98+/-2.02	12.64+/-0.59	5.23+/-1.51	9.54+/-1.14	6.81+/-1.97
L-Isoleucine	9.60+/-2.77	5.64+/-1.63	9.95+/-0.78	4.71+/-2.33	7.85+/-0.89	5.31+/-1.53
L-Leucine	8.23+/-3.20	6.20+/-1.79	14.08+/-3.96	5.53+/-1.60	10.23+/-2.96	5.97+/-1.72
L-Valine	8.28+/-2.36	3.92+/-1.14	9.09+/-2.59	3.28+/-0.95	6.71+/-1.92	3.79+/-1.10
L-Tyrosine	5.28+/-1.52	2.29+/-0.66	5.51+/-1.52	1.54+/-0.44	4.04+/-1.15	2.04+/-0.59
L-Methionine	4.07+/-0.94	3.35+/-0.97	5.46+/-0.17	3.14+/-0.91	3.94+/-0.72	3.08+/-0.11
L-Tryptophan	3.76+/-1.08	2.87+/-0.83	3.32+/-0.91	2.33+/-0.67	2.70+/-0.74	2.94+/-0.85
L-Phenylalanine	3.24+/-1.91	3.06+/1.22	6.92+/-1.91	2.54+/-1.12	4.90+/-1.35	3.12+/-1.36

B.

Metabolites Produced	T_N Optimal (mg/L)	T_N Low (mg/L)	T_{CM} Optimal (mg/L)	T_{CM} Low (mg/L)	T_{EM} Optimal (mg/L)	T_{EM} Low (mg/L)
Lactate	12271.47+/-1471.81	587.28+/-41.94	9826.15+/-684.33	629.17+/-39.20	6373.29+/-377.56	616.05+/-61.78
Ammonia	25.43+/-6.14	34.52+/-7.57	24.14+/-6.46	33.08+/-9.39	22.61+/-6.37	28.77+/-7.13
L-Glutamic Acid	11.83+/-2.66	11.44+/-2.92	6.71+/-0.90	6.96+/-1.88	7.40+/-1.18	2.52+/-0.82

L-Alanine	1.17+/-0.51	8.43+/-1.56	1.84+/-1.01	8.55+/-2.31	1.50+/-0.42	3.65+/-1.37
L-Aspartic Acid	nq	4.51+-/1.49	nq	2.81+/-1.54	nq	2.51+/-1.96

Table 3-3: Production and consumption of metabolites by activated T cell subsets.

Indicated T cell subsets were activated with anti-CD3/CD28 coated beads for 48 hours.

A. Rates of consumption of selected amino acids and organic acids were determined by

HPLC of supernatant and comparing that to un-used respective media kept at cell

culture conditions for 48 hours. B. Rates of production of selected amino acids and

organic acids were determined by HPLC of supernatant and comparing that to un-used

respective media kept at cell culture conditions for 48 hours. nq= below limit of

detection, not quantifiable. Rates of production are +/- SEM.

Chapter 4- Understanding mitochondrial remodeling during T cell activation

Introduction

T cells undergo significant mitochondria biogenesis upon T cell activation and upregulate mitochondrial function (Ron-Harel et al., 2016). Researchers have observed increases in numerous mitochondrial pathways including oxidative phosphorylation, fatty acid metabolism, and one-carbon metabolism upon activation (Procaccini et al., 2016). Oxidative phosphorylation and electron transport are essential for proliferation following TCR stimulation, while fatty acid and one-carbon metabolism can generate the necessary building blocks for proliferating cells. Furthermore the mitochondrion generates reactive oxygen species that are vital for nuclear factor of activated T cells (NFAT), translocation into the nucleus and IL-2 production during T cell activation (Chang et al., 2013; Sena et al., 2013). Thus mitochondria are critical for T cell proliferation and serve necessary functions well beyond energy production.

It is widely believed that mitochondrial shape and cristae structure are inherently tied to mitochondrial function (Cogliati et al., 2013; Paumard et al., 2002). Although most of this evidence was obtained during the context of apoptosis induction or in Opa1 knockout cells. During T cell activation, mitochondria begin to loosen their mitochondrial cristae and begin increasing rates of mitochondrial fission (Buck et al., 2016). It remains unknown which activation signals initiate mitochondrial morphology

changes, and what effects those morphology changes have on respiration and other mitochondrial functions.

We sought to identify the activation signals responsible for mitochondrial morphology changes, and how those changes affected cellular respiration and ROS production. We found that human CD4 T cells significantly and reversibly alter mitochondrial structure upon activation. Mitochondria undergo dramatic swelling and cristae disruption that is glucose and mammalian target of rapamycin complex 1 (mTORC1) dependent. Swelling and cristae disruption were strongly correlated, and were reversed as cells rest down or more quickly when cells were transferred to limiting glucose. We also observe that cytochrome C, an essential component of the electron transport chain and pro-apoptotic protein, is cytoplasmic in T cells activated in abundant glucose, but can readily sequester cytochrome C in the mitochondria if those cells are transferred to low glucose environments. By utilizing multiple pharmacological inhibitors/nutrient conditions, we found that cristae disturbance strongly correlated to rates of glycolysis, reactive oxygen species production, and voltage potential. From this data we have generated a model that proposes glucose uptake and mTORC1 signaling are required to induce an activation signal that induces mitochondrial swelling and cristae disruption. We speculate that the cristae disturbance and mitochondrial swelling drive ROS production, which is known to be required for optimal T cell proliferation. When mitochondria are unable to restore structure, ROS production remains elevated, T cells are able to exhibit increased proliferation but at cost of increased death. When

mitochondria are not able to alter mitochondrial structure, they are unable to produce

ROS and generate appropriate proliferation signals. Taken together, we propose

Warburg metabolism promotes cellular division by a novel mechanism of altering

mitochondrial structure and ROS production.

Results

CD4 T cells reversibly alter mitochondrial structure upon activation in a glucose

dependent manner

Numerous reports have also linked nutrient availability to mitochondrial

structure (Liesa and Shirihai, 2013; Mishra and Chan, 2016). We first noticed large

mitochondrial structure differences during CD4 T cell activation when cells were grown

in optimal (35mM) or low (0.35mM) glucose in previous work done by our laboratory

(Ecker et al., 2018). To better understand how human CD4 T cells altered mitochondria

structure upon stimulation, we kinetically examined how mitochondria cristae,

mitochondrial area, and shape changed in CD4 T cells grown in optimal and low glucose

using anti-CD3/CD28 coated beads. We found that cells grown in optimal glucose had

large changes to mitochondrial cristae. Mitochondrial cristae lost strict, parallel

patterning, became less frequent in number, and even became circular structures within

the mitochondria themselves in a term we call "cristae disturbance". We quantified

cristae disturbance using a scale ranging from 1 to 5 (**Fig 4-1**). A numerical value of 1

represents "normal mitochondria" with tight, parallel, abundant cristae, while 5

represents the "most disturbed" mitochondria with loose, few and erratic patterning of

cristae.   We observed that cells experienced maximal disturbance by day 2 post-

activation, and slowly restored mitochondrial shape as cells began to rest (**Fig 4-2 A,B**).

This followed a similar kinetic pattern in cells grown in low glucose, although the

magnitude of disruption was decreased. Individual mitochondrial area drastically

increased following near identical kinetics to cristae disruption, again with low glucose

experiencing less dramatic swelling (**Fig 4-2 C**). As mitochondria swelling increased,

mitochondria became less elongated (**Fig 4-2 D**). All of this was largely temporary, and

as cells began to slow rates of proliferation their mitochondria cristae, size, and shape

began to normalize to baseline. Interestingly, the mitochondria of cells in low glucose

began to elongate even further than baseline by day 5 post-activation. Fascinatingly

despite the loss in both cristae structure and patterning, T cells experience large

increases in oxygen consumption rate (OCR, an indirect measurement of oxidative

phosphorylation) by 24 hours post-activation, maintain the ability for heightened

oxidative phosphorylation, and begin to slowly decrease oxidative phosphorylation back

down to baseline (**Fig 4-2 E**). Extracellular acidification rate (ECAR, an indirect

measurement of glycolysis) increases until 48 hours post-activation, before slowly

decreasing (**Fig 4-2 F**). ECAR was not observed to decrease entirely back to baseline by

10 days post-activation.

While cells were able to restore mitochondrial size and cristae structure several

days following activation, it was unclear whether individual mitochondria would be able

to recover, or whether the swollen mitochondria were removed by mitophagy and new

mitochondrial were generated. We activated T cells in optimal glucose until maximal cristae disturbance was observed (48 hours post activation) and switched some of the cells acutely to low glucose media for several hours (**Fig 4-3 A**).   We found that within 1 hour, the mitochondria from cells moved from optimal glucose to low glucose, were indistinguishable in cristae disturbance or size from mitochondria grown in low glucose the entire duration of activation (**Fig 4-3 B-D**). This data suggests that mitochondria are able to adapt readily to nutrient alterations by quickly altering their native cristae morphology and size.

Cytochrome C is not sequestered in the mitochondria of activated T cells in optimal glucose

Mitochondrial swelling often occurs from a large influx of water and solutes from the cytoplasm and frequently associated with induction of intrinsic apoptosis pathways (Cai et al., 1998; Crompton, 1999). The mitochondria permeability transition pore (MPTP) forms a pore connecting the inner and outer mitochondrial membranes and regulates the permeability of the mitochondria. The individual components of the MPTP have been frequently debated and highly controversial, but can permit the release of cytochrome C from the mitochondria (Gogvadze et al., 2006). Cytochrome C is a highly soluble protein typically involved in the electron transport chain, and can be released from the mitochondria and initiate apoptosis under certain stimuli. Despite seeing very little cell death and no observable caspase cleavage upon T cell activation at

48 hours post-activation during maximal mitochondrial swelling, we sought to examine

if the MPTP was indeed opening upon activation.

We first transduced CD4+ T cells with a lentiviral construct expressing

cytochrome C fused to GFP. We found that T cells grown in optimal glucose expressed

cytochrome C throughout the cytoplasm and nucleus (**Fig 4-4 A**). However as we placed

cells into low glucose, we found that cytochrome C began accumulating in distinct

cytoplasmic punctae. We later verified that these cytoplasmic punctae were indeed

mitochondria. This process took up to 48 hours-post activation for complete loss of

nuclear fluorescence. Lentiviral overexpression and fusion protein dynamics can

interfere with proper localization of expressed proteins, and subsequently used cellular

fractionation to confirm cytochrome C localization in wild-type activated T cells. Once

again we found that cytochrome C largely did not localize to the membrane fraction

(which includes endoplasmic reticulum, golgi apparatus, mitochondria contents) in T

cells activated in optimal glucose (**Fig 4-4 B**). Whereas T cells stimulated in low glucose

localized cytochrome C entirely to the membrane fraction. Again matching similar

kinetics, when cells are moved from optimal to low glucose, cytochrome C levels in the

cytoplasmic over the next 48 hours are slowly decreased (**Fig 4-4 C**). This process

appears to be unique to T cells, because embryonic kidney 293T cells do not have

cytoplasmic cytochrome C in optimal glucose.

Mitochondrial dysfunction correlates to glycolytic rate and not oxidative phosphorylation

Several studies have reported that common pharmacological drugs/nutrient conditions can have a range of effects on mitochondrial shape or fusion/fission dynamics in different cell types (Buck et al., 2016; Liesa and Shirihai, 2013; Mishra and Chan, 2016; Trudeau et al., 2012). We found that CD4 T cells activated in hypoxia or Mdivi1 (a mitochondrial fusion inhibitor) had significantly higher cristae disturbance at day 5 post-activation than cells simply activated in optimal glucose (**Fig 4-5 A,B**). Furthermore, we found that cells grown in rapamycin (an mTORC1 inhibitor) had reduced levels of cristae disturbance compared to cells in optimal glucose. This directly correlated to their basal glycolytic rates as measured by the extracellular acidification rate (ECAR, **Fig 4-5 C,E**).   Surprisingly mitochondrial cristae disruption had no significant correlation to basal rates of oxidative phosphorylation as measured by oxygen consumption rate (OCR, **Fig 4-5 D**).

Mitochondrial dysfunction correlates to ROS production and voltage potential

We started to ask if these mitochondrial morphology changes could affect other mitochondrial functions or products. We found that the most swollen and disturbed mitochondria also generated the highest levels of ROS and voltage potential (Mdivi1 or hypoxia), whereas the cells with the least disruption had the least ROS or voltage potential (low glucose or rapamycin treatment, **Fig 4-6 A-B**). While our data currently indicates correlations, we hypothesize that these mitochondrial morphology changes are causing the increase in ROS production following activation.

Future Directions and Discussion

Our data supports a model where an activation signal drives mitochondrial

morphology changes, which subsequently drives ROS production. With the recent data

that reactive oxygen species facilitates tumor and T cell proliferation, we hypothesize

ROS are needed at a careful balance in T cells (Kong and Chandel, 2018; Sena et al.,

2013). Too little ROS, and T cells may not be able to make the important proliferative

signals (IL-2 production, NFAT nuclear localization, ERK MAPK or JNK pathway activation)

needed to support proliferation, while too much ROS can cause excessive cellular

damage and death (**Fig 4-7**). Much of our current work is focused on altering ROS in

settings of cristae disturbance and examining effects on cellular viability and

proliferation. We have developed two lentiviral constructs that overexpress a

mitochondria-targeted catalase and superoxide dismutase, two enzymes with

antioxidant activity.

We are also attempting to identify the "activation signal" responsible for these

mitochondrial morphology changes. We are attempting to create a minimalist system

where we isolate mitochondria and test the identity of the "signal" by solely adding

activation signals, activated T cell cytoplasm, or glucose to induce morphology changes.

The process is incredibly slow because our only method of examining cristae is through

low-throughput, expensive electron microscopy. However most of our experiments

have indicated mitochondrial size and cristae disturbance are strongly related, and we

may be able speed these up in confocal experiments by examining isolating and

quantifying individual mitochondrial size. One of the other major concerns is that if this "signal" is needed for other parts of T cell activation, it may be hard to exclusively examine its role in mitochondrial morphology.

Our data that cytochrome C is not sequestered in the mitochondria is particularly surprising, considering its role in apoptosis. Identifying the maturation state of cytochrome C may also play a large role in better understanding of this process.   We will need increased resolution using inducible cytochrome C expression and/or translation inhibitors to fully identify cytochrome C kinetics, maturity and localization status. Formation of mature cytochrome C (holocytochrome C) requires mitochondrial localization and its release is sufficient to induce apoptosis (Cai et al., 1998). The precursor apocytochrome C travels to the mitochondria and can spontaneously insert into the mitochondrial outer membrane, and is not able to induce apoptosis. Apocytochrome C eventually binds to heme lyase where it becomes fully matured bearing a heme group and refolded and traveling to the mitochondrial inner membrane. We cannot conclude from our current data whether holocytochrome C is leaving the mitochondria upon activation due to the opening of the MPTP, or whether newly made apocytochrome C cannot somehow enter the mitochondria in optimal glucose. If the former is true, we must seek to understand why mature, cytoplasmic C is not able to induce caspase activation in activated T cells. If the latter is true, it may explain why the cells are not inducing apoptosis but does not explain why apocytochrome C cannot enter the mitochondria.

Our data provides another example of the importance of mitochondria outside of oxidative phosphorylation and energy production. This project further underscores an important theme throughout my thesis the surprising roles certain metabolic pathways or metabolic byproducts (in this case ROS) play during T cell activation and act on proliferative signals or production of a specific cytokine (in this study IL-2).

Materials and Methods

Study Design

The purpose of this study was to identify how mitochondria are functionally affected from the mitochondrial swelling and cristae disturbance observed following T cell activation. The number of replicates per experiment are indicated in the figure legends and performed in a controlled and non-blinded manner.

Cell Culture and Activation

Human CD4 T cells are isolated, washed twice in PBS, and then placed in IB2H serum-free medium containing optimal (35mM) low (0.35mM) glucose concentrations.   The medium was supplemented with 1x chemically defined lipid mixture (ThermoFisher Scientific, 11905031, individual lipid concentrations available online) and 8mM L-glutamine.   Cells were then activated at 1 million cells per mL using Dynabeads® Human T-Expander CD3/CD28 (ThermoFisher Scientific, 11131D) at a concentration of 3 beads per cell. Additional volumes of medium were added on Day 3 and every other day after so that each culture was at 0.5 million cells/mL after feeding. Cells were treated with vehicle (DMSO), rapamycin (500nM, Sigma Aldrich, 553210), mdivi1 (20μM, Sigma Aldrich, M0199), or placed in hypoxia (1% oxygen) or normoxia (21% oxygen).   cDNA encoding cytochrome C-GFP was synthesized (IDT) and transferred into pTRPE, a lentiviral transfer vector (Leibman et al, submitted). Lentiviral supernatants and T cell transduction were generated and performed as previously described (Parry et al., 2003)

Western Blotting

Cells were fractionated using the Subcellular Protein Fractionation Kit for Cultured Cells (Thermofisher Scientific, 78840) according to manufacturer's instructions. Proteins were resolved by SDS-PAGE and transferred to nitrocellulose. Blots were probed with anti-Cytochrome c (Cell Signaling Technology, 11940), HSP90 (Cell Signaling Technology, 4877S), SDHA (Cell Signaling Technology, 11998), COX IV (Cell Signaling Technology, 4850)

anti-LC3B (Cell Signaling Technology, 3868) and anti-β-actin (Cell Signaling Technology, 4970). Protein was visualized using Odyssey CLx LI-COR instrument.

Confocal Microscopy

To quantify neutral lipid droplets, cells were stained with 500ng/mL Bodipy 493/503 (ThermoFisher Scientific, D3922) in serum free medium at 37 degrees Celsius for 30 minutes. Cells were then washed 2x with PBS and placed in their respective media. Cells were live imaged at 37 degrees Celsius using a stage heater on the Leica TCS SP8 Confocal microscope.

Mitochondrial Dyes

Mitochondrial mass was observed by staining cells using Mitotracker Deep Red (Thermofisher Scientific, M22426) at 5nM for 15 minutes at 37 degrees Celsius in serum-free media. Mitochondrial super oxide production was quantified by staining cells using Mitosox Red Mitochondrial Superoxide Indicator (Thermofisher Scientific, M36008) at

5μM for 15 minutes at 37 degrees Celsius in serum-free media. Voltage potential was

quantified by staining cells using Tetramethylrhodamine, ethyl ester perchlorate (TMRE,

Thermofisher Scientific, T669) a 20nM for 15 minutes at 37 degrees Celsius in serum-free media.

All stained cells were washed 1-2x with PBS before confocal microscopy or flow cytometry.

Transmission Electron Microscopy

Tissues for electron microscopic examination were fixed with 2.5% glutaraldehyde, 2.0%

paraformaldehyde in 0.1M sodium cacodylate buffer, pH7.4, overnight at 4°C.   After

subsequent buffer washes, the samples were post-fixed in 2.0% osmium tetroxide for 1

hour at room temperature, and then washed again in buffer followed by water. After

dehydration through a graded ethanol series, the tissue was infiltrated and embedded

in EMbed-812 (Electron Microscopy Sciences, Fort Washington, PA). Thin sections were

stained with uranyl acetate and lead citrate and examined with a JEOL 1010 electron

microscope fitted with a Hamamatsu digital camera and AMT Advantage image capture

software.

Seahorse XF Assay

OCR and ECAR were measured using a 96-well XF extracellular flux analyzer (Seahorse

Bioscience). 250k cells per well at 48 hours post-activation in optimal or low glucose

IB2H medium , washed with PBS, and transferred to warm, optimal or low glucose

supplemented, XF Seahorse medium.

Statistics

Statistical analysis on correlational data was performed using linear regression analysis.

Significance determined at $p < 0.05$, and error bars indicating mean plus or minus SEM.

All calculations were made using GraphPad Prism 5 software (GraphPad Software Inc.)

or Microsoft Excel.

Figures

"Normal Cristae"   "Disturbed Cristae"
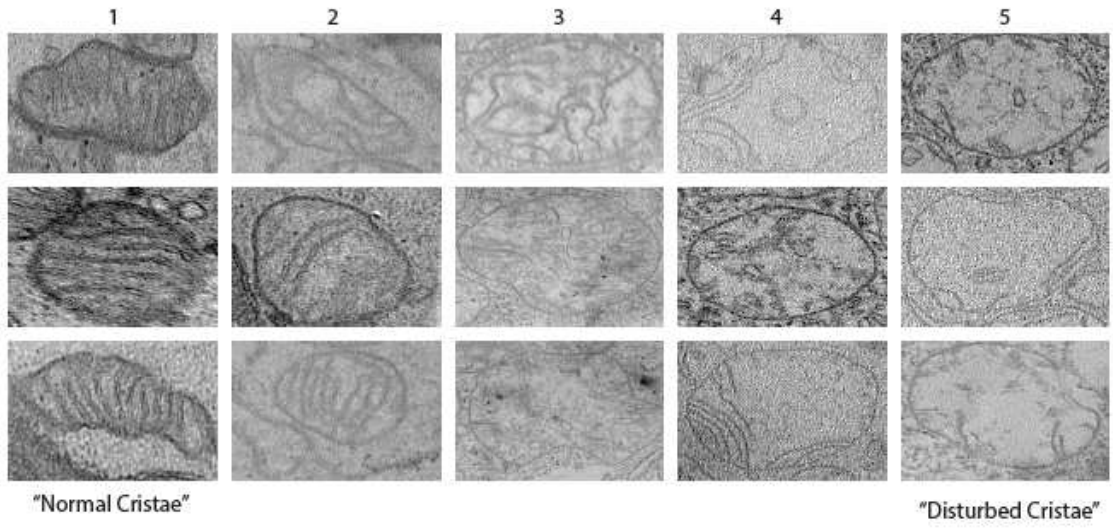
Figure 4-1

Figure 4-1: Quantitative Scale of Cristae Disturbance.

Representation of mitochondria with range of cristae disturbance observed in T cells during activation. Scale is a numerical range from 1 to 5. 1 represents normal mitochondria with tight, parallel cristae morphology, while 5 represents disturbed mitochondria with few, loose, non-parallel cristae.
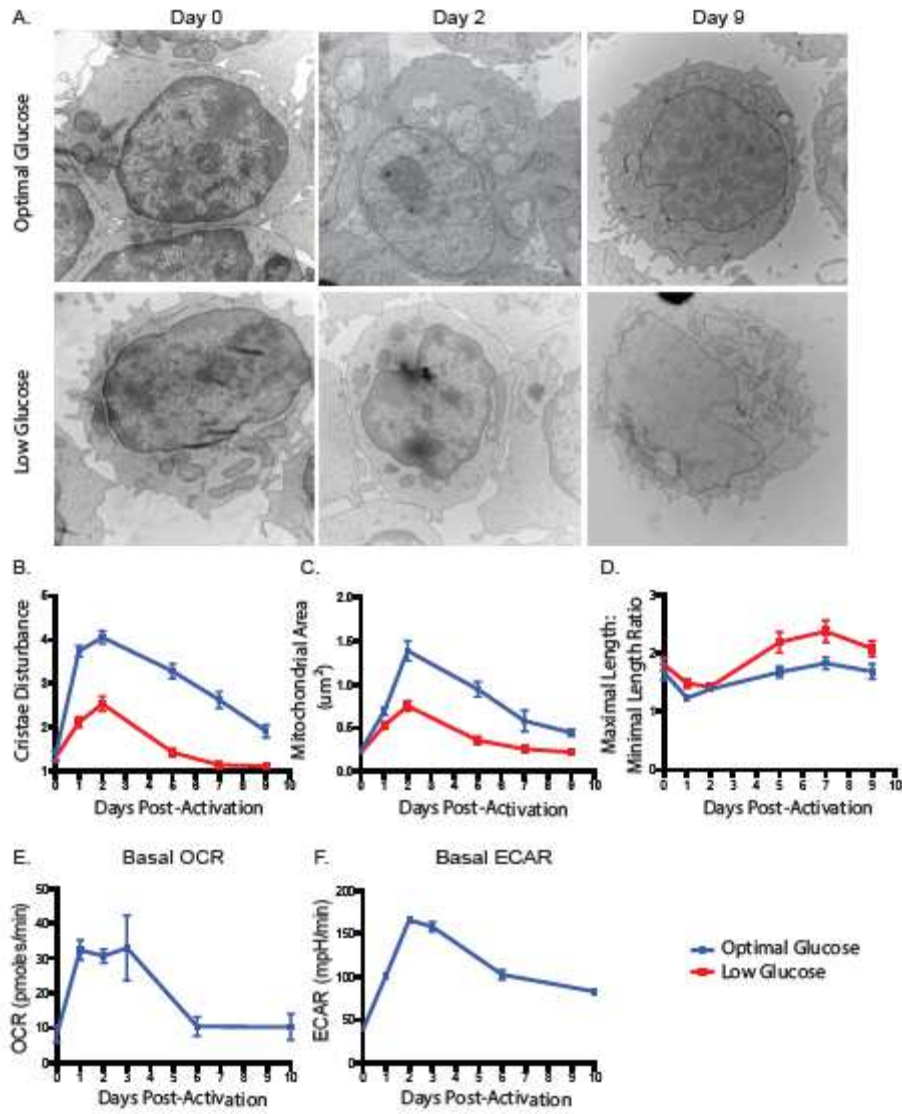
Figure 4-2

Figure 4-2: CD4 T cells reversibly alter mitochondrial structure upon activation in a glucose dependent manner.

A. Total CD4 T cells are activated with anti-CD3/CD28 coated beads in optimal (35mM) or low glucose (0.35mM) and cultured for 9 days. Cells are fixed on days 1, 2, 5, 7, and 9 days- post-activation for transmission electron microscopy (TEM). Representative images are shown. **B.** Cristae disturbance was measured via TEM Approximately 40 cells were measured per indicated time point and condition. **C.** Mitochondrial area was measured via TEM. Approximately 40 mitochondria, and at least 20 cells were measured per indicated time point and condition. **D.** The maximal length of each mitochondria was determined and ratioed to the minimal length of each mitochondria via TEM. Approximately 40 mitochondria, and at least 20 cells were measured per indicated time point and condition. Error bars represent SEM.

A.

Day 2:   Optimal Glucose   Opt. to Low 1hr   Opt. to Low 24hrs   Low Glucose

B.

Cristae Disturbance

Opt. Glucose / Opt. to Low 1hr / Opt. to Low 24hrs / Low Glucose

C.

Mitochondrial Area (um^2)

Opt. Glucose / Opt. to Low 1hr / Opt. to Low 24hrs / Low Glucose

D.

Maximal Length: Minimal Length Ratio

Opt. Glucose / Opt. to Low 1hr / Opt. to Low 24hrs / Low Glucose
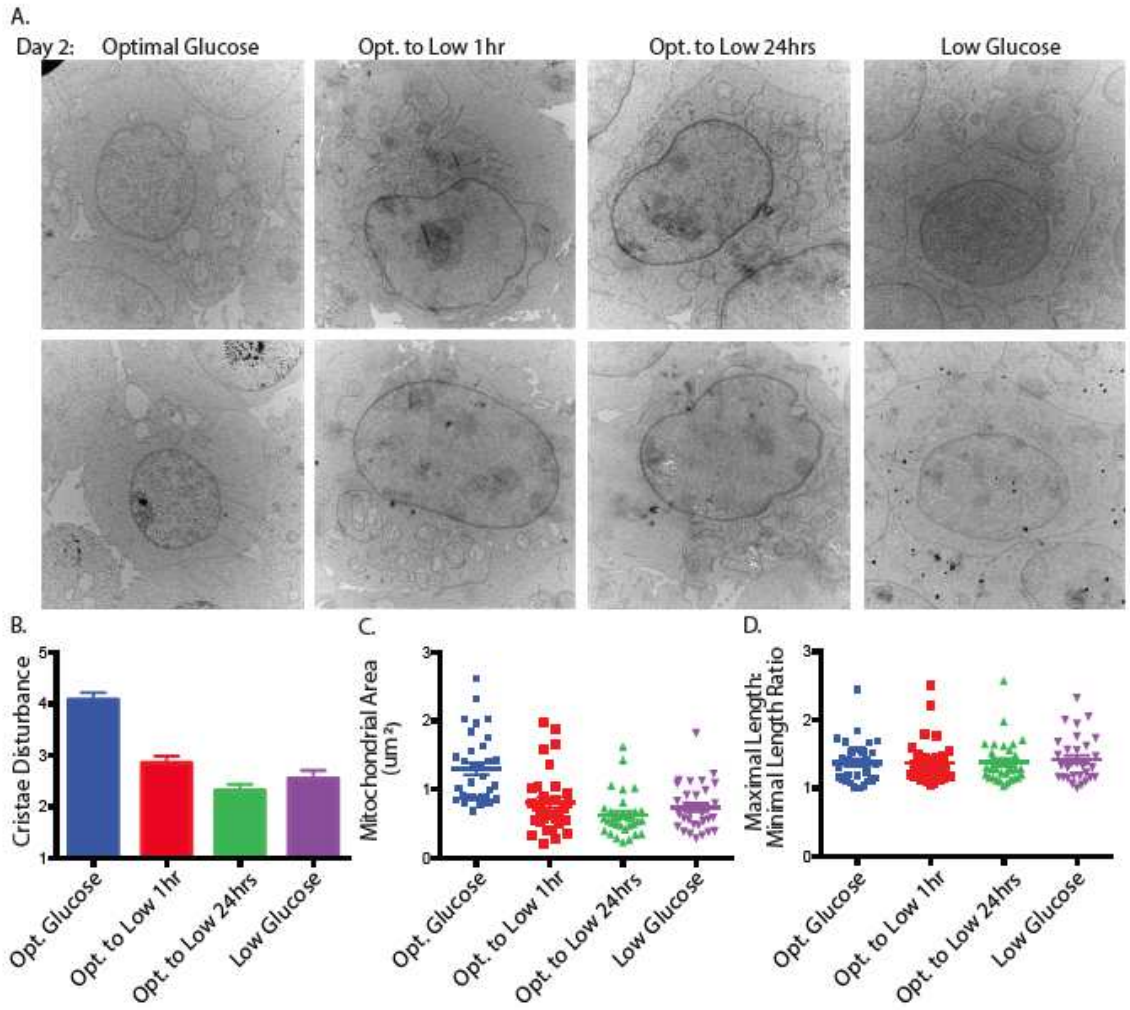
Figure 4-3

123

Figure 4-3: CD4 T cells adjust mitochondrial structure acutely to changes in glucose availability.

A. Total CD4 T cells are activated with anti-CD3/CD28 coated beads and grown in optimal or low glucose for 48 hours, or moved from optimal to low glucose for 1 or 24 hours at 48 hours post-activation. Representative images are shown. **B.** Cristae disturbance was measured via TEM (scale 1-5, 1 represents normal, parallelel, tight cristae morphology, while 5 represents few, loose, non-parallel cristae). Approximately 40 cells were measured per indicated time point and condition. **C.** Mitochondrial area was measured via TEM. Approximately 40 mitochondria, and at least 20 cells were measured per indicated time point and condition. **D.** The maximal length of each mitochondria was determined and ratioed to the minimal length of each mitochondria via TEM. Approximately 40 mitochondria, and at least 20 cells were measured per indicated time point and condition. Error bars represent SEM.

A.

Optimal Glucose

Opt to Low 6hrs

Opt to Low 48hrs

Mitotracker Overlay

B.

	Cytoplasmic		Membrane		
	Optimal Glucose	Low Glucose	Optimal Glucose	Low Glucose	

Cytochrome C

HSP90

SDHA (Mt. Complex II)

COX (Mt. Complex IV)

C.

	Cytoplasmic					
	Optimal Glucose	Low Glucose	Opt. to Low 6hrs	Opt to Low 24hrs	Opt to Low 48hrs	293T

Cytochrome C

HSP90

Figure 4-4

125

Figure 4-4: Cytochrome C is not sequestered in the mitochondria of activated T cells in optimal glucose.

A. Total CD4 T cells were stimulated with anti-CD3/CD28 coated beads and transduced with cytochrome C-GFP (green) in optimal glucose. After 72 hours of activation, cells were left in optimal or transferred into low glucose for the indicated time points. The right column are cells transduced with cytochrome C-GFP (green) and co-stained with mitotracker Deep Red (red) in the indicated conditions. **B.** Total CD4 T cells were activated with anti-CD3/CD28 coated beads in optimal or low glucose for 72 hours. Cell were fractionated into cytoplasmic and membrane fractions, and these fractions were probed for Cytochrome C, HSP90, SDHA, and COX. **C.** T cells were activated with anti-CD3/CD28 coated beads in optimal or low glucose for 72 hours, or moved from optimal to low glucose in the indicated time point. Cell lysates from these T cell conditions or 293T cells were fractionated into cytoplasmic fractions and probed for cytochrome C and HSP90.

A.

Day 5: Optimal Glucose | Optimal Glucose +Rapamycin | Optimal Glucose + Hypoxia | Optimal Glucose+ Mdivi1

B.

Cristae Disturbance

Opt. Glucose, Low Glucose, Rapamycin, Hypoxia, Mdivi1

C.

ECAR (mpH/min)

Opt. Glucose, Low Glucose, Rapamycin, Hypoxia, Mdivi1

D.

$r^2 = 0.0507$
$p = 0.7207$

Basal OCR (pmoles/min)

Cristae Disturbance

E.

$r^2 = 0.8263$
$p = 0.0467$

Basal ECAR (mpH/min)

Cristae Disturbance

Figure 4-5

127
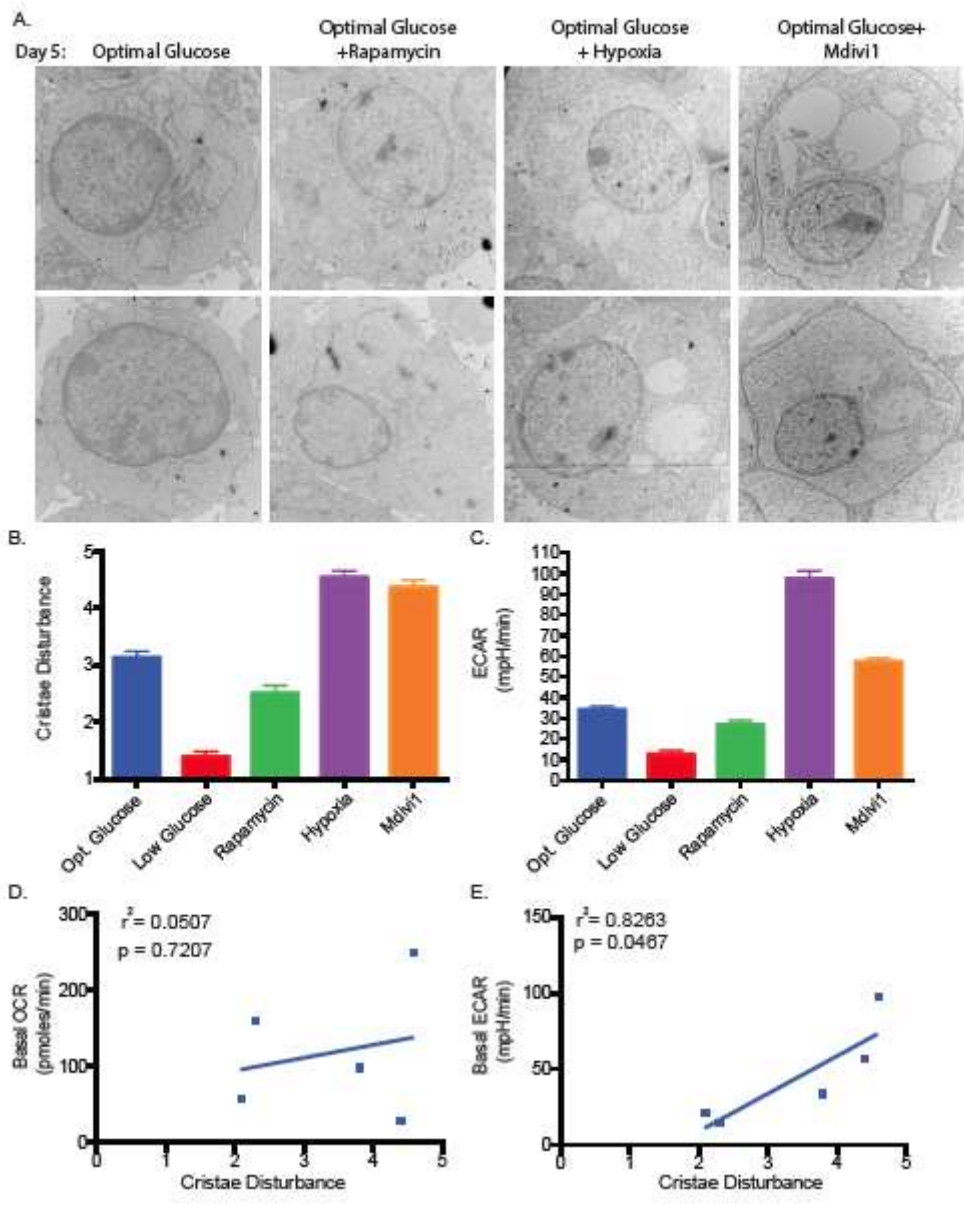
Figure 4-5: Mitochondrial dysfunction correlates to glycolytic rate and not oxidative phosphorylation.

A. Total CD4 T cells are activated with anti-CD3/CD28 coated beads and grown in optimal glucose or during the indicated condition in optimal glucose for 5 days. Representative images are shown. **B.** Cristae disturbance was measured via TEM (scale 1-5, 1 represents normal, parallel, tight cristae morphology, while 5 represents few, loose, non-parallel cristae). Approximately 40 cells were measured per indicated time point and condition. **C-E.** Total CD4 T cells are activated with anti-CD3/CD28 coated beads and grown in optimal or during the indicated condition for 5 days. Basal extracellular acidification rate (ECAR) and basal oxygen consumption rate (OCR) were measured by XF Seahorse Analyzer. For correlation analyses, linear regression analysis was used. A *p*-value of <0.05 was considered significant.

A. ROS Production

B. Voltage Potential

Optimal Glucose

Low Glucose

Rapamycin

Hypoxia

Mdivi1

Mitosox

TMRE

Figure 4-6

129
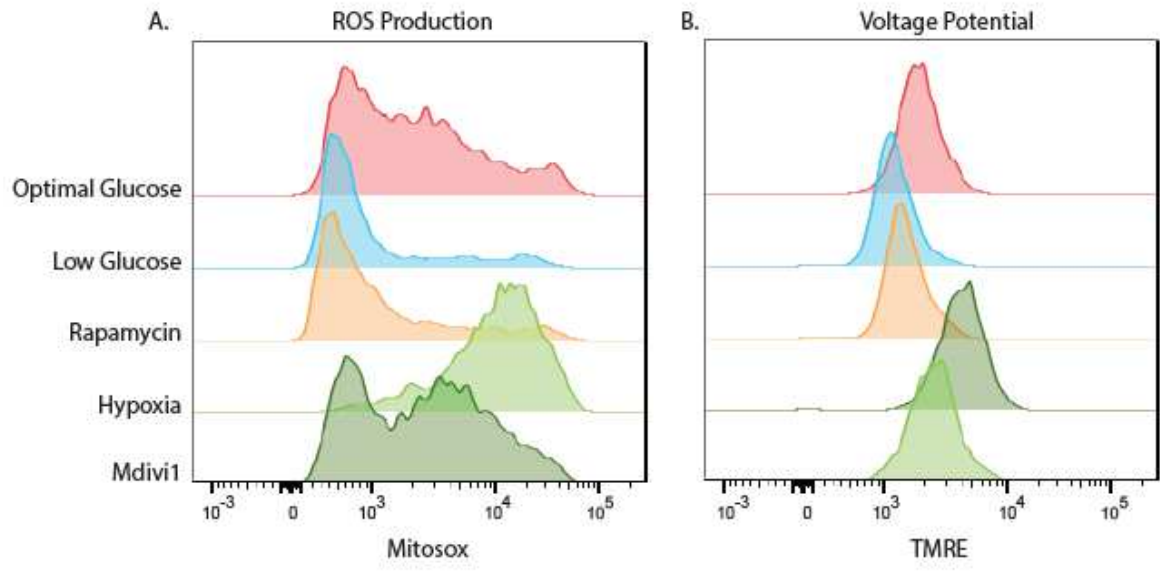
Figure 4-6: Mitochondrial dysfunction correlates to mitochondrial ROS production and polarization.

A-B. Total CD4 T cells are activated with anti-CD3/CD28 coated beads and grown in optimal glucose, low glucose or the indicated condition in optimal glucose for 5 days and stained with Mitosox (A) or TMRE (B).

Working Model:
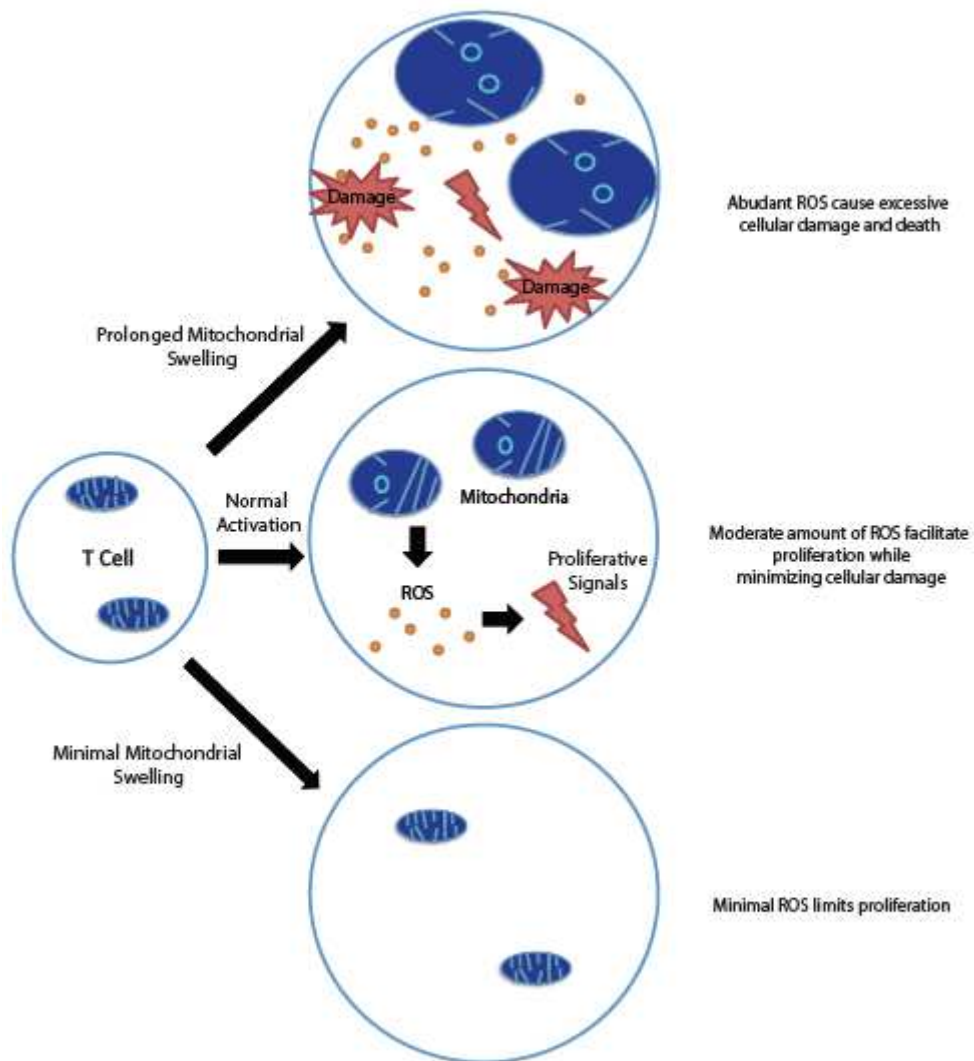
Figure 4-7

Figure 4-7: Working model for cellular outcomes of mitochondrial disturbance.

When T cells are activated in sufficient nutrients, an activation signal triggers mitochondrial swelling and cristae disturbance. These morphological changes are temporary and reverse over the course of T cell activation. Temporary swelling of mitochondria promotes moderate mitochondrial ROS production, and subsequently facilitates cellular signals (IL-2, NFAT nuclear localization, JNK, ERK MAPK pathways) that promote proliferation. If the mitochondria swelling is prolonged (as in the case of hypoxia or Mdivi1 treatment), these mitochondria make significant amounts of ROS. Too much ROS promotes cellular damage and eventual cell death in these cells. If the mitochondria swelling is largely prevented (as in the case of low glucose or rapamycin production), ROS production is minimal. Without ROS production, proliferation is inhibited.

Chapter 5- Summary, Discussion, and Future Directions

The full implications of Warburg metabolism during T cell activation are numerous, complex, and still not fully understood. Warburg metabolism endows T cells with the ability to not only rapidly proliferate but also to engage effector functions upon T cell stimulation. The tumor microenvironment presents a major challenge to T cell activation by restricting glucose availability. How do T cells and tumor cells, which both rely on Warburg metabolism, compete in the solid tumor microenvironment?   My first project sought to understand how T cells relied on mitochondrial pathways when they could no longer rely on Warburg metabolism because nutrients were limiting. Specifically we asked what metabolic pathways do T cells rely on when glucose is absent or limiting, and how does T cell reliance on alternative metabolic pathways interplay with their proliferation and functionality. My second project identified a novel relationship between Warburg metabolism and mitochondrial structural changes during T cell activation. We attempted to identify the activation signals responsible for these structural changes, as well as how these mitochondrial changes may subsequently promote T cell activation.   Collectively my thesis projects have sought to understand how mitochondria adapt to glucose availability to fulfill the requirements of T cell activation. My thesis has identified novel connections between Warburg metabolism and mitochondrial pathways, and how together they contribute to T cell functionality in diverse environments.

Summary, Discussion, and Future Directions for Chapter 3

Recent clinical trials focused on augmenting T cell responses through adoptive transfer of tumor-specific T cells have had breakthrough successes in treatment of leukemia and lymphomas. However, these therapies have failed to be effective in many solid tumors, where cancer cells can set up an immunosuppressive niche. We speculate that these failures in solid tumors are caused by the tumor microenvironment's limiting supply of key nutrients critical for T cell activation. The existing literature that has explored nutrient limitation has focused on the total population of T cells found in the blood. We hypothesized that due to more frequent exposure to nutrient limitation, effector memory T (T_{EM}) cells may be more adept at maintaining proliferative and functional capacity during nutrient deprivation than naïve or central memory T cells. We found that during glucose limitation, T_N and T_{CM} cells begin to rely on mitochondrial pathways. T_N and T_{CM} cells upregulate oxidative phosphorylation by utilizing fatty acid oxidation and rerouting glutamine for *de novo* fatty acid synthesis. Conversely, T_{EM} cells are unable to increase oxidative phosphorylation or fatty acid synthesis. We then discovered a surprising regulatory role for fatty acid synthesis on effector functions. T_N cells which relied heavily on fatty acid synthesis for survival and proliferation downregulated IFN-γ production during glucose depletion, while T_{EM} cells preserved IFN-γ production in glucose depletion by not relying on fatty acid synthesis. Pharmacological inhibition of fatty acid synthesis was sufficient to promote IFN-γ production only in T_N cells. We hypothesize this independence from fatty acid synthesis

134

in T_{EM} cells allows them to maintain functionality in all sites of nutrient limitation (commonly observed in inflammation or cancer). More broadly our study uncovered a novel role for metabolic salvage pathways in cytokine production. We discovered that alternative metabolic pathways are not simply used for survival during nutrient stress, but can also regulate cellular functionality by modifying cytokine production.

Whether T_{EM} cells completely unable to rely on fatty acid synthesis remains unclear.   While T_{EM} may not rely on fatty acid synthesis during glucose limitation, they can survive in fatty acid-free media for longer than T_N or T_{CM} cells. Thus we wondered whether T_{EM} cells might have been able to perform fatty acid synthesis in fatty-acid free media, or that they might need less fatty acids to survive. T_{EM} cells might simply require lower amounts of fatty acids (from fatty acid synthesis and exogenous fatty acids), because they proliferate less than T_N or T_{CM} cells and thus may require fewer membrane components. In our hands, several enzymes (ACC1, FAS) in the fatty acid synthesis pathway exhibit equivalent gene expression in T_{EM} as their T_N or T_{CM} counterparts. However, we have not examined the RNA expression of every enzyme involved in fatty acid synthesis nor have we quantified protein expression of these enzymes. We also would need to perform more tracing studies of glutamine and glucose to fully examine if T_{EM} under certain contexts can perform fatty acid synthesis and reductive glutaminolysis. Furthermore manipulation of fatty acid pathways appear tightly regulated and feature redundant pathways. We had little success studying the role of fatty acid pathways in T cells by overexpressing known fatty acid transporters (CD36,

135

FABP4, FABP5). While we were able to achieve surface overexpression of these fatty

acid transporters, we never observed an increase in fatty acid uptake (data not shown).

Our data indicate that while lipid metabolism may promote survival during

nutrient depletion, they may frequently hamper T cell function. However, more work

will be needed to clarify the role of fatty acid metabolism in T cell function *in vivo*.

Several solid tumors (like ovarian cancer) can form in adipose rich tissue and could be a

useful model to better understand fatty acid metabolism during nutrient deprivation.

Future studies may help elucidate the spatial organization of immune cells, adipocytes,

and tumor cells in human clinical samples.   Unpublished, but publically presented work

by Susan Kaech's group has demonstrated that CD36 knockout, tumor-specific T cells

have enhanced anti-tumor efficacy compared to wild-type T cells in multiple models of

solid tumors. This is largely consistent with our *in vitro* findings that exogenous fatty

acids inhibit T cell functionality. Further evidence of the importance of lipid metabolism

in nutrient deprived T cells comes from a paper demonstrating TILS (tumor infiltrating

lymphocytes) in a mouse model of melanoma had large increases in lipid uptake

compared to T cells in the spleen (Zhang et al., 2017). The authors found that utilizing

peroxisome proliferator activated receptor-α (PPAR-α) agonist that promoted fatty acid

catabolism and simultaneously promoted higher T cell engraftment and

polyfunctionality. Interestingly, suppressing fatty acid catabolism by knocking out PPAR-

α inhibited anti-tumor functionality of T cells. While this study appears opposed to both

ours and Susan Kaech's data, it could be that a careful balance of fatty acid metabolism

is needed for survival of T cells in the solid tumor microenvironment, while too much reliance on fatty acid metabolism can harm functionality. Alternatively, it may be that altering exogenous fatty acid uptake, and fatty acid oxidation pathways are not synonymous processes. Long-chain fatty acids can have a diverse range of fates including components of phospholipid bilayers which all membranes are made of in the cell, secondary signaling messengers (which are known to play key roles in early T cell signaling), TCA cycle intermediates and energy. Thus increasing fatty acid uptake may serve a large number of cellular processes, while fatty acid oxidation may only increase TCA cycle intermediate concentrations and energy production.

The role of fatty acids in immunity may not be entirely surprising, as links between fat metabolism and immunity have been evolutionarily conserved since at least invertebrates. The fat bodies in insects act as important immune organs that can secrete key effector molecules like antimicrobial peptides and factors for wound healing (Zasloff, 2002). Many of these responses are released only after immune stimulation via damage signal receptors such as Toll (Krautz et al., 2014). Adipocytes and immune cells resident in adipose tissue are also widely recognized to be involved in inflammatory processes in higher eukaryotes (Kolodin et al., 2015; Mathis, 2013; Trayhurn and Wood, 2004). Anatomically many lymph nodes are surrounded by adipose rich tissue. Very few studies have attempted to understand how the adipocytes around lymph nodes respond during immune activation, and this will need to be explored in a variety of immune contexts (Pond and Mattacks, 1995).

Consistent with previous studies we found that T cells rely on futile cycling of fatty acids, a paradoxical process in which cells utilize fatty acid synthesis and fatty acid oxidation. In limiting glucose, T cells increased both fatty acid oxidation and fatty acid synthesis. Energetically this appears to be inefficient, to essentially use ATP and NADPH to generate new fatty acids only to break them down again for ATP. Technically we can only measure these processes from large numbers of cells, and thus we don't know if these processes are occurring simultaneously in a single cell. Previously published work determined that during activation IL-15 treated T cells utilized futile cycling more so than IL-2 treated T cells (O'Sullivan et al., 2014). The authors believed that futile cycling may be required for long-term survival of memory T cells, and might be extended to stem cells and other long-lived cell types. While the exact reason for futile cycling remains largely unknown, researchers have proposed that it may be for generation of heat or allow for quicker adaption to regulatory/initiation signals (Curi et al., 2016; Katz and Rognstad, 1976). The role of heat produced by metabolism in T cell activation remains unexplored and requires further investigation.

We also need to examine whether our results on effector memory T cell metabolism reflect tumor infiltrating lymphocytes (at least before exhaustion begins) and how exhaustion may perturb metabolic adaptation. In collaboration with Shaun O'Brien, Steven Albelda, Jason Standalick, and Sunil Singhal we have received advanced stage non-small cell lung cancer patient (NSCLC) samples. As well described by other studies, we found that cells in the adjacent lung and diseased lung tissue are largely

effector memory (T_{EM}) or effector memory RA phenotype (T_{EMRA}), losing both CCR7 and

CD27 expression compared to patient PBMC. Other studies have observed that tumor

infiltrating lymphocytes have fewer mitochondria which are smaller and have less

voltage potential and perform less oxidative phosphorylation (Scharping et al., 2016;

Siska et al., 2017a).   These defects have largely been confined only to the cells in the

tumor microenvironment, and not to the T cells in the blood or lymph nodes. We

identified that these defects corresponded to all T cells in the lung, both near and far

away from the tumor microenvironment. We do not have lung tissue from healthy

lungs to distinguish whether this might be a lung-specific phenonomena or whether the

mitochondrial defects observed in the tumor microenvironment apply to the entire lung

tissue. However, these data certainly suggest the possibility that tissue-signals, rather

than tumor-signals act to regulate metabolic signatures of T cells in specific tissues.

These mitochondrial differences between blood T cells and lung T cells from

NSCLC patients appear to be highly reversible (data not shown). We found that

prolonged *in vitro* stimulation of NSCLC patient lung TILS and PBMC *in vitro* removes all

differences in mitochondrial mass between both populations.   These recent data were

extremely reminiscent of some of my earliest thesis work, where we sorted T cells based

on mitochondrial mass. We isolated CD4 T cells with the highest mitochondrial mass

and lowest mitochondrial mass. Upon stimulation, these isolated populations reverted

back to having an equal mitochondrial mass distribution. Furthermore, those

populations did not have observable differences in memory potential or proliferation

following expansion. This appears in contrast to earlier work where cells sorted on mitochondrial voltage potential exhibited differences in memory phenotype upon isolation and maintained those differences in differentiation and proliferation during *in vitro* expansion (Sukumar et al., 2016). These differences in conservation of *in vivo* phenotype during *in vitro* expansion may simply be because mitochondrial voltage potential may act as a surrogate for memory phenotype, whereas mitochondrial mass may not. This work is largely a testament to how much *in vivo* metabolism information may be lost during *in vitro* expansion.

Mitochondrial mass may be significantly regulated by tissue location via tissue-specific signals. T cells in white adipose tissue have much higher mitochondrial mass compared to T cells in the lamina propria (Han et al., 2017). Interestingly, this phenomena was not confined to only resident memory cells but all effector memory T cells in the white adipose tissue. These tissue-specific phenotypes may well extend beyond mitochondrial mass and extend to entire metabolic programs. The authors in the previous study found white adipose tissue T cells uptake large amounts of extracellular lipids in vivo compared to T cells in the spleen or lamina propria. Skin resident memory T cells appear to rely heavily on extracellular lipids for survival and persistence (Pan et al., 2017).   Lung resident memory T cells have elevated expression of numerous hypoxia inducible factor 1α (HIF1α) and a signature associated with glucose depletion (Hombrink et al., 2016) compared to T cells from the blood. These metabolic signatures were linked to the specific transcription factor Notch, which was

demonstrated to be vital for survival of lung resident T cells. Identifying tissue-specific

metabolic signatures for T cells, and the factors that regulate those signatures may be

critical for enhancing resident memory responses. What tissue-specific signals regulate

these metabolic programs in T cells and how permanent are these metabolic programs?

Furthermore, by identifying the signals driving metabolic signatures *in vivo* we may be

able to maintain tissue-specific metabolic programs *in vitro*.

Summary, Discussion, and Future Directions for Chapter 4

My second major project attempted to identify the activation signals responsible

for large l structural changes to mitochondria during T cell activation. Mitochondria can

swell up to five times their initial size within the first 48 hours of activation, and their

cristae lose standard shape and patterning. Despite these sweeping mitochondrial

changes, we found that T cells were able to upregulate oxidative phosphorylation.

Cytochrome C is not sequestered inside the mitochondria in T cells activated in optimal

glucose, and only becomes sequestered when cells are moved into low glucose. Despite

observable cytoplasmic cytochrome C, we did not observe caspase activation or cell

death. Furthermore using a variety of pharmacological inhibitors and altered

metabolite concentrations, we observed that mitochondria cristae disruption strongly

correlated with glycolysis, reactive oxygen species production, and voltage potential but

not oxidative phosphorylation.   Several studies have indicated that tightly folded cristae

are required for supercomplex organization which promotes efficient electron transport

and ATP production (Cogliati et al., 2013; Gomes et al., 2011). Our data stand in

141

contrast, and strongly indicate that mitochondria can have highly unfolded cristae and perform high levels of oxidative phosphorylation. These data may highlight a novel role for Warburg metabolism in modulation of mitochondrial structure and may apply to other cell types engaged in aerobic glycolysis.

The strong correlation between glycolysis, mitochondrial changes, and ROS production suggest a potential model relating T cell activation to mitochondrial changes. Our model suggests that glucose drives T cell activation signals such as mTOR, Akt, and NF-κB. Potentially one or several of these intermediate signals directly or indirectly alter mitochondrial size and cristae patterning, and we have evidence that at least mTORC1 activity is required for these mitochondrial changes. Mitochondrial swelling and cristae structure may drive ROS induction and our dta suggest that the two are strongly correlated. ROS production appears to facilitate proliferation in tumor cells and subsequent proliferation via IL-2 and NFAT signaling in T cells (Kong and Chandel, 2018; Sena et al., 2013). Thus mitochondria may swell during activation to produce ROS and subsequently proliferate. However, in conditions of sustained mitochondrial swelling and cristae disruption, these cells have large increases in ROS production that can not only promote proliferation but can begin to induce cell death, which we observe at highly increased levels in in hypoxia (data not shown). T cells in hypoxia have very swollen and cristae disturbed mitochondria and high ROS production. They also actually proliferate better than normoxic cells, although this is not reflected by cell number due

to increased cell death. This is our first model derived from largely correlational data, and of course as we learn more the order of events in this model may change.

The flexibility and rapid adaption of mitochondrial structure to changes in nutrient availability revealed by our data is quite striking. We found that by moving activated cells with highly disturbed cristae from optimal glucose to low glucose, the mitochondria were able to largely recover patterning and mitochondrial size within 1 hour. The speed of these changes likely indicates that they are not regulated by transcriptional events. Traditionally proteins involved in electron transport and mitochondria fusion/fission dynamics are thought to regulate cristae shape. ATP synthase dimers are known to be sufficient to induce membrane curvature in lipid bilayers (Jiko et al., 2015). Other proteins like optic atrophy 1 (Opa1), dynamin related protein-1 (Drp1), and members of the mitochondrial contact site and cristae-organizing system (MICOS) complex also further contribute and cooperate to regulate cristae shape. Several of these proteins like Drp1 are modified post-translationally through phosphorylation, which is critical for their activation or inhibition (Marsboom et al., 2012). While recent work demonstrates that T cells promote mitochondrial fission during activation, how all of these regulators work in tandem to control T cell cristae during activation remains elusive (Buck et al., 2016).

If the mitochondrial permeability transition pore (MPTP) is truly open in activated T cells, many proteins and metabolites are potentially leaving and entering the mitochondria. While our initial hypothesis has proposed that these swollen

143

mitochondria promote ROS species to propagate proliferation signals, it is highly possible that the migration of mitochondrial proteins into the cytoplasm could further contribute to T cell proliferation/function. Our data suggest cytochrome C is a potential protein that leaves the mitochondria, but the possibilities could include many other cytoplasmic and mitochondrial proteins or metabolites. Several laboratories have publically presented unpublished data indicating that specific TCA cycle metabolites modulate cytokine production. For example, Luke O'Neill's group has suggested that succinate can control IL-1β production, while citrate controls IFNα production in TLR-stimulated macrophages. There is a large amount of interest in how these metabolites may control epigenetic regulation. Metabolites can serve as both essential donors or cofactors for epigenetic modifying enzymes, and regulate protein activity via post-translational modifications or post-transcriptional regulation (Minocherhomji et al., 2012; Pietrocola et al., 2015; Reid et al., 2017; Siska and Rathmell, 2016). However no work to date has focused on how these metabolites leave the mitochondria during immune stimulation. Metabolite transport across the inner mitochondrial membrane appears complex and tightly regulated, with the human genome encoding a large number of mitochondrial transporters and channels (Kunji, 2004; Passarella et al., 2003; Wohlrab, 2009). Could opening of these channels or pores during T cell activation promote an efflux from the mitochondria and facilitate non-metabolic roles for mitochondrial metabolites?

Defining the Next Frontiers of Immunometabolism

It has become clear that the metabolic states of immune cells are fundamental to immune function, differentiation, and cellular identity. Transcription factors critical for cellular identity like FOXP3 regulate many cellular processes including metabolism (Angelin et al., 2017; Gerriets et al., 2016). In addition, alterations in metabolism are sufficient to induce dramatic changes in cellular functionality, polarization, and differentiation.   T regulatory cells typically rely on a careful balance of fatty acid oxidation and synthesis, as well as glycolysis for proliferation, migration and suppression (Kishore et al., 2017; O'Sullivan and Pearce, 2014; Procaccini et al., 2016).   Excessive phosphatidylinositol-3-OH kinase (PI(3)K) activity in T regulatory cells promotes elevated glycolysis and as a result these cells lose suppressive activity and have unstable lineage commitment (Huynh et al., 2015; Shrestha et al., 2015). Furthermore, these studies demonstrate that while the T regulatory cell population size decreases, a simultaneous expansion of the follicular helper T cell population or T helper type 1 cells is observed. The links between glycolysis and effector function and fatty acid metabolism with suppressive function is continually echoed in the literature in a variety of cell types. Immunosuppressive tumor-associated macrophages or alternatively activated macrophages utilize higher levels of fatty acid oxidation and oxidative phosphorylation compared to more inflammatory macrophages that utilize glycolysis (Galván-Peña and O'Neill, 2014; Hao et al., 2018).

If such a careful balance of different metabolic processes are needed for cell identity, how do T cells operate in such a diverse array of tissue environments? Which

metabolic pathways are required in which tissues or inflammatory contexts? To answer

these questions, we need to move beyond studying the cells from the blood and spleen.

Skin resident memory T cells require exogenous fatty acids for survival and protective

responses during infection with skin vaccinia virus (Pan et al., 2017). The transcription

factor Notch is required for maintenance of resident memory T cells in the lung and

regulates oxidative phosphorylation, glycolysis, and fatty acid synthesis-associated

genes (Hombrink et al., 2016). Single tissues have started to be examined, but large-

scale, systematic metabolomic analysis of cells present in different tissues in different

inflammatory contexts has not been examined. Recent studies clearly documented that

immune cells in separate tissues exhibit large phenotypical and metabolic differences

and are exposed to distinct pathogens over the host's lifetime (Gosselin et al., 2014;

Granot et al., 2017; Thome et al., 2014). Which gene expression differences or tissue-

specific signals drive distinct metabolic phenotypes of cells in different tissues?

Alternatively, which gene expression differences are due to distinct metabolic

phenotypes?

Theoretically it appears dangerous to tie cellular identity and function too tightly

to metabolism, especially in immune cells that travel to a diverse range of metabolic

niches. It appears to limit a cell's ability to respond appropriately in specific contexts.

For example, if exposure to exogenous fatty acids promotes a T-regulatory cell gene

expression profile, what if a strong immune response is needed from T effector cells in

adipose tissue? Alternatively, how is the immune system able to function in people

consuming high fat or high sugar diets? How does the immune system adapt to large

diet changes between people or even overtime within the same person? A large body

of work has characterized known immune-associated phenotypes in mice consuming

different diets.   However, it remains unknown how many of these phenotypes are due

to changes in nutrient uptake specifically by immune cells.

Much of the current work on nutrient availability in immune responses has

focused on nutrient limitation in the solid tumor microenvironment. Current work has

focused on the intense competition for glucose in the tumor microenvironment

between tumor cells and T cells. By specifically elevating tumor glycolysis, Ho et al. and

Chang et al. have uncovered the critical need for glucose in the solid tumor

microenvironment for immune-mediated tumor rejection (Chang et al., 2015b; Ho et

al., 2015b). Glucose is not the only key nutrient being competed for between T cells and

tumor cells, and many other nutrients may be required for anti-tumor responses.

However studies have not systematically manipulated other specific metabolic

pathways in tumor cells *in vivo* to search for additional critical nutrients regulating anti-

tumor responses. While overexpressing or inhibiting metabolic pathways in tumor cells

may be useful tools to explore nutrient competition and *in vivo* relevance of key

nutrients for tumor responses, we must be careful that our interpretations are not

caused by alterations to tumor growth independently of immune cells. For example,

Chang et al. utilized tumor cells with lentiviral overexpression of various glycolytic

enzyme in immune deficient Rag$^{-/-}$ mice and found no differences in tumor growth. We

also still lack a more holistic view of the competition between the multiple cell populations (tumor, effector T cells, T regulatory cells, stromal cells, suppressive myeloid populations, etc.) present in the tumor microenvironment.

Viral, bacterial and parasitic infections can also cause large changes in nutrient availability in the serum and tissue (Cui et al., 2018; Eltzschig and Carmeliet, 2011; Zhou et al., 2016). While these changes have been examined, very few studies have sought to understand how these nutrient changes during infection can impact subsequent immune responses. In one of these studies, increased acetate availability during systemic bacterial infection drove augmented immune function through enhanced memory recall responses (Balmer et al., 2016). Fascinatingly increased T cell activity alone is sufficient to decrease serum levels of many amino acids (Miyajima et al., 2017). More work is needed to understand how local tissue nutrient gradients promote or inhibit immune responses, and which nutrient changes are the most impactful on subsequent immune responses *in vivo*. Surprisingly little work has sought to understand how nutrient availability changes during infections in the lymph node. During potent immune responses, densely packed T cells are rapidly proliferating in the T cell zone, swarming around antigen presenting cells and performing large amounts of glycolysis. The massive influx and expansion of cells (via trapping of additional naive lymphocytes and proliferation of responding T cells) is enough to cause dramatic lymph node swelling and stromal remodeling. Can all responding T cells receive the same amount of glucose or other nutrients needed for proliferation and activation? Are nutrients limiting and do

different T cell clones (or even daughters of the same T cell) compete for their

acquisition of nutrients? Could memory T cells arise from naïve T cells during infection

because they were unable to acquire sufficient nutrients upon antigen exposure?

The utilization of mass spectrometry imaging (MSI, mentioned briefly in Chapter

3) will likely be a key tool in visualizing nutrient gradients and localization of immune

cells *in situ* (Dilillo et al., 2017; Holzlechner et al., 2017). Combined with tissue

sectioning and technical advancements in improving resolution of MSI, detailed spatial

organization of nutrient availability and immune cells can be overlaid. Although nutrient

gradients and immune cells have been examined separately through MSI, together the

data can usher in a new understanding of how T cells operate in a variety of contexts.

This technology has the potential to create detailed maps of nutrient availability and

how nutrients change during a variety of contexts (infection, cancer, obesity, diabetes)

and how successful therapeutic or immune interventions alternutrient availabilities.

Metabolites play large roles in immune function and differentiation by a diverse

array of mechanisms. Mitochondria produced ROS are required for NFAT nuclear

localization in T cells, adipocyte differentiation through PPARγ, and activation of the

inflammasome (Sena et al., 2013; Tormos et al., 2011; Zhou et al., 2011). The glycolytic

enzyme GAPDH can regulate translation of IFN-γ production, while publically presented

data by Luke O'Neill's lab suggests the TCA cycle metabolite, succinate, regulates IL-1β

production (Chang et al., 2013).   Acetyl-CoA can donate an acetyl group for histone

acetyltransferase-dependent acetylation of histones (Wellen et al., 2009). Thus multiple

metabolites can take on a multitude of functions in the cytoplasm, nucleus, or mitochondria. What are the mechanisms by which these metabolites act? And how are these metabolites (most notably mitochondrial metabolites) able to travel between compartments? Recent evidence indicates that while nuclear and cytoplasmic pools of acetyl-CoA are not physically separated because acetyl-CoA can pass through nuclear pores, some of the enzymes that generate acetyl CoA can travel to different compartments depending on environmental conditions and create local gradients (Sivanand et al., 2018).   Thus potentially a cell can temporarily enhance acetyl-CoA levels in specific compartments and modify compartment-specific activities.   Both global changes and gene-specific changes have been observed by modulating histone acetylation through metabolic changes (Lee et al., 2014b; Peng et al., 2016). Furthermore while metabolism plays a role in regulating global epigenetic enzyme activity, what directs their enzymatic activity to specific genes in the nucleus?   One answer may be that acetylation and other post-translational modifications of transcription factors can directly regulate their activity at specific loci. Acetylation is well described to modulate the activity of NF-κB, HIF 1α, Nrf2, and the FOXO family (and likely many others) which are known to regulate immunity (Thiagarajan et al., 2016).

We are still discovering new ways in which metabolic pathways influence immunity. Together my thesis offers some new insight into how fuel choice affects cytokine production and how T cell activation can influence mitochondrial structure. By

identifying metabolic axes of regulation in immunity, we may be able to create new

methods to improve existing immunotherapies and vaccines.

References

Airley, R., Loncaster, J., Davidson, S., Bromley, M., Roberts, S., Patterson, A., Hunter, R., Stratford, I., and West, C. (2001). Glucose transporter glut-1 expression correlates with tumor hypoxia and predicts metastasis-free survival in advanced carcinoma of the cervix. Clinical cancer research : an official journal of the American Association for Cancer Research *7*, 928-934.

Angelin, A., Gil-de-Gómez, L., Dahiya, S., Jiao, J., Guo, L., Levine, M.H., Wang, Z., Quinn, W.J., Kopinski, P.K., Wang, L.*, et al.* (2017). Foxp3 Reprograms T Cell Metabolism to Function in Low-Glucose, High-Lactate Environments. Cell Metab *25*, 1282-45098112.

Araki, K., Turner, A.P., Shaffer, V.O., Gangappa, S., Keller, S.A., Bachmann, M.F., Larsen, C.P., and Ahmed, R. (2009). mTOR regulates memory CD8 T-cell differentiation. Nature *460*, 108-112.
Balmer, M.L., Ma, E.H., Bantug, G.R., Grählert, J., Pfister, S., Glatter, T., Jauch, A., Dimeloe, S., Slack, E., Dehio, P.*, et al.* (2016). Memory CD8(+) T Cells Require Increased Concentrations of Acetate Induced by Stress for Optimal Function. Immunity *44*, 1312-1324.

Barneda, D., and Christian, M. (2017). Lipid droplet growth: regulation of a dynamic organelle. Curr Opin Cell Biol *47*, 9-15.

Bengsch, B., Johnson, A.L., Kurachi, M., Odorizzi, P.M., Pauken, K.E., Attanasio, J., Stelekati, E., McLane, L.M., Paley, M.A., Delgoffe, G.M.*, et al.* (2016). Bioenergetic Insufficiencies Due to Metabolic Alterations Regulated by the Inhibitory Receptor PD-1 Are an Early Driver of CD8(+) T Cell Exhaustion. Immunity *45*, 358-373.

Bennewith, K.L., and Durand, R.E. (2004). Quantifying transient hypoxia in human tumor xenografts by flow cytometry. Cancer research *64*, 6183-6189.

Berod, L., Friedrich, C., Nandan, A., Freitag, J., Hagemann, S., Harmrolfs, K., Sandouk, A., Hesse, C., Castro, C.N., Bähre, H.*, et al.* (2014). De novo fatty acid synthesis controls the fate between regulatory T and T helper 17 cells. Nat Med *20*, 1327-1333.

Beura, L.K., Hamilton, S.E., Bi, K., Schenkel, J.M., Odumade, O.A., Casey, K.A., Thompson, E.A., Fraser, K.A., Rosato, P.C., Filali-Mouhim, A.*, et al.* (2016). Normalizing the environment recapitulates adult human immune traits in laboratory mice. Nature *532*, 512-516.

Bhutia, Y.D., and Ganapathy, V. (2016). Glutamine transporters in mammalian cells and their functions in physiology and cancer. Biochimica et biophysica acta *1863*, 2531-2539.

Blagih, J., Coulombe, F., Vincent, E.E., Dupuy, F., Galicia-Vázquez, G., Yurchenko, E., Raissi, T.C., van der Windt, G.J., Viollet, B., Pearce, E.L*., et al.* (2015). The energy sensor AMPK regulates T cell metabolic adaptation and effector responses in vivo. Immunity *42*, 41-54.

Brand, A., Singer, K., Koehl, G.E., Kolitzus, M., Schoenhammer, G., Thiel, A., Matos, C., Bruss, C., Klobuch, S., Peter, K*., et al.* (2016). LDHA-Associated Lactic Acid Production Blunts Tumor Immunosurveillance by T and NK Cells. Cell metabolism *24*, 657-671.

Buck, M.D., O'Sullivan, D., Klein Geltink, R.I., Curtis, J.D., Chang, C.-H.H., Sanin, D.E., Qiu, J., Kretz, O., Braas, D., van der Windt, G.J*., et al.* (2016). Mitochondrial Dynamics Controls T Cell Fate through Metabolic Programming. Cell *166*, 63-76.

Cai, J., Yang, J., and Jones, D.P. (1998). Mitochondrial control of apoptosis: the role of cytochrome c. Biochimica et biophysica acta *1366*, 139-149.

Calcinotto, A., Filipazzi, P., Grioni, M., Iero, M., De Milito, A., Ricupito, A., Cova, A., Canese, R., Jachetti, E., Rossetti, M*., et al.* (2012). Modulation of microenvironment acidity reverses anergy in human and murine tumor-infiltrating T lymphocytes. Cancer research *72*, 2746-2756.

Carmeliet, P. (2005). VEGF as a key mediator of angiogenesis in cancer. Oncology *69 Suppl 3*, 4-10.

Carr, E.L., Kelman, A., Wu, G.S., Gopaul, R., Senkevitch, E., Aghvanyan, A., Turay, A.M., and Frauwirth, K.A. (2010). Glutamine uptake and metabolism are coordinately regulated by ERK/MAPK during T lymphocyte activation. Journal of immunology (Baltimore, Md : 1950) *185*, 1037-1044.

Cham, C.M., and Gajewski, T.F. (2005). Glucose availability regulates IFN-gamma production and p70S6 kinase activation in CD8+ effector T cells. J Immunol *174*, 4670-4677.

Chang, C.-H., Qiu, J., O'Sullivan, D., Buck, M.D., Noguchi, T., Curtis, J.D., Chen, Q., Gindin, M., Gubin, M.M., van der Windt, G*., et al.* (2015a). Metabolic Competition in the Tumor Microenvironment Is a Driver of Cancer Progression. Cell *162*, 1229-1241.

Chang, C.-H.H., Curtis, J.D., Maggi, L.B., Faubert, B., Villarino, A.V., O'Sullivan, D., Huang, S.C., van der Windt, G.J., Blagih, J., Qiu, J*., et al.* (2013). Posttranscriptional control of T cell effector function by aerobic glycolysis. Cell *153*, 1239-1251.

Chang, C.-H.H., Qiu, J., O'Sullivan, D., Buck, M.D., Noguchi, T., Curtis, J.D., Chen, Q., Gindin, M., Gubin, M.M., van der Windt, G.J.*, et al.* (2015b). Metabolic Competition in the Tumor Microenvironment Is a Driver of Cancer Progression. Cell *162*, 1229-1241. Chen, W.W., Freinkman, E., Wang, T., Birsoy, K., and Sabatini, D.M. (2016). Absolute Quantification of Matrix Metabolites Reveals the Dynamics of Mitochondrial Metabolism. Cell *166*, 1324-1963042816.

Cluntun, A.A., Lukey, M.J., Cerione, R.A., and Locasale, J.W. (2017). Glutamine Metabolism in Cancer: Understanding the Heterogeneity. Trends in cancer *3*, 169-180.

Cogliati, S., Frezza, C., Soriano, M.E., Varanita, T., Quintana-Cabrera, R., Corrado, M., Cipolat, S., Costa, V., Casarin, A., Gomes, L.C.*, et al.* (2013). Mitochondrial cristae shape determines respiratory chain supercomplexes assembly and respiratory efficiency. Cell *155*, 160-171.

Colegio, O.R., Chu, N.-Q.Q., Szabo, A.L., Chu, T., Rhebergen, A.M., Jairam, V., Cyrus, N., Brokowski, C.E., Eisenbarth, S.C., Phillips, G.M.*, et al.* (2014). Functional polarization of tumour-associated macrophages by tumour-derived lactic acid. Nature *513*, 559-563.

Crompton, M. (1999). The mitochondrial permeability transition pore and its role in cell death. The Biochemical journal *341 (Pt 2)*, 233-249.

Cruz, C.R., Micklethwaite, K.P., Savoldo, B., Ramos, C.A., Lam, S., Ku, S., Diouf, O., Liu, E., Barrett, A.J., Ito, S.*, et al.* (2013). Infusion of donor-derived CD19-redirected virus-specific T cells for B-cell malignancies relapsed after allogeneic stem cell transplant: a phase 1 study. Blood *122*, 2965-2973.

Cui, L., Pang, J., Lee, Y.H., Ooi, E.E., Ong, C.N., Leo, Y.S., and Tannenbaum, S.R. (2018). Serum metabolome changes in adult patients with severe dengue in the critical and recovery phases of dengue infection. PLoS neglected tropical diseases *12*.

Curi, R., Newsholme, P., Marzuca-Nassr, G.N., Takahashi, H.K., Hirabara, S.M., Cruzat, V., Krause, M., and de Bittencourt, P.I. (2016). Regulatory principles in metabolism-then and now. The Biochemical journal *473*, 1845-1857.

Dang, E.V., Barbi, J., Yang, H.-Y.Y., Jinasena, D., Yu, H., Zheng, Y., Bordman, Z., Fu, J., Kim, Y., Yen, H.-R.R.*, et al.* (2011). Control of T(H)17/T(reg) balance by hypoxia-inducible factor 1. Cell *146*, 772-784.

DeBerardinis, R.J., and Chandel, N.S. (2016). Fundamentals of cancer metabolism. Science advances *2*.

DeBerardinis, R.J., and Cheng, T. (2010). Q's next: the diverse functions of glutamine in metabolism, cell biology and cancer. Oncogene *29*, 313-324.

Dilillo, M., Ait-Belkacem, R., Esteve, C., Pellegrini, D., Nicolardi, S., Costa, M., Vannini, E., Graaf, E.L., Caleo, M., and McDonnell, L.A. (2017). Ultra-High Mass Resolution MALDI Imaging Mass Spectrometry of Proteins and Metabolites in a Mouse Model of Glioblastoma. Scientific reports *7*, 603.

Dimeloe, S., Mehling, M., Frick, C., Loeliger, J., Bantug, G.R., Sauder, U., Fischer, M., Belle, R., Develioglu, L., Tay, S.*, et al.* (2016a). The Immune-Metabolic Basis of Effector Memory CD4+ T Cell Function under Hypoxic Conditions. Journal of immunology (Baltimore, Md : 1950) *196*, 106-114.

Dimeloe, S., Mehling, M., Frick, C., Loeliger, J., Bantug, G.R., Sauder, U., Fischer, M., Belle, R., Develioglu, L., Tay, S.*, et al.* (2016b). The Immune-Metabolic Basis of Effector Memory CD4+ T Cell Function under Hypoxic Conditions. J Immunol *196*, 106-114.

Doedens, A.L., Phan, A.T., Stradner, M.H., Fujimoto, J.K., Nguyen, J.V., Yang, E., Johnson, R.S., and Goldrath, A.W. (2013). Hypoxia-inducible factors enhance the effector responses of CD8(+) T cells to persistent antigen. Nature immunology *14*, 1173-1182.

Dunn, G.P., Bruce, A.T., Ikeda, H., Old, L.J., and Schreiber, R.D. (2002). Cancer immunoediting: from immunosurveillance to tumor escape. Nat Immunol *3*, 991-998.

Ecker, C., Guo, L., Voicu, S., Gil-de-Gómez, L., Medvec, A., Cortina, L., Pajda, J., Andolina, M., Torres-Castillo, M., Donato, J.L.*, et al.* (2018). Differential reliance on lipid metabolism as a salvage pathway underlies functional differences of T cell subsets in poor nutrient environments. Cell Reports *3, 741-755.*

Ecker, C., and Riley, J.L. (Submitted). Translating in vitro T cell metabolic findings to in vivo tumor models of nutrient competition. Cell Metab.

Eltzschig, H.K., and Carmeliet, P. (2011). Hypoxia and inflammation. N Engl J Med *364*, 656-665.

Etchegaray, J.-P.P., and Mostoslavsky, R. (2016). Interplay between Metabolism and Epigenetics: A Nuclear Adaptation to Environmental Changes. Molecular cell *62*, 695-711.

Everts, B., Amiel, E., Huang, S.C., Smith, A.M., Chang, C.-H.H., Lam, W.Y., Redmann, V., Freitas, T.C., Blagih, J., van der Windt, G.J.*, et al.* (2014). TLR-driven early glycolytic

reprogramming via the kinases TBK1-IKKε supports the anabolic demands of dendritic cell activation. Nature immunology *15*, 323-332.

Fallarino, F., Grohmann, U., Vacca, C., Bianchi, R., Orabona, C., Spreca, A., Fioretti, M.C., and Puccetti, P. (2002). T cell apoptosis by tryptophan catabolism. Cell death and differentiation *9*, 1069-1077.
Farber, D.L., Yudanin, N.A., and Restifo, N.P. (2014). Human memory T cells: generation, compartmentalization and homeostasis. Nat Rev Immunol *14*, 24-35.

Fendt, S.-M.M., Bell, E.L., Keibler, M.A., Olenchock, B.A., Mayers, J.R., Wasylenko, T.M., Vokes, N.I., Guarente, L., Vander Heiden, M.G., and Stephanopoulos, G. (2013). Reductive glutamine metabolism is a function of the α-ketoglutarate to citrate ratio in cells. Nat Commun *4*, 2236.

Fischer, K., Hoffmann, P., Voelkl, S., Meidenbauer, N., Ammer, J., Edinger, M., Gottfried, E., Schwarz, S., Rothe, G., Hoves, S.*, et al.* (2007). Inhibitory effect of tumor cell-derived lactic acid on human T cells. Blood *109*, 3812-3819.

Fletcher, M., Ramirez, M.E., Sierra, R.A., Raber, P., Thevenot, P., Al-Khami, A.A., Sanchez-Pino, D., Hernandez, C., Wyczechowska, D.D., Ochoa, A.C.*, et al.* (2015). l-Arginine depletion blunts antitumor T-cell responses by inducing myeloid-derived suppressor cells. Cancer research *75*, 275-283.

Frauwirth, K.A., Riley, J.L., Harris, M.H., Parry, R.V., Rathmell, J.C., Plas, D.R., Elstrom, R.L., June, C.H., and Thompson, C.B. (2002). The CD28 signaling pathway regulates glucose metabolism. Immunity *16*, 769-777.

Frey, A.J., Feldman, D.R., Trefely, S., Worth, A.J., Basu, S.S., and Snyder, N.W. (2016). LC-quadrupole/Orbitrap high-resolution mass spectrometry enables stable isotope-resolved simultaneous quantification and ^{13}C-isotopic labeling of acyl-coenzyme A thioesters. Analytical and bioanalytical chemistry *408*, 3651-3658.

Galván-Peña, S., and O'Neill, L.A. (2014). Metabolic reprograming in macrophage polarization. Frontiers in immunology *5*, 420.

Gattinoni, L., Lugli, E., Ji, Y., Pos, Z., Paulos, C.M., Quigley, M.F.F., Almeida, J.R., Gostick, E., Yu, Z., Carpenito, C.*, et al.* (2011). A human memory T cell subset with stem cell-like properties. Nature medicine *17*, 1290-1297.

Gauron, C., Rampon, C., Bouzaffour, M., Ipendey, E., Teillon, J., Volovitch, M., and Vriz, S. (2013). Sustained production of ROS triggers compensatory proliferation and is required for regeneration to proceed. Scientific reports *3*, 2084.

Geiger, R., Rieckmann, J.C., Wolf, T., Basso, C., Feng, Y., Fuhrer, T., Kogadeeva, M., Picotti, P., Meissner, F., Mann, M.*, et al.* (2016). L-Arginine Modulates T Cell Metabolism and Enhances Survival and Anti-tumor Activity. Cell *167*, 829-84033536.

Gerriets, V.A., Kishton, R.J., Johnson, M.O., Cohen, S., Siska, P.J., Nichols, A.G., Warmoes, M.O., de Cubas, A.A., MacIver, N.J., Locasale, J.W.*, et al.* (2016). Foxp3 and Toll-like receptor signaling balance Treg cell anabolic metabolism for suppression. Nat Immunol *17*, 1459-1466.

Glatz, J.F., and Luiken, J.J. (2016). From fat to FAT (CD36/SR-B2): Understanding the regulation of cellular fatty acid uptake. Biochimie *136*, 21-26.

Gogvadze, V., Orrenius, S., and Zhivotovsky, B. (2006). Multiple pathways of cytochrome c release from mitochondria in apoptosis. Biochimica et biophysica acta *1757*, 639-647.

Gomes, L.C., Di Benedetto, G., and Scorrano, L. (2011). During autophagy mitochondria elongate, are spared from degradation and sustain cell viability. Nature cell biology *13*, 589-598.

Gosselin, D., Link, V.M., Romanoski, C.E., Fonseca, G.J., Eichenfield, D.Z., Spann, N.J., Stender, J.D., Chun, H.B., Garner, H., Geissmann, F.*, et al.* (2014). Environment drives selection and function of enhancers controlling tissue-specific macrophage identities. Cell *159*, 1327-1340.

Granot, T., Senda, T., Carpenter, D.J., Matsuoka, N., Weiner, J., Gordon, C.L., Miron, M., Kumar, B.V., Griesemer, A., Ho, S.-H.H.*, et al.* (2017). Dendritic Cells Display Subset and Tissue-Specific Maturation Dynamics over Human Life. Immunity *46*, 504-515.

Grupp, S.A., Kalos, M., Barrett, D., Aplenc, R., Porter, D.L., Rheingold, S.R., Teachey, D.T., Chew, A., Hauck, B., Wright, J.F.*, et al.* (2013). Chimeric antigen receptor-modified T cells for acute lymphoid leukemia. The New England journal of medicine *368*, 1509-1518.

Gubser, P.M., Bantug, G.R., Razik, L., Fischer, M., Dimeloe, S., Hoenger, G., Durovic, B., Jauch, A., and Hess, C. (2013). Rapid effector function of memory CD8+ T cells requires an immediate-early glycolytic switch. Nat Immunol *14*, 1064-1072.

Guo, L., Worth, A.J., Mesaros, C., Snyder, N.W., Glickson, J.D., and Blair, I.A. (2016). Diisopropylethylamine/hexafluoroisopropanol-mediated ion-pairing ultra-high-performance liquid chromatography/mass spectrometry for phosphate and carboxylate metabolite analysis: utility for studying cellular metabolism. Rapid Commun Mass Spectrom *30*, 1835-1845.

Han, S.-J.J., Glatman Zaretsky, A., Andrade-Oliveira, V., Collins, N., Dzutsev, A., Shaik, J., Morais da Fonseca, D., Harrison, O.J., Tamoutounour, S., Byrd, A.L.*, et al.* (2017). White Adipose Tissue Is a Reservoir for Memory T Cells and Promotes Protective Memory Responses to Infection. Immunity *47*, 1154-1168000000.

Hao, J., Yan, F., Zhang, Y., Triplett, A., Zhang, Y., Schultz, D.A., Sun, Y., Zeng, J., Silverstein, K.A.T.A.T., Zheng, Q.*, et al.* (2018). Expression of adipocyte/macrophage fatty acid binding protein in tumor associated macrophages promotes breast cancer progression. Cancer research.

He, F., Deng, X., Wen, B., Liu, Y., Sun, X., Xing, L., Minami, A., Huang, Y., Chen, Q., Zanzonico, P.B.*, et al.* (2008). Noninvasive molecular imaging of hypoxia in human xenografts: comparing hypoxia-induced gene expression with endogenous and exogenous hypoxia markers. Cancer research *68*, 8597-8606.

He, H., Dang, Y., Dai, F., Guo, Z., Wu, J., She, X., Pei, Y., Chen, Y., Ling, W., Wu, C.*, et al.* (2003). Post-translational modifications of three members of the human MAP1LC3 family and detection of a novel type of modification for MAP1LC3B. J Biol Chem *278*, 29278-29287.

Hensley, C.T., Faubert, B., Yuan, Q., Lev-Cohain, N., Jin, E., Kim, J., Jiang, L., Ko, B., Skelton, R., Loudat, L.*, et al.* (2016). Metabolic Heterogeneity in Human Lung Tumors. Cell *164*, 681-694.

Ho, P.-C.C., Bihuniak, J.D., Macintyre, A.N., Staron, M., Liu, X., Amezquita, R., Tsui, Y.-C.C., Cui, G., Micevic, G., Perales, J.C.*, et al.* (2015a). Phosphoenolpyruvate Is a Metabolic Checkpoint of Anti-tumor T Cell Responses. Cell *162*, 1217-1228.

Ho, P.C., Bihuniak, J.D., Macintyre, A.N., Staron, M., Liu, X., Amezquita, R., Tsui, Y.C., Cui, G., Micevic, G., Perales, J.C.*, et al.* (2015b). Phosphoenolpyruvate Is a Metabolic Checkpoint of Anti-tumor T Cell Responses. Cell *162*, 1217-1228.

Holzlechner, M., Strasser, K., Zareva, E., Steinhäuser, L., Birnleitner, H., Beer, A., Bergmann, M., Oehler, R., and Marchetti-Deschmann, M. (2017). In Situ Characterization of Tissue-Resident Immune Cells by MALDI Mass Spectrometry Imaging. Journal of proteome research *16*, 65-76.

Hombrink, P., Helbig, C., Backer, R.A., Piet, B., Oja, A.E., Stark, R., Brasser, G., Jongejan, A., Jonkers, R.E.E., Nota, B.*, et al.* (2016). Programs for the persistence, vigilance and control of human CD8+lung-resident memory T cells. Nature immunology *17*, 1467-1478.

Hsiao, H.-W.W., Hsu, T.-S.S., Liu, W.-H.H., Hsieh, W.-C.C., Chou, T.-F.F., Wu, Y.-J.J., Jiang, S.-T.T., and Lai, M.-Z.Z. (2015). Deltex1 antagonizes HIF-1α and sustains the stability of regulatory T cells in vivo. Nature communications *6*, 6353.

Huang, A.C., Postow, M.A., Orlowski, R.J., Mick, R., Bengsch, B., Manne, S., Xu, W., Harmon, S., Giles, J.R., Wenz, B.*, et al.* (2017). T-cell invigoration to tumour burden ratio associated with anti-PD-1 response. Nature *545*, 60-65.

Huynh, A., DuPage, M., Priyadharshini, B., Sage, P.T., Quiros, J., Borges, C.M., Townamchai, N., Gerriets, V.A., Rathmell, J.C., Sharpe, A.H.*, et al.* (2015). Control of PI(3) kinase in Treg cells maintains homeostasis and lineage stability. Nat Immunol *16*, 188-196.
Jacobs, S.R., Herman, C.E., Maciver, N.J., Wofford, J.A., Wieman, H.L., Hammen, J.J., and Rathmell, J.C. (2008). Glucose uptake is limiting in T cell activation and requires CD28-mediated Akt-dependent and independent pathways. J Immunol *180*, 4476-4486.

Jiko, C., Davies, K.M., Shinzawa-Itoh, K., Tani, K., Maeda, S., Mills, D.J., Tsukihara, T., Fujiyoshi, Y., Kühlbrandt, W., and Gerle, C. (2015). Bovine F1Fo ATP synthase monomers bend the lipid bilayer in 2D membrane crystals. eLife *4*.

Kalos, M., Levine, B.L., Porter, D.L., Katz, S., Grupp, S.A., Bagg, A., and June, C.H. (2011). T cells with chimeric antigen receptors have potent antitumor effects and can establish memory in patients with advanced leukemia. Science translational medicine *3*.

Kamphorst, J.J., Nofal, M., Commisso, C., Hackett, S.R., Lu, W., Grabocka, E., Vander Heiden, M.G., Miller, G., Drebin, J.A., Bar-Sagi, D.*, et al.* (2015). Human pancreatic cancer tumors are nutrient poor and tumor cells actively scavenge extracellular protein. Cancer research *75*, 544-553.

Katz, J., and Rognstad, R. (1976). Futile cycles in the metabolism of glucose. Current topics in cellular regulation *10*, 237-289.

Keppel, M.P., Saucier, N., Mah, A.Y., Vogel, T.P., and Cooper, M.A. (2015). Activation-specific metabolic requirements for NK Cell IFN-γ production. J Immunol *194*, 1954-1962.

Kishore, M., Cheung, K.C.P.C.P., Fu, H., Bonacina, F., Wang, G., Coe, D., Ward, E.J., Colamatteo, A., Jangani, M., Baragetti, A.*, et al.* (2017). Regulatory T Cell Migration Is Dependent on Glucokinase-Mediated Glycolysis. Immunity *47*, 875.

Klebanoff, C.A., Gattinoni, L., and Restifo, N.P. (2006). CD8+ T-cell memory in tumor immunology and immunotherapy. Immunological reviews *211*, 214-224.

Klysz, D., Tai, X., Robert, P.A., Craveiro, M., Cretenet, G., Oburoglu, L., Mongellaz, C., Floess, S., Fritz, V., Matias, M.I.*, et al.* (2015). Glutamine-dependent α-ketoglutarate production regulates the balance between T helper 1 cell and regulatory T cell generation. Science signaling *8*.

Kolodin, D., van Panhuys, N., Li, C., Magnuson, A.M., Cipolletta, D., Miller, C.M., Wagers, A., Germain, R.N., Benoist, C., and Mathis, D. (2015). Antigen- and cytokine-driven accumulation of regulatory T cells in visceral adipose tissue of lean mice. Cell metabolism *21*, 543-557.

Kong, H., and Chandel, N.S. (2018). Regulation of redox balance in cancer and T cells. The Journal of biological chemistry *293*, 7499-7507.

Krautz, R., Arefin, B., and Theopold, U. (2014). Damage signals in the insect immune response. Frontiers in plant science *5*, 342.

Kunji, E.R. (2004). The role and structure of mitochondrial carriers. FEBS letters *564*, 239-244.

Kusmartsev, S., Nefedova, Y., Yoder, D., and Gabrilovich, D.I. (2004). Antigen-specific inhibition of CD8+ T cell response by immature myeloid cells in cancer is mediated by reactive oxygen species. Journal of immunology (Baltimore, Md : 1950) *172*, 989-999.

Lanitis, E., Irving, M., and Coukos, G. (2015). Targeting the tumor vasculature to enhance T cell activity. Current opinion in immunology *33*, 55-63.

Laplante, M., and Sabatini, D.M. (2012). mTOR signaling in growth control and disease. Cell *149*, 274-293.

Lee, D.W., Kochenderfer, J.N., Stetler-Stevenson, M., Cui, Y.K., Delbrook, C., Feldman, S.A., Fry, T.J., Orentas, R., Sabatino, M., Shah, N.N.*, et al.* (2015). T cells expressing CD19 chimeric antigen receptors for acute lymphoblastic leukaemia in children and young adults: a phase 1 dose-escalation trial. Lancet (London, England) *385*, 517-528.

Lee, J., Walsh, M.C., Hoehn, K.L., James, D.E., Wherry, E.J., and Choi, Y. (2014a). Regulator of fatty acid metabolism, acetyl coenzyme a carboxylase 1, controls T cell immunity. J Immunol *192*, 3190-3199.

Lee, J.V., Carrer, A., Shah, S., Snyder, N.W., Wei, S., Venneti, S., Worth, A.J., Yuan, Z.-F.F., Lim, H.-W.W., Liu, S.*, et al.* (2014b). Akt-dependent metabolic reprogramming regulates tumor cell histone acetylation. Cell metabolism *20*, 306-319.

Liberti, M.V., and Locasale, J.W. (2016). The Warburg Effect: How Does it Benefit Cancer Cells? Trends in biochemical sciences *41*, 211-218.

Liesa, M., and Shirihai, O.S. (2013). Mitochondrial dynamics in the regulation of nutrient utilization and energy expenditure. Cell metabolism *17*, 491-506.

Ligtenberg, M.A., Mougiakakos, D., Mukhopadhyay, M., Witt, K., Lladser, A., Chmielewski, M., Riet, T., Abken, H., and Kiessling, R. (2016). Coexpressed Catalase Protects Chimeric Antigen Receptor-Redirected T Cells as well as Bystander Cells from Oxidative Stress-Induced Loss of Antitumor Activity. Journal of immunology (Baltimore, Md : 1950) *196*, 759-766.

Liu, K., and Czaja, M.J. (2013). Regulation of lipid stores and metabolism by lipophagy. Cell death and differentiation *20*, 3-11.
Locasale, J.W., and Cantley, L.C. (2011). Metabolic flux and the regulation of mammalian cell growth. Cell metabolism *14*, 443-451.

Lu, W., Zhang, Y., McDonald, D.O., Jing, H., Carroll, B., Robertson, N., Zhang, Q., Griffin, H., Sanderson, S., Lakey, J.H.*, et al.* (2014). Dual proteolytic pathways govern glycolysis and immune competence. Cell *159*, 1578-1590.

Ma, E.H., Bantug, G., Griss, T., Condotta, S., Johnson, R.M., Samborska, B., Mainolfi, N., Suri, V., Guak, H., Balmer, M.L.*, et al.* (2017a). Serine Is an Essential Metabolite for Effector T Cell Expansion. Cell Metab *25*, 345-357.

Ma, E.H., Bantug, G., Griss, T., Condotta, S., Johnson, R.M., Samborska, B., Mainolfi, N., Suri, V., Guak, H., Balmer, M.L.*, et al.* (2017b). Serine Is an Essential Metabolite for Effector T Cell Expansion. Cell metabolism *25*, 345-357.

Macintyre, A.N., Gerriets, V.A., Nichols, A.G., Michalek, R.D., Rudolph, M.C., Deoliveira, D., Anderson, S.M., Abel, E.D., Chen, B.J., Hale, L.P.*, et al.* (2014). The glucose transporter Glut1 is selectively essential for CD4 T cell activation and effector function. Cell Metab *20*, 61-72.

Marsboom, G., Toth, P.T., Ryan, J.J., Hong, Z., Wu, X., Fang, Y.-H.H., Thenappan, T., Piao, L., Zhang, H.J., Pogoriler, J.*, et al.* (2012). Dynamin-related protein 1-mediated mitochondrial mitotic fission permits hyperproliferation of vascular smooth muscle cells

and offers a novel therapeutic target in pulmonary hypertension. Circulation research *110*, 1484-1497.

Mathis, D. (2013). Immunological goings-on in visceral adipose tissue. Cell metabolism *17*, 851-859.

Maude, S.L., Frey, N., Shaw, P.A., Aplenc, R., Barrett, D.M., Bunin, N.J., Chew, A., Gonzalez, V.E., Zheng, Z., Lacey, S.F.*, et al.* (2014). Chimeric antigen receptor T cells for sustained remissions in leukemia. The New England journal of medicine *371*, 1507-1517.

Maude, S.L., Teachey, D.T., Porter, D.L., and Grupp, S.A. (2015). CD19-targeted chimeric antigen receptor T-cell therapy for acute lymphoblastic leukemia. Blood *125*, 4017-4023.

Medvec, A.R., Ecker, C., Kong, H., Winters, E.A., Glover, J., Varela-Rohena, A., and Riley, J.L. (2018). Improved Expansion and In Vivo Function of Patient T Cells by a Serum-free Medium. Molecular Therapy - Methods & Clinical Development *8*, 65-74.

Metallo, C.M., Gameiro, P.A., Bell, E.L., Mattaini, K.R., Yang, J., Hiller, K., Jewell, C.M., Johnson, Z.R., Irvine, D.J., Guarente, L.*, et al.* (2011). Reductive glutamine metabolism by IDH1 mediates lipogenesis under hypoxia. Nature *481*, 380-384.
Michalek, R.D., Gerriets, V.A., Jacobs, S.R., Macintyre, A.N., MacIver, N.J., Mason, E.F., Sullivan, S.A., Nichols, A.G., and Rathmell, J.C. (2011). Cutting edge: distinct glycolytic and lipid oxidative metabolic programs are essential for effector and regulatory CD4+ T cell subsets. J Immunol *186*, 3299-3303.

Milone, M.C., Fish, J.D., Carpenito, C., Carroll, R.G., Binder, G.K., Teachey, D., Samanta, M., Lakhal, M., Gloss, B., Danet-Desnoyers, G.*, et al.* (2009). Chimeric receptors containing CD137 signal transduction domains mediate enhanced survival of T cells and increased antileukemic efficacy in vivo. Molecular therapy : the journal of the American Society of Gene Therapy *17*, 1453-1464.

Minocherhomji, S., Tollefsbol, T.O., and Singh, K.K. (2012). Mitochondrial regulation of epigenetics and its role in human diseases. Epigenetics *7*, 326-334.

Mishra, P., and Chan, D.C. (2016). Metabolic regulation of mitochondrial dynamics. The Journal of cell biology *212*, 379-387.

Miyajima, M., Zhang, B., Sugiura, Y., Sonomura, K., Guerrini, M.M., Tsutsui, Y., Maruya, M., Vogelzang, A., Chamoto, K., Honda, K.*, et al.* (2017). Metabolic shift induced by systemic activation of T cells in PD-1-deficient mice perturbs brain monoamines and emotional behavior. Nature immunology *18*, 1342-1352.

Moon, E.K., Wang, L.C., Dolfi, D.V., Wilson, C.B., Ranganathan, R., Sun, J., Kapoor, V., Scholler, J., Pure, E., Milone, M.C.*, et al.* (2014). Multifactorial T-cell hypofunction that is reversible can limit the efficacy of chimeric antigen receptor-transduced human T cells in solid tumors. Clin Cancer Res *20*, 4262-4273.

O'Sullivan, D., and Pearce, E.L. (2014). Fatty acid synthesis tips the TH17-Treg cell balance. Nat Med *20*, 1235-1236.

O'Sullivan, D., van der Windt, G.J., Huang, S.C., Curtis, J.D., Chang, C.-H.H., Buck, M.D., Qiu, J., Smith, A.M., Lam, W.Y., DiPlato, L.M.*, et al.* (2014). Memory CD8(+) T cells use cell-intrinsic lipolysis to support the metabolic programming necessary for development. Immunity *41*, 75-88.

Pagès, F., Berger, A., Camus, M., Sanchez-Cabo, F., Costes, A., Molidor, R., Mlecnik, B., Kirilovsky, A., Nilsson, M., Damotte, D.*, et al.* (2005). Effector memory T cells, early metastasis, and survival in colorectal cancer. N Engl J Med *353*, 2654-2666.

Pan, Y., Tian, T., Park, C.O., Lofftus, S.Y., Mei, S., Liu, X., Luo, C., O'Malley, J.T., Gehad, A., Teague, J.E.*, et al.* (2017). Survival of tissue-resident memory T cells requires exogenous lipid uptake and metabolism. Nature *543*, 252-256.

Parry, R.V., Rumbley, C.A., Vandenberghe, L.H., June, C.H., and Riley, J.L. (2003). CD28 and inducible costimulatory protein Src homology 2 binding domains show distinct regulation of phosphatidylinositol 3-kinase, Bcl-xL, and IL-2 expression in primary human CD4 T lymphocytes. J Immunol *171*, 166-174.

Passarella, S., Atlante, A., Valenti, D., and de Bari, L. (2003). The role of mitochondrial transport in energy metabolism. Mitochondrion *2*, 319-343.

Paumard, P., Vaillier, J., Coulary, B., Schaeffer, J., Soubannier, V., Mueller, D.M., Brèthes, D., di Rago, J.-P.P., and Velours, J. (2002). The ATP synthase is involved in generating mitochondrial cristae morphology. The EMBO journal *21*, 221-230.

Pavlova, N.N., and Thompson, C.B. (2016). The Emerging Hallmarks of Cancer Metabolism. Cell metabolism *23*, 27-47.

Pearce, E.L., and Pearce, E.J. (2013). Metabolic pathways in immune cell activation and quiescence. Immunity *38*, 633-643.

Peng, M., Yin, N., Chhangawala, S., Xu, K., Leslie, C.S., and Li, M.O. (2016). Aerobic glycolysis promotes T helper 1 cell differentiation through an epigenetic mechanism. Science *354*, 481-484.

Pfeiffer, T., Schuster, S., and Bonhoeffer, S. (2001). Cooperation and competition in the evolution of ATP-producing pathways. Science (New York, NY) *292*, 504-507.

Pietrocola, F., Galluzzi, L., Bravo-San Pedro, J.M.M., Madeo, F., and Kroemer, G. (2015). Acetyl coenzyme A: a central metabolite and second messenger. Cell Metab *21*, 805-821.

Platten, M., Wick, W., and Van den Eynde, B.J.J. (2012). Tryptophan catabolism in cancer: beyond IDO and tryptophan depletion. Cancer research *72*, 5435-5440.

Pollizzi, K.N., and Powell, J.D. (2014). Integrating canonical and metabolic signalling programmes in the regulation of T cell responses. Nat Rev Immunol *14*, 435-446.

Pond, C.M., and Mattacks, C.A. (1995). Interactions between adipose tissue around lymph nodes and lymphoid cells in vitro. Journal of lipid research *36*, 2219-2231.

Porter, D.L., Levine, B.L., Kalos, M., Bagg, A., and June, C.H. (2011). Chimeric antigen receptor-modified T cells in chronic lymphoid leukemia. N Engl J Med *365*, 725-733.

Procaccini, C., Carbone, F., Di Silvestre, D., Brambilla, F., De Rosa, V., Galgani, M., Faicchia, D., Marone, G., Tramontano, D., Corona, M.*, et al.* (2016). The Proteomic Landscape of Human Ex Vivo Regulatory and Conventional T Cells Reveals Specific Metabolic Requirements. Immunity *44*, 406-421.

Rambold, A.S., Kostelecky, B., Elia, N., and Lippincott-Schwartz, J. (2011). Tubular network formation protects mitochondria from autophagosomal degradation during nutrient starvation. Proceedings of the National Academy of Sciences of the United States of America *108*, 10190-10195.

Reid, M.A., Dai, Z., and Locasale, J.W. (2017). The impact of cellular metabolism on chromatin dynamics and epigenetics. Nature cell biology *19*, 1298-1306.

Ricciardi, M.R., Mirabilii, S., Allegretti, M., Licchetta, R., Calarco, A., Torrisi, M.R., Foà, R., Nicolai, R., Peluso, G., and Tafuri, A. (2015). Targeting the leukemia cell metabolism by the CPT1a inhibition: functional preclinical effects in leukemias. Blood *126*, 1925-1929.

Ron-Harel, N., Santos, D., Ghergurovich, J.M., Sage, P.T., Reddy, A., Lovitch, S.B., Dephoure, N., Satterstrom, F.K., Sheffer, M., Spinelli, J.B.*, et al.* (2016). Mitochondrial Biogenesis and Proteome Remodeling Promote One-Carbon Metabolism for T Cell Activation. Cell metabolism *24*, 104-117.

Ron-Harel, N., Sharpe, A.H., and Haigis, M.C. (2015). Mitochondrial metabolism in T cell activation and senescence: a mini-review. Gerontology *61*, 131-138.

Sabatini, D.M. (2017). Twenty-five years of mTOR: Uncovering the link from nutrients to growth. Proceedings of the National Academy of Sciences of the United States of America *114*, 11818-11825.

Sallusto, F., Lenig, D., Förster, R., Lipp, M., and Lanzavecchia, A. (1999). Two subsets of memory T lymphocytes with distinct homing potentials and effector functions. Nature *401*, 708-712.

Samudio, I., Harmancey, R., Fiegl, M., Kantarjian, H., Konopleva, M., Korchin, B., Kaluarachchi, K., Bornmann, W., Duvvuri, S., Taegtmeyer, H.*, et al.* (2010). Pharmacologic inhibition of fatty acid oxidation sensitizes human leukemia cells to apoptosis induction. J Clin Invest *120*, 142-156.

Schafer, C.C., Wang, Y., Hough, K.P., Sawant, A., Grant, S.C., Thannickal, V.J., Zmijewski, J., Ponnazhagan, S., and Deshane, J.S. (2016). Indoleamine 2,3-dioxygenase regulates anti-tumor immunity in lung cancer by metabolic reprogramming of immune cells in the tumor microenvironment. Oncotarget *7*, 75407-75424.

Scharping, N.E., Menk, A.V., Moreci, R.S., Whetstone, R.D., Dadey, R.E., Watkins, S.C., Ferris, R.L., and Delgoffe, G.M. (2016). The Tumor Microenvironment Represses T Cell Mitochondrial Biogenesis to Drive Intratumoral T Cell Metabolic Insufficiency and Dysfunction. Immunity *45*, 374-388.

Schwenk, R.W., Holloway, G.P., Luiken, J.J., Bonen, A., and Glatz, J.F. (2010). Fatty acid transport across the cell membrane: regulation by fatty acid transporters. Prostaglandins Leukot Essent Fatty Acids *82*, 149-154.

Sena, L.A., Li, S., Jairaman, A., Prakriya, M., Ezponda, T., Hildeman, D.A., Wang, C.-R.R., Schumacker, P.T., Licht, J.D., Perlman, H.*, et al.* (2013). Mitochondria are required for antigen-specific T cell activation through reactive oxygen species signaling. Immunity *38*, 225-236.

Shrestha, S., Yang, K., Guy, C., Vogel, P., Neale, G., and Chi, H. (2015). Treg cells require the phosphatase PTEN to restrain TH1 and TFH cell responses. Nat Immunol *16*, 178-187.

Shrestha, S., Yang, K., Wei, J., Karmaus, P.W., Neale, G., and Chi, H. (2014). Tsc1 promotes the differentiation of memory CD8+ T cells via orchestrating the

transcriptional and metabolic programs. Proceedings of the National Academy of Sciences of the United States of America *111*, 14858-14863.

Sinclair, L.V., Rolf, J., Emslie, E., Shi, Y.-B.B., Taylor, P.M., and Cantrell, D.A. (2013). Control of amino-acid transport by antigen receptors coordinates the metabolic reprogramming essential for T cell differentiation. Nature immunology *14*, 500-508.

Singh, R., Kaushik, S., Wang, Y., Xiang, Y., Novak, I., Komatsu, M., Tanaka, K., Cuervo, A.M., and Czaja, M.J. (2009). Autophagy regulates lipid metabolism. Nature *458*, 1131-1135.

Siska, P.J., Beckermann, K.E., Mason, F.M., Andrejeva, G., Greenplate, A.R., Sendor, A.B., Chiang, Y.-C.J., Corona, A.L., Gemta, L.F., Vincent, B.G.*, et al.* (2017a). Mitochondrial dysregulation and glycolytic insufficiency functionally impair CD8 T cells infiltrating human renal cell carcinoma. JCI Insight *2*.

Siska, P.J., Beckermann, K.E., Mason, F.M., Andrejeva, G., Greenplate, A.R., Sendor, A.B., Chiang, Y.J., Corona, A.L., Gemta, L.F., Vincent, B.G.*, et al.* (2017b). Mitochondrial dysregulation and glycolytic insufficiency functionally impair CD8 T cells infiltrating human renal cell carcinoma. JCI Insight *2*.

Siska, P.J., and Rathmell, J.C. (2016). Metabolic Signaling Drives IFN-γ. Cell Metab *24*, 651-652.

Siska, P.J., van der Windt, G.J., Kishton, R.J., Cohen, S., Eisner, W., MacIver, N.J., Kater, A.P., Weinberg, J.B., and Rathmell, J.C. (2016). Suppression of Glut1 and Glucose Metabolism by Decreased Akt/mTORC1 Signaling Drives T Cell Impairment in B Cell Leukemia. J Immunol *197*, 2532-2540

Sivanand, S., Viney, I., and Wellen, K.E. (2018). Spatiotemporal Control of Acetyl-CoA Metabolism in Chromatin Regulation. Trends in biochemical sciences *43*, 61-74.

Snyder, N.W., Tombline, G., Worth, A.J., Parry, R.C., Silvers, J.A., Gillespie, K.P., Basu, S.S., Millen, J., Goldfarb, D.S., and Blair, I.A. (2015). Production of stable isotope-labeled acyl-coenzyme A thioesters by yeast stable isotope labeling by essential nutrients in cell culture. Analytical biochemistry *474*, 59-65.

Sugiura, A., and Rathmell, J.C. (2018). Metabolic Barriers to T Cell Function in Tumors. The Journal of Immunology *200*, 400-407.

Sukumar, M., Liu, J., Ji, Y., Subramanian, M., Crompton, J.G., Yu, Z., Roychoudhuri, R., Palmer, D.C., Muranski, P., Karoly, E.D.*, et al.* (2013). Inhibiting glycolytic metabolism

enhances CD8+ T cell memory and antitumor function. The Journal of clinical investigation *123*, 4479-4488.

Sukumar, M., Liu, J., Mehta, G.U., Patel, S.J., Roychoudhuri, R., Crompton, J.G., Klebanoff, C.A., Ji, Y., Li, P., Yu, Z*., et al.* (2016). Mitochondrial Membrane Potential Identifies Cells with Enhanced Stemness for Cellular Therapy. Cell metabolism *23*, 63-76.

Sukumar, M., Roychoudhuri, R., and Restifo, N.P. (2015). Nutrient Competition: A New Axis of Tumor Immunosuppression. Cell *162*, 1206-1208.

Sun, R.C., Fan, T.W., Deng, P., Higashi, R.M., Lane, A.N., Le, A.-T.T., Scott, T.L., Sun, Q., Warmoes, M.O., and Yang, Y. (2017). Noninvasive liquid diet delivery of stable isotopes into mouse models for deep metabolic network tracing. Nature communications *8*, 1646.

Svensson, R.U., Parker, S.J., Eichner, L.J., Kolar, M.J., Wallace, M., Brun, S.N., Lombardo, P.S., Van Nostrand, J.L., Hutchins, A., Vera, L*., et al.* (2016). Inhibition of acetyl-CoA carboxylase suppresses fatty acid synthesis and tumor growth of non-small-cell lung cancer in preclinical models. Nat Med *22*, 1108-1119.

Tafani, M., Sansone, L., Limana, F., Arcangeli, T., De Santis, E., Polese, M., Fini, M., and Russo, M.A. (2016). The Interplay of Reactive Oxygen Species, Hypoxia, Inflammation, and Sirtuins in Cancer Initiation and Progression. Oxidative medicine and cellular longevity *2016*, 3907147.

Thiagarajan, D., Vedantham, S., Ananthakrishnan, R., Schmidt, A.M., and Ramasamy, R. (2016). Mechanisms of transcription factor acetylation and consequences in hearts. Biochimica et biophysica acta *1862*, 2221-2231.

Thome, J.J., Yudanin, N., Ohmura, Y., Kubota, M., Grinshpun, B., Sathaliyawala, T., Kato, T., Lerner, H., Shen, Y., and Farber, D.L. (2014). Spatial map of human T cell compartmentalization and maintenance over decades of life. Cell *159*, 814-828.

Tormos, K.V., Anso, E., Hamanaka, R.B., Eisenbart, J., Joseph, J., Kalyanaraman, B., and Chandel, N.S. (2011). Mitochondrial complex III ROS regulate adipocyte differentiation. Cell metabolism *14*, 537-544.

Trayhurn, P., and Wood, I.S. (2004). Adipokines: inflammation and the pleiotropic role of white adipose tissue. The British journal of nutrition *92*, 347-355.

Trudeau, K., Muto, T., and Roy, S. (2012). Downregulation of mitochondrial connexin 43 by high glucose triggers mitochondrial shape change and cytochrome C release in retinal endothelial cells. Investigative ophthalmology & visual science *53*, 6675-6681.

van der Windt, G.J., Everts, B., Chang, C.-H.H., Curtis, J.D., Freitas, T.C., Amiel, E., Pearce, E.J., and Pearce, E.L. (2012). Mitochondrial respiratory capacity is a critical regulator of CD8+ T cell memory development. Immunity *36*, 68-78.

Van Gulik, W.M., Canelas, A.B., Taymaz-Nikerel, H., Douma, R.D., de Jonge, L.P., and Heijnen, J.J. (2012). Fast sampling of the cellular metabolome. Methods in molecular biology (Clifton, NJ) *881*, 279-306.

Vander Heiden, M.G., Cantley, L.C., and Thompson, C.B. (2009). Understanding the Warburg effect: the metabolic requirements of cell proliferation. Science (New York, NY) *324*, 1029-1033.

Vaupel, P., Fortmeyer, H.P., Runkel, S., and Kallinowski, F. (1987). Blood flow, oxygen consumption, and tissue oxygenation of human breast cancer xenografts in nude rats. Cancer research *47*, 3496-3503.

Vuckovic, D., de Lannoy, I., Gien, B., Shirey, R.E., Sidisky, L.M., Dutta, S., and Pawliszyn, J. (2011). In vivo solid-phase microextraction: capturing the elusive portion of metabolome. Angewandte Chemie (International ed in English) *50*, 5344-5348.

Waickman, A.T., and Powell, J.D. (2012). mTOR, metabolism, and the regulation of T-cell differentiation and function. Immunological reviews *249*, 43-58.

Weinberg, F., Hamanaka, R., Wheaton, W.W., Weinberg, S., Joseph, J., Lopez, M., Kalyanaraman, B., Mutlu, G.M.M., Budinger, G.R., and Chandel, N.S. (2010). Mitochondrial metabolism and ROS generation are essential for Kras-mediated tumorigenicity. Proceedings of the National Academy of Sciences of the United States of America *107*, 8788-8793.

Wellen, K.E., Hatzivassiliou, G., Sachdeva, U.M., Bui, T.V., Cross, J.R., and Thompson, C.B. (2009). ATP-citrate lyase links cellular metabolism to histone acetylation. Science (New York, NY) *324*, 1076-1080.

Wohlrab, H. (2009). Transport proteins (carriers) of mitochondria. IUBMB life *61*, 40-46.

Xu, Y., Chaudhury, A., Zhang, M., Savoldo, B., Metelitsa, L.S., Rodgers, J., Yustein, J.T., Neilson, J.R., and Dotti, G. (2016). Glycolysis determines dichotomous regulation of T cell subsets in hypoxia. J Clin Invest *126*, 2678-2688.

Yang, X., Ma, Y., Li, N., Cai, H., and Bartlett, M.G. (2017). Development of a Method for the Determination of Acyl-CoA Compounds by Liquid Chromatography Mass Spectrometry to Probe the Metabolism of Fatty Acids. Analytical chemistry *89*, 813-821.

Zasloff, M. (2002). Antimicrobial peptides of multicellular organisms. Nature *415*, 389-395.

Zea, A.H., Rodriguez, P.C., Culotta, K.S., Hernandez, C.P., DeSalvo, J., Ochoa, J.B., Park, H.-J.J., Zabaleta, J., and Ochoa, A.C. (2004). L-Arginine modulates CD3zeta expression and T cell function in activated human T lymphocytes. Cellular immunology *232*, 21-31.

Zeng, H., and Chi, H. (2017). mTOR signaling in the differentiation and function of regulatory and effector T cells. Current opinion in immunology *46*, 103-111.

Zhang, Y., Kurupati, R., Liu, L., Zhou, X.Y., Zhang, G., Hudaihed, A., Filisio, F., Giles-Davis, W., Xu, X., Karakousis, G.C.*, et al.* (2017). Enhancing CD8+ T Cell Fatty Acid Catabolism within a Metabolically Challenging Tumor Microenvironment Increases the Efficacy of Melanoma Immunotherapy. Cancer cell *32*, 377-157976064.

Zhou, C.-X.X., Zhou, D.-H.H., Elsheikha, H.M., Zhao, Y., Suo, X., and Zhu, X.-Q.Q. (2016). Metabolomic Profiling of Mice Serum during Toxoplasmosis Progression Using Liquid Chromatography-Mass Spectrometry. Scientific reports *6*, 19557.

Zhou, R., Yazdi, A.S., Menu, P., and Tschopp, J. (2011). A role for mitochondria in NLRP3 inflammasome activation. Nature *469*, 221-225.